Chemical Engineering Journal 503 (2025) 158467

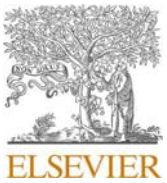

Contents lists available at ScienceDirect

Chemical Engineering Journal

journal homepage: www.elsevier.com/locate/cej

Review

State-of-the-art advancements in the thermocatalytic conversion of CO_2 into ethanol and higher alcohols: recent progress in catalyst development and reaction mechanisms

Andrii Kostyniuk *, Blaž Likozar

Department of Catalysis and Chemical Reaction Engineering, National Institute of Chemistry, Hajdrihova 19, Ljubljana 1001, Slovenia

ARTICLE INFO

Keywords:
CO_2 hydrogenation
Heterogeneous catalysts
Ethanol synthesis
Higher alcohols synthesis
Reaction mechanisms

ABSTRACT

The production of ethanol and higher alcohols (HA) via CO_2 hydrogenation with achieving high product selectivity and catalyst stability is a difficult scientific and technological challenge due to chemical inertness of CO_2, complexity in various reaction routes, and uncontrollability of C–C coupling from untamed surface moieties in HA synthesis. One of the main solutions is a catalyst design, which can overcome these issues. Hence, in this review, we summarize and analyze the recent advances in thermocatalytic direct CO_2 hydrogenation into ethanol and HA in batch and continuous fixed-bed reactors. The introductory section delves into the discourse surrounding carbon capture and utilization, highlighting the constraints imposed by reaction thermodynamics, and emphasizing the indispensable role of catalysts in the conversion of CO_2 to ethanol and HA. The second section highlights the potential promising catalyst families, in a batch reactor, including modified Cu-based catalysts, modified Co-based catalysts, and a noble-metal catalysts, together with various promoters, supports, and solvent effects specified in each case. The third section reviews the family most active catalysts, but in continuous fixed-bed reactor, including modified Cu-, Co–, Fe-based and noble metals catalysts. The fourth section reviews the possible reaction mechanisms (CO-mediated pathway, formate/methoxy-mediated pathway, and C–C coupling pathways) for ethanol and HA production. Ultimately, the conclusion and future perspectives are provided to offer a forward-looking assessment of catalyst development including approaches to enhance selectivity towards ethanol/HA based on the available experimental results.

1. Introduction

Every day, huge amounts of greenhouse gases (GHG) are emitted and accumulate in the atmosphere which in turn causes global warming. Notably, carbon dioxide (CO_2) contributes to 72 % of the GHG emissions, mainly due to the combustion of large amounts of fossil resources, and its emission keeps rising in recent years (Fig. 1**a**) [1]. The global CO_2 emissions in 2018 were approximately 33.9 Gt [2]. Therefore, carbon capture and utilization (CCU) and/or carbon capture and storage (CCS) are critical to reducing CO_2 emissions, a major air pollutant, and mitigating global warming (Fig. 1**b**) [2], where CCU is a more attractive and promising pathway [3]. These technologies provide substantial advantages in carbon emissions reduction. The latter specifically fosters a circular economy by encouraging industrial symbiosis among high CO_2 footprint industries and facilitating renewable energy storage. These efforts align with the European policy objective of achieving a 40 % reduction in GHG emissions by 2030, relative to 1990 levels [4].

At present, approximately 22 million tons of coal, 10 billion m^3 of natural gas, and 12 million tons of oil are combusted daily to fulfill 82 % of the current total energy demand. This results in an annual emission exceeding 30 billion tons of CO_2 into the environment [5]. CO_2 as feedstock for chemical processes has attracted great attention since it can reduce the cost and increase the profit for reducing CO_2 emissions. At the same time, the CO_2 molecule exhibits remarkable thermodynamic and chemical stability. When employed as a sole reactant, its utilization demands substantial energy. However, a fascinating shift occurs when introduced a coreactant possessing higher Gibbs free energy, such as H_2. In this context, the reaction becomes more thermodynamically favorable, facilitating the transformation of CO_2 into a valuable resource [6].

The "Power-to-Fuel" strategy, which utilizes excess renewable energy from wind and solar, has gained significant attention [4]. A key component of this approach is CO_2 hydrogenation, especially when

* Corresponding author.
E-mail address: andrii.kostyniuk@ki.si (A. Kostyniuk).

https://doi.org/10.1016/j.cej.2024.158467
Received 3 July 2024; Received in revised form 19 September 2024; Accepted 8 December 2024
Available online 12 December 2024

combined with CO_2 capture and renewable H_2 production via electrolysis. As a result, extensive research has focused on CO_2 hydrogenation to create a direct route for producing chemicals used as fuels or feedstocks in alternative processes. Among the various technologies explored, catalytic hydrogenation stands out as the most advanced and promising, with different catalysts enabling the conversion of CO_2 into a wide range of products, as shown in Fig. 2**a** [4]. As illustrated in Fig. 2**b**, the principal outcomes of CO_2 activation and transformation/hydrogenation encompass methane, methanol, higher alcohols (HA), dimethyl ether (DME), and hydrocarbons, including olefins, liquefied petroleum gas (LPG), gasoline, and aromatics [4,7–26].

In recent years, the research studies related to "CO_2 or ethanol" have experienced significant intensification, and the number of related scientific publications has tremendously increased, as shown in **Fig. S1**. In Fig. 3**a**, it is evident that CO_2 serves as a versatile feedstock for numerous processes, with a diverse array of technologies available at varying levels of technological maturity – ranging from laboratory experiments, small pilots, and demonstrations to readily accessible commercial-off-the-shelf (COTS) options. The analysis conducted by the International Energy Agency (IEA) emphasizes that a substantial 75 % of the requisite emission reductions for achieving carbon neutrality must be derived from a multitude of technologies that are currently in an immature state. Importantly, this does not necessitate the invention of entirely new technologies but rather the swift scaling-up of existing benchtop technologies from laboratories to pilot projects, then demonstrations, and ultimately integration into the market for actual industrial processes [27]. Fig. 3**b** indicates a potential reduction of 50 % in CO_2 emissions in the near future when utilizing fossil CO_2, and a complete elimination of emissions in the case of atmospheric or biogenic CO_2 in the long term. However, caution is necessary to prevent lock-in effects, as the majority of fossil CO_2 sources must be phased out to achieve ambitious climate targets. Additionally, Fig. 3**b** underscores that CCU should only utilize CO_2 from sources with hard-to-abate emissions, avoiding those where low-carbon energy could have been used more directly. Regarding e-fuels or other synthesized fuels, achieving net-zero or even net-negative emissions depends on the origin and destination of the CO_2. To attain the ultimate goal of carbon negativity, the CO_2 must be biogenic (from biomass) or sourced from direct air capture (DAC), followed by permanent sequestration. Throughout the entire process, upstream and downstream GHG emissions must be smaller than the quantity of GHGs removed [27].

Thus, together with the generation of renewable H_2, which can be produced by water electrolysis with electricity generated from solar or wind sources, CO_2 capture and conversion provide a sustainable way for the synthesis of fuels and chemicals including CO, CH_4, olefins, aromatics, dimethyl ether, liquid hydrocarbons, formates/formic acid, and alcohols [28–48]. One of the most promising approaches toward CO_2 valorization is the direct hydrogenation of the latter into ethanol and/or HA. The reduction of CO_2 can be achieved through thermal catalysis [1,2,5,49,50], photocatalysis [51–56], or electrocatalysis [57–63], with thermal catalysis standing out for its advantageous kinetics and garnering considerable attention [64].

Between 1913 and 1928, BASF secured a series of German patents [65–68] that laid the foundation for the production of a range of alcohols, hydrocarbons, aldehydes, ketones, and carboxylic acids from the hydrogenation of CO under high-pressure conditions. These processes were typically carried out at pressures of 100–200 bar and temperatures ranging from 300 to 500 °C, employing metal oxide catalysts [69]. The primary catalysts disclosed in these patents were predominantly ZnO, often combined with Cr_2O_3 and/or MnO. Additionally, a variety of other oxides, such as uranium, vanadium, and cadmium oxides, were also explored. The inclusion of various metals, including Cu, Ag, and Pb, was noted to enhance catalytic activity or selectivity in some cases. These early contributions represent significant advances in the field of catalytic hydrogenation and laid crucial groundwork for future developments in the field of synthetic fuel production. Intentional incorporation of CO_2 into the traditional CO/H_2 feed gas was rarely documented before the 1960 s. One significant exception came from Schmidt and Ufer [70] of BASF, who in 1925 secured a patent for a variety of mixed oxide (Cu, Na, Ti, U, V, Cr, Mg, etc.) catalysts. These catalysts were designed to facilitate methanol production from carbon oxides, whether CO, CO_2, or a combination of both, in the presence of H_2. Although innovative, this approach to using CO_2 in methanol synthesis was not widely adopted until much later. In the 1980 s, efforts began to develop a process for synthesizing ethanol (C_2H_5OH) and HA from CO_2 using catalysts derived from syngas conversion methods [71]. However, the inherent low reactivity of the CO_2 molecule, coupled with competition from hydrocarbons and C_1 compounds for selectivity, posed significant limitations on achieving desirable yields of HA. Intensive investigation and practical implementations have centered around catalyzing the conversion of CO_2 into methanol (CH_3OH), with a particular emphasis on utilizing the $Cu/ZnO/Al_2O_3$ catalyst [6,69]. In contrast, the conversion to C_2H_5OH, a safer alternative with a higher energy density, has seen limited exploration. The primary industrial catalyst for synthesizing CH_3OH from CO_2 hydrogenation ($CO_2 + 3H_2 \rightarrow CH_3OH + H_2O$) is the $Cu/ZnO/Al_2O_3$ catalyst, as highlighted in literature [72]. This catalyst predominantly produces CO and CH_3OH as the main products. However, its limitations prevent the synthesis of C_2H_5OH ($2CO_2 + 6H_2 \rightarrow C_2H_5OH + 3H_2O$), attributed to challenges in C – O bond scission and C – C coupling through adsorbed formyl (*CHO) or formaldehyde ($*CH_2O$) precursors [73]. The first catalytic demonstration of ethanol and HA synthesis from CO_2 hydrogenation dates back

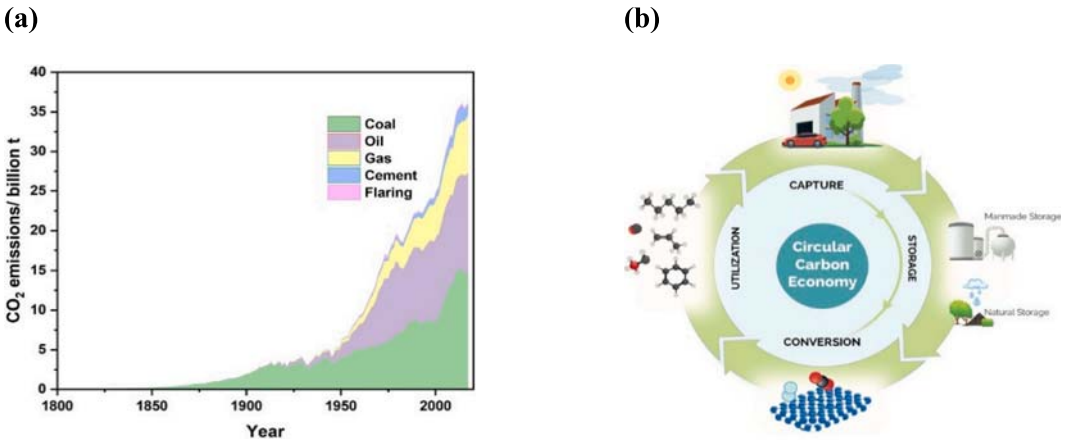

Fig. 1. (a) – Annual CO_2 emissions from various sources. Adapted with permission from Ref. [1]; (b) – Schematic representation of the circular carbon economy. Adapted with permission from Ref. [2].

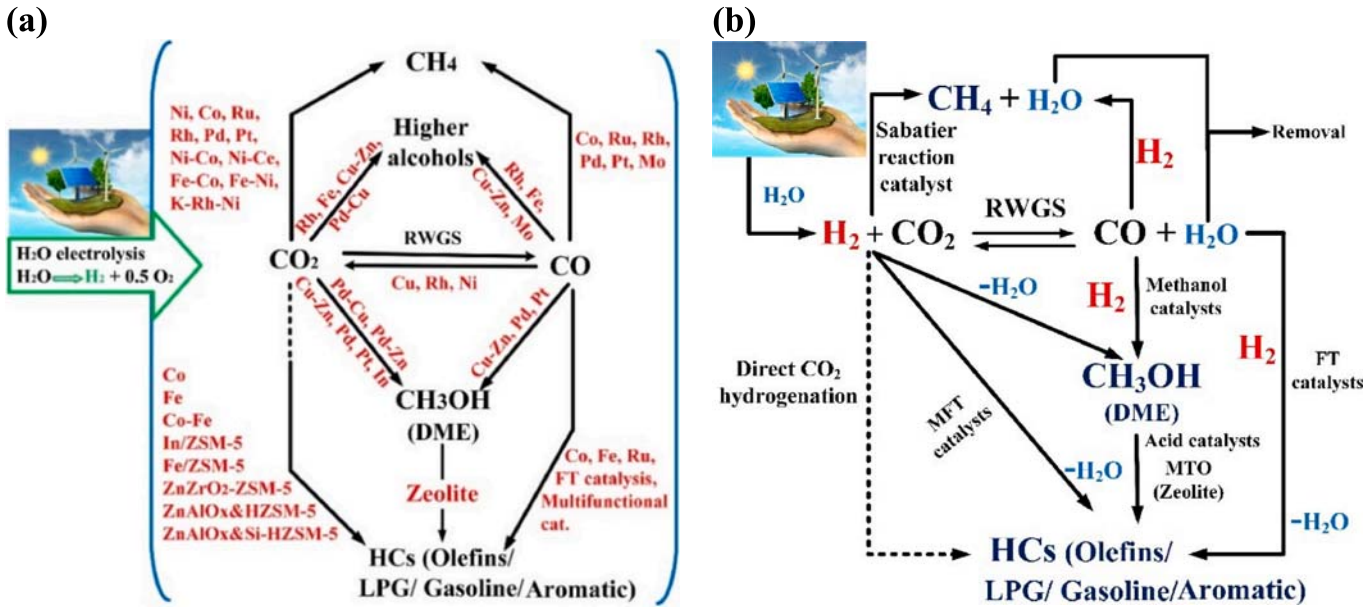

Fig. 2. (a) – Showcases an assortment of products derived from CO_2 hydrogenation using different catalysts, and (b) – Demonstrates various potential routes for creating value-added products via CO_2 hydrogenation.
Reproduced with permission from Ref. [4].

to 1985, when Tatsumi et al. [74] successfully employed a Mo-KCl/SiO_2 catalyst. This catalyst showed moderate activity in converting CO_2 into $C_{2+}OH$ compounds, marking a significant early step in the development of catalytic processes for the production of ethanol and higher alcohols from CO_2.

The combustion of petroleum-derived fuels results in significant CO_2 emissions, and alcohols derived from CO_2 offer a potential substitution or blending option to reduce their overall consumption. Methanol, ethanol, 1-propanol, 1-butanol, 1-pentanol, and 1-hexanol possess energy densities of 22, 30, 33, 36, 38, and 39 MJ/kg, respectively, with the latter three closely approaching the lower thresholds of natural gas, diesel, and gasoline (approximately 42 MJ/kg). These alcohols exhibit superior combustion characteristics due to their higher octane numbers compared to gasoline. The combination of alcohols with conventional fuels has demonstrated a reduction in greenhouse gas emissions and particulate matter during combustion, while also delivering engine performance equivalent to or exceeding that of gasoline. Additionally, these alcohols maintain a liquid state under standard temperature and pressure conditions, allowing for storage in nonpressurized tanks [75].

Ethanol has various applications such as a clean fuel, engine fuel, fuel additive, intermediate of manufacturing industries, feedstock, solvent, low-temperature liquid, etc. The global bioethanol production is estimated to increase from 120 billion liters in 2017 to 131 billion liters by 2027, where a half of this increase is expected to originate from Brazil, and the other large contributors to the expansion in bioethanol production are Thailand, China, India, and the Philippines with 12 %, 10 %, 9 %, and 5 %, respectively [76]. Ethanol can be obtained by synthetic routes (Fig. 4a) through the hydration of ethylene over a solid acid catalyst or by the fermentation of sugar, grain crops, and waste biomass. The production of ethanol from ethylene has many disadvantages, mainly including high production cost, non-environmentally friendly route, unsustainable production, and hazardous feedstock. Therefore, the fermentation method is more favorable. At the same time, the toxicity of ethanol to yeast limits the concentration of ethanol in a fermentation reaction, and further distillation is necessary to obtain the high concentrated ethanol [76]. Moreover, ethanol production via fertilization of corn and sugar cane is considered non-ethical (food versus fuel discussions).

Methods for the hydrogenation of CO_2 into ethanol or HA are in great demand but their development is still challenging. Typically, noble-metal-based catalysts such as Pd, Pt, and Rh were employed to address the initial challenges of C–O activation and subsequent C–C coupling hurdles in ethanol production via CO_2 hydrogenation. However, due to the high cost associated with these catalysts, there has been a shift in focus within the research community towards exploring abundant transition metals as alternative options [77]. The combination of a metal (s), metal oxides and zeolites can be considered as a multifunctional catalyst [77–82] where impregnated transition and alkali metals will be responsible for the hydrogenation function, C – C coupling and help to prolong the zeolite support lifetime which possesses unique shape selectivity and acidity (Fig. 4b).

It is still a challenge to achieve highly efficient conversion of CO_2 due to the low selectivity and poor catalyst stability. Moreover, the direct CO_2-to-ethanol transformation or HA, which is more challenging than the multiple reaction processes, still exhibits poor ethanol productivity. Achieving the direct production of ethanol or HA through CO_2 hydrogenation poses significant challenges. This difficulty arises not only due to the thermodynamic stability and chemical inertness of CO_2 but also because of the intricate nature of multiple reaction pathways and the uncontrollable coupling of C–C bonds from unregulated surface moieties. Furthermore, this process necessitates both dissociative and non-dissociative adsorptions of C – O bonds to generate surface alkyl and C(H)O species, respectively. The inherent mismatch in the kinetics of these processes, coupled with the presence of various side reactions, typically leads to low activity and selectivity in the production of HA from CO_2 hydrogenation. Over the past four decades, and notably in recent years, significant advancements were made in the preparation methods and *in situ* characterization techniques for catalysts of this nature. This includes thermodynamic calculations specific to HA synthesis in comparison to other reactions involved in direct CO_2 hydrogenation. The principal reactions in CO_2 hydrogenation encompass the following list of reactions [5]:

Reverse water–gas shift (RWGS):

$$CO_2 + H_2 \rightarrow CO + H_2O \quad (1)$$

CO_2 hydrogenation to alkanes:

$$nCO_2 + (3n + 1)H_2 \rightarrow C_nH_{2n+2} + 2nH_2O \quad (2)$$

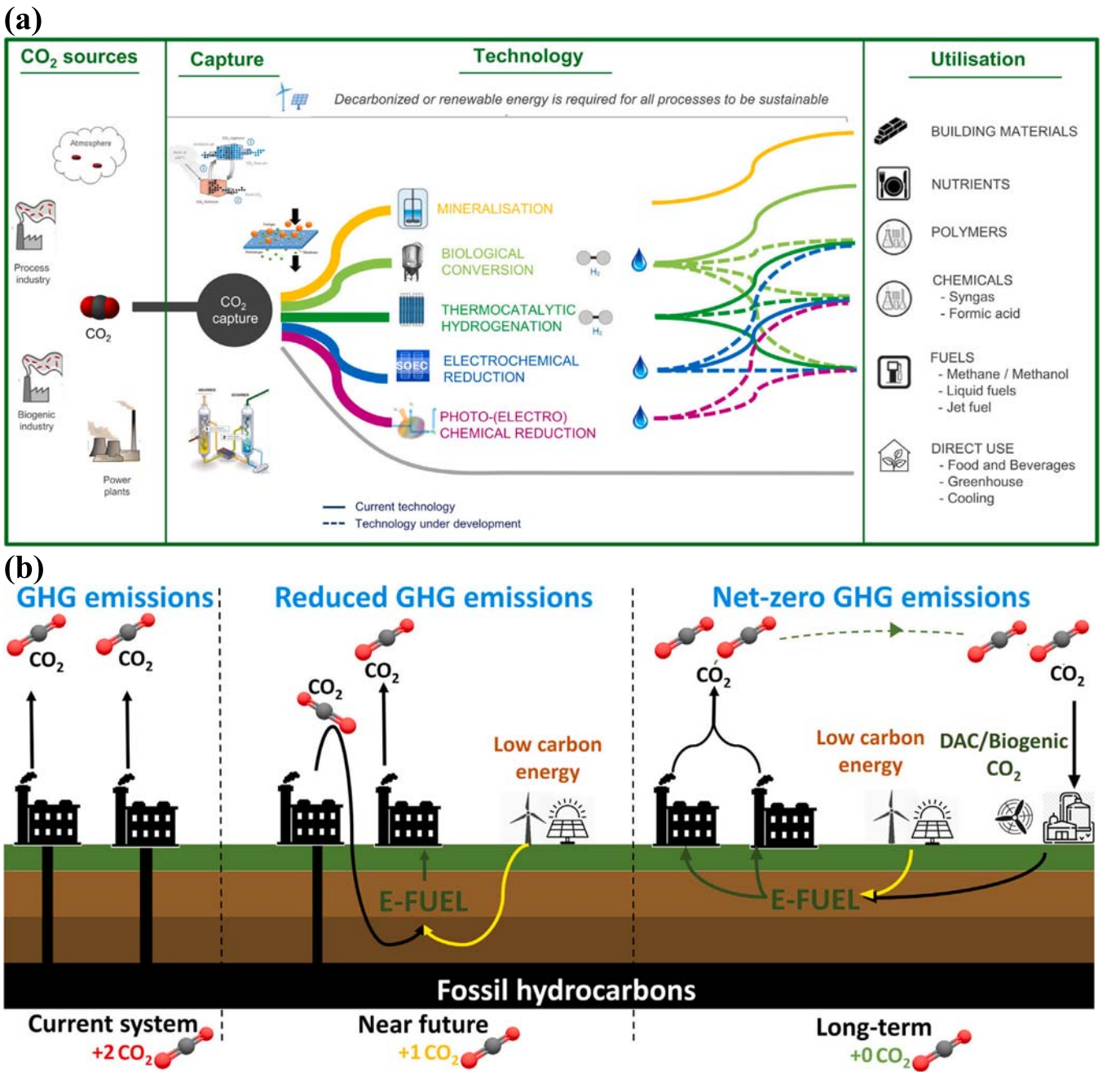

Fig. 3. (a) – Routes to various CO_2-derived e-molecules for a range of applications; (b) – Environmental benefits of low-carbon CCU: potential reduction of emissions by up to 50 % through the recycling of fossil CO_2. Adapted with permission from Ref. [27].

CO_2 hydrogenation to alkenes:

$$nCO_2 + 3nH_2 \rightarrow C_nH_{2n} + 2nH_2O \quad (3)$$

Methanol synthesis:

$$CO_2 + 3H_2 \rightarrow CH_3OH + H_2O \quad (4)$$

HA synthesis:

$$nCO_2 + 3nH_2 \rightarrow C_nH_{2n+1}OH + (2n-1)H_2O \quad (5)$$

As illustrated in Fig. 5**A** and Fig. 5**B**, most CO_2 hydrogenation pathways exhibit exothermicity and thermodynamic favorability at low temperatures, with the exception of the RWGS reaction. Consequently, the RWGS reaction is unlikely to occur independently, but it may act as a parallel side-product when overall thermodynamics are favorable for all reactions. Ethanol synthesis emerges as more favorable than methanol synthesis at lower temperatures, attributed to its lower Gibbs free energy of reaction and a higher equilibrium constant value. It is important to highlight that the formation of alkanes is highly exothermic, with calculated equilibrium constants considerably surpassing those of HA at all temperatures, making alkanes, such as CH_4 and C_{2+}, the most thermodynamically favored products. In Fig. 5**C**, it is demonstrated that allowing methanation as a reaction leads to an equilibrium yield of ethanol approaching zero. This underscores the need for selective catalysts to inhibit or significantly reduce methanation, which is strongly thermodynamically driven. When restricting carbon products to only CO and ethanol, substantial equilibrium concentrations of ethanol can be achieved at temperatures below 350 °C (Fig. 5**D**). Consequently, ethanol synthesis should be conducted at low temperatures through a different kinetic route, introducing a barrier to the formation of alkanes before

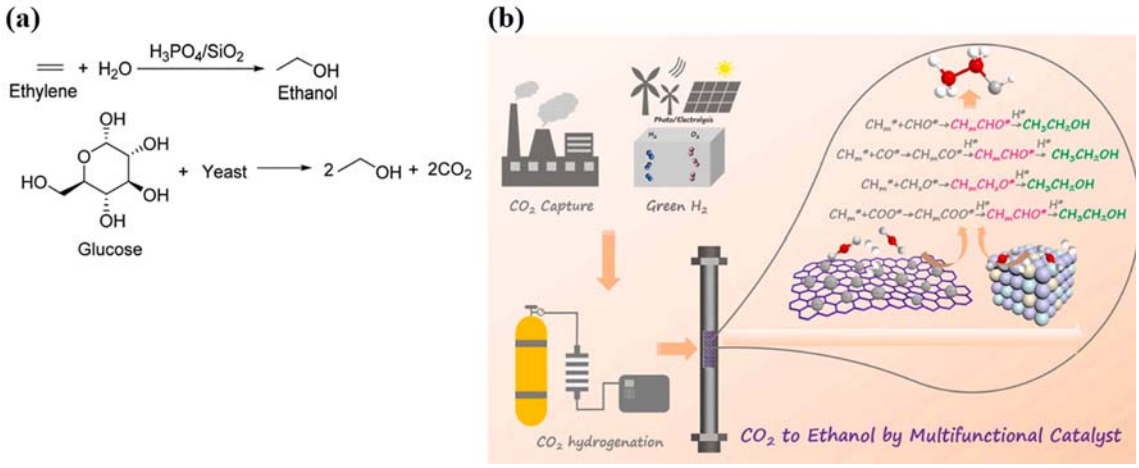

Fig. 4. (a) – Methods for producing ethanol on an industrial scale. Adapted with permission from Ref. [76]. (b) – Directly transforming CO_2 into ethanol using multifunctional catalysts. Adapted with permission from Ref. [77].

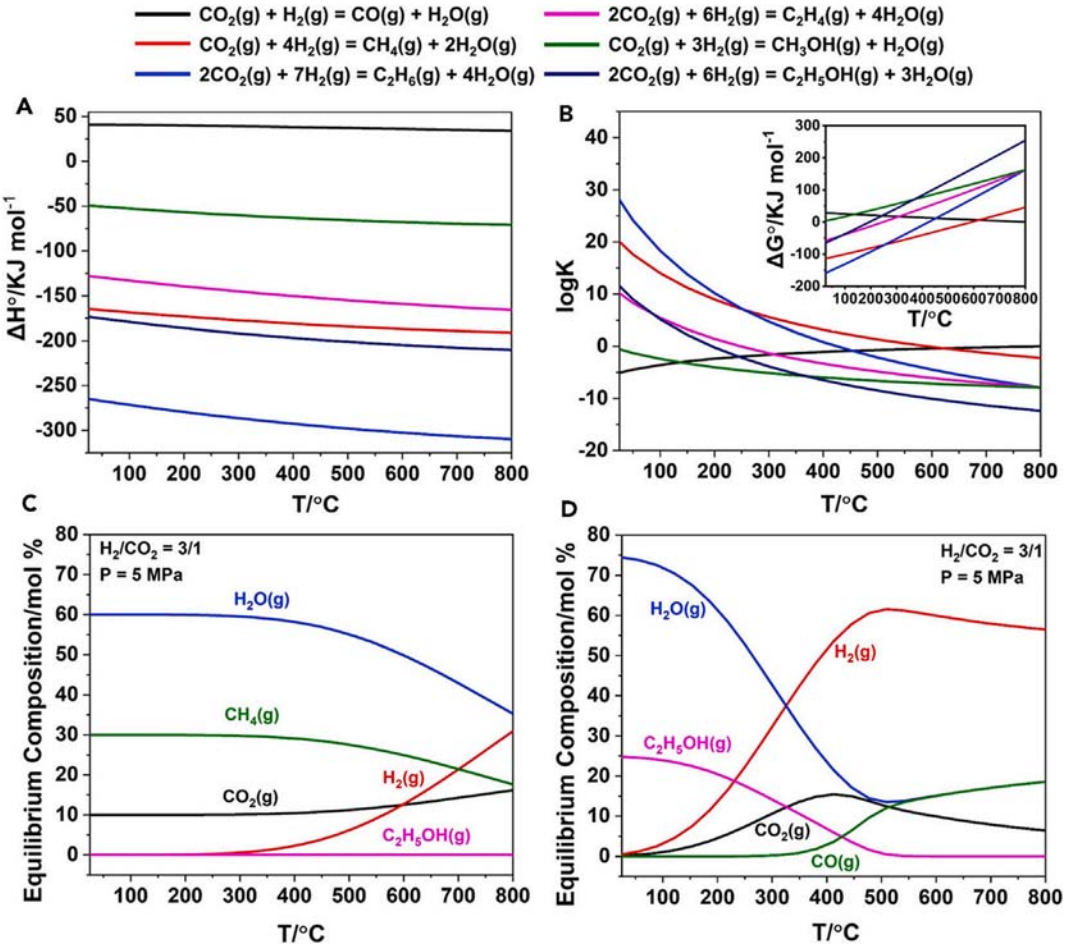

Fig. 5. An analysis of the thermodynamics involved in CO_2 hydrogenation reactions. Panels A and B display diagrams that illustrate (A) the variation in standard enthalpy (ΔH°) and (B) the equilibrium constant (K) along with the standard Gibbs free energy change (ΔG°) for the reactions, both as functions of temperature. Panels C and D show the equilibrium composition of the hydrogenation of CO_2, leading to (C) methane and ethanol and (D) CO and ethanol, under conditions of 5 MPa with a H_2/CO_2 ratio of 3:1. Reprinted with permission from Ref. [5].

they become predominant products, given that all equilibria are established at high temperatures. While methanol formation is less thermodynamically favorable than ethanol synthesis, it remains a competitive kinetic route. This is due to the likelihood of methanol synthesis and HA synthesis sharing the same active site for the hydrogenation of C–O bonds without the cleavage of C–O bonds in alcohol formation. Kinetically, HA synthesis is more intricate than methanol synthesis and is generally considered a combination of Fischer-Tropsch synthesis and methanol synthesis. Therefore, based on the analysis above, an effective HA synthesis catalyst should possess the ability to create a substantial

kinetic barrier for alkanes formation and methanol synthesis, ensuring high selectivity towards HA under the given reaction conditions.

He et al. [83] investigated the thermodynamics of CO_2 hydrogenation to HA using Aspen Plus. They examined the effects of alcohol isomers and methane on the reaction system, finding that methane is the most thermodynamically favorable product, which hinders HA formation. However, low temperatures, high pressures, a high H_2/CO_2 ratio, and the formation of longer-chain alcohols can mitigate CH_4 negative impact on HA synthesis. Additionally, the same authors [84] demonstrated that recycling unreacted tail gas, as well as co-feeding CO, plays a crucial role in improving CO_2 conversion to ethanol. Their thermodynamic study, conducted using Aspen Plus, analyzed the effects of tail gas recycling and CO co-feeding on CO_2 conversion and ethanol selectivity under varying temperatures and pressures. The results revealed that optimizing the recycle ratio and the $CO/(CO + CO_2)$ ratio in the feed could significantly enhance ethanol synthesis. He and colleagues [85] recognized that the process (CO_2 to EtOH), despite its potential, may generate additional CO_2 emissions due to the consumption of heat, electricity, and the emission of tail gas. To address this, the authors model and investigate the influence of critical parameters, such as CO_2 conversion rate per pass, tail gas splitting ratio, and reaction temperature, on the overall CO_2 conversion efficiency, energy consumption, and emission reduction. Their results indicate that a moderate single pass CO_2 conversion rate (around 15 %), a high tail gas splitting ratio (around 0.8), and a relatively high reaction temperature (around 250 °C) are optimal for practical applications of this process. With a CO_2 processing capacity of 268 kt per year, their study demonstrates that up to 86.9 % of CO_2 emissions could be eliminated, resulting in an annual ethanol production of 141 kt. This highlights the high efficiency of the hydrogenation process in reducing CO_2 emissions.

The techno-economic analysis indicates that the synthesis of alcohols from CO_2 and green hydrogen has the potential to be economically viable, provided that the separation of alcohols from other reaction byproducts is performed efficiently [49]. Optimizing this separation process is a key factor in improving overall process economics and ensuring the commercial feasibility of CO_2-to-alcohol conversion technologies. In the work by Vo and colleagues [86], process systems engineering analysis is used to assess the techno-economic and environmental performance of three thermocatalytic CO_2-based plants individually producing liquid hydrocarbon transportation fuels (LHTF), methanol, and 1-propanol. The study concluded that, unlike LHTF and methanol plants, the 1-propanol plant generates a substantial profit. The key limiting factor for LHTF and methanol is the cost of CO_2 and H_2 inputs, which need to drop by approximately 80 % for these plants to break even. The analysis also indicated that implementing a tax structure is not a viable solution, as it would need to be more than four times the highest carbon tax currently applied in the country. In terms of environmental performance, CO_2 utilization efficiencies were reported as 45.5 % for LHTF, 60.1 % for methanol synthesis, and –33.8 % for 1-propanol synthesis. The negative efficiency observed in the 1-propanol plant highlights the critical need for more sustainable ethylene production, as ethylene serves as the key raw material for the hybrid process involved. Despite this, when comparing the entire lifecycle of these products to their conventional counterparts, the 1-propanol plant still shows a significant reduction in CO_2 emissions, with 85.9 % less CO_2 emitted, compared to reductions of 77.4 % for methanol and 35.9 % for LHTF.

One year later, Vo et al. [75] conducted a more comprehensive techno-economic and environmental evaluation for the synthesis of 1-propanol, 1-butanol, 1-pentanol, and 1-hexanol using captured CO_2 and green hydrogen via the syngas route (CO_2 to syngas to higher alcohols). This analysis demonstrated that, under ideal conditions for conversion and selectivity, 1-pentanol and 1-hexanol plants exhibit economic viability, while the costs of manufacturing 1-propanol and 1-butanol exceed their revenues. Specifically, raw materials accounted for 83 % of the total cost of manufacturing, utilities for 12 %, and wastewater treatment for 5 %, excluding capital expenditures (CAPEX). Sensitivity analysis highlights that for the 1-propanol and 1-butanol processes to break even, the cost of hydrogen must fall from the current level of approximately \$2500 t^{-1} to around \$2100 t^{-1} and \$1700 t^{-1}, respectively. One of the key challenges is that 55–60 % of the hydrogen is lost to byproduct water in these processes, an inherent issue with thermocatalytic CO_2 hydrogenation. While a standalone green 1-propanol plant is not economically viable at present, the authors propose a hybrid process combining a recently studied route using ethylene and CO_2-derived syngas with the novel route based solely on CO_2. This hybrid approach has the potential to reduce the carbon footprint without relying on carbon sequestration and could also be profitable at the prevailing hydrogen costs.

Several research groups are actively investigating CO_2 hydrogenation, and a series of recent reviews [1,2,5,49,50,87–98] were released, shedding light on the latest progress in catalytic CO_2 hydrogenation. These reviews offer brief summaries of catalyst classifications and potential reaction routes, building upon previous research discoveries. However, to the best of our knowledge, there is a noticeable lack (or only a limited number) of comprehensive and detailed review articles specifically dedicated to CO_2 hydrogenation with a focus on the production of ethanol and HA. The field of ethanol and HA production from CO_2 hydrogenation lacks an integrated and thorough analysis of active metals, support and promoter effects, as well as the underlying reaction mechanisms. This review aims to fill this gap by summarizing and analyzing the progress made in the direct CO_2 hydrogenation to ethanol and HA through heterogeneous catalysis over the past decade. The initial section will concentrate on catalyst systems utilized in fixed-bed and batch reactors, shedding light on the roles played by promoters and supports. The subsequent section will provide an overview of the disclosed reaction mechanisms found in the literature. Through this, we aim to extract valuable guidance and insights from prior works. Furthermore, we identified key areas for further investigation based on our critical analysis, encompassed in sections addressing strategies for enhancing ethanol and HA selectivity. The outlook (challenges and future perspectives) and conclusions sections provide a summary of our findings and future directions for interested readers. This review aspires to serve as a comprehensive resource for researchers and practitioners in the field, fostering a deeper understanding of the challenges and opportunities in the quest for efficient CO_2 hydrogenation to ethanol and HA.

2. Catalysts in batch reactors

The use of a batch reactor in a solvent offers a distinct advantage over a fixed-bed reactor for ethanol and HA production, primarily due to its enclosed recirculating environment. Developing an efficient catalyst for ethanol and HA production through CO_2 hydrogenation necessitates a dual focus on enhancing CO_2 activation and facilitating $C-C$ coupling on the catalyst's surface [50]. Addressing this challenge entailed significant endeavors in designing and synthesizing selective catalytic systems. These encompass transition-based systems including Cu, Co and bimetallic configurations, mono-metallic noble metal catalysts such as Rh, Ru, Ir, Pd, Pt, and Au, multimetallic/multifunctional catalysts, and metal–organic frameworks (MOFs). Within this chapter, catalysts for the conversion of CO_2 to ethanol and HA are systematically classified into three distinct groups: Cu-based catalysts, Co-based catalysts, and noble-metal-based catalysts. Each of these categories plays a pivotal role in contributing unique advancements to catalytic efficiency in the targeted conversion processes.

2.1. Cu-based catalysts with different promoters, supports, and solvents

Cu-based catalysts are widely employed in methanol synthesis [99–106]. Additionally, owing to the RWGS activity inherent in Cu-based systems, various modified catalysts were utilized for the

synthesis of ethanol and HA from syngas [6,80,107–110]. Batch reactors, employing Cu-based catalysts for the hydrogenation of CO_2, demonstrated superior catalytic activity compared to fixed-bed reactors, resulting in higher selectivity towards ethanol and HA (Table 1). An illustrative example is presented by An et al. [111], who employed a Cs^+-modified MOF catalyst (Zr_{12}-bpdc-CuCs) in achieving highly selective (>99 %) hydrogenation of CO_2 to ethanol. This reaction was conducted at 100 °C for 10 h under 350 bar in tetrahydrofuran (THF), resulting in an outstanding space–time yield (STY) of 728 mmol·g_{cat}^{-1}·h^{-1}, currently unmatched in the literature (Fig. 6**b**). The study revealed a notable decrease in Cu TON (turnover number) as the Cu loadings decreased. Specifically, Cu TON dropped from 279 (in 10 h) with N_{Cu}/SBU = 11 to 82 with N_{Cu}/SBU = 7, and further declined to 10 with N_{Cu}/SBU = 3 (Fig. 6**a**). The authors propose, as depicted in Fig. 6**c**, that alkali plays a crucial role in the catalytic process, influencing the selectivity of ethanol in the order of Li < Na < K < Cs. The catalytic activity is ascribed to the cooperative behavior of bimetallic CuI_2 centers, which not only facilitate H_2 activation but also enable the direct C–C coupling of methanol and formyl species. The alkali-metal promoters further contribute by creating an electron-rich environment for the Cu center, enhancing activity, and stabilizing a formyl intermediate.

Bai et al. [112] successfully synthesized highly organized Pd-Cu nanoparticles (NPs) designed for the hydrogenation of CO_2 to ethanol (Fig. 7). Through careful adjustments to the catalyst composition and support, the optimized 1.23 %Pd_2Cu NPs/P25 catalyst demonstrated remarkable results, achieving a noteworthy ethanol selectivity of up to 92.0 % and a substantial STY of 41.5 mmol·g_{cat}^{-1}·h^{-1} at 200 °C under 24 bar in a water medium after 5 h (Fig. 7 **I**).

The study proposed that the enhanced selectivity observed in the optimized Pd_2Cu NPs/P25 catalyst is likely attributed to the charge transfer between Pd and Cu in the well-ordered Pd-Cu NPs/P25 structure. This charge transfer is believed to enhance the reducibility of surface oxides. Additionally, results from DRIFTS indicated (Fig. 7 **II**) that the hydrogenation of *CO to *HCO is a crucial step, leading to a reduction in *CO coverage and mitigating the adverse effects of *CO poisoning. This particular step was identified as the rate-determining process for the overall CO_2 hydrogenation to ethanol. The high catalytic activity of Pd_2Cu NPs/P25 in CO_2 hydrogenation to ethanol can be attributed to the low coverage of *CO over Pd atoms, particularly in the form of 3-fold bridge-bonded *CO species. These species are more readily converted to ethanol compared to 2-fold bridge-bonded *CO species present on other Pd-Cu NPs/P25 structures.

A comprehensive investigation was conducted, integrating theoretical insights with experimental observations, to analyze the dual impact of surface segregation and diverse CO coverage over the CoCu (111) surface in CO_2 hydrogenation [113]. The results showcased a remarkable achievement, with a selectivity exceeding 60 % towards ethanol and a notable STY of 10 mmol·g_{cat}^{-1}·h^{-1}. The investigation revealed that the crucial step in promoting ethanol production involves the scission of the C − O bond and subsequent hydrogenation of the intermediate *CH_2O. This relationship was identified as a key factor influencing the overall efficiency of the ethanol production process. Wang et al. [114] employed CoCu-based catalysts supported on mesoporous silica MCM-41, achieving an impressive ethanol selectivity of up to 85.3 %, with an ethanol STY of 0.229 mmol/(g_{metal}•h). The study revealed that adsorbed oxygen (O*) generated through CO_2 dissociation has the ability to occupy cobalt hollow sites on the CoCu surfaces. Significantly, these cobalt hollow sites serve as adsorption sites for C_1 intermediates, facilitating further C − C coupling in the catalytic process.

2.2. Co-based catalysts with different promoters, supports, and solvents

Co is a well-established element in the classic Fischer-Tropsch synthesis [127–129] and found extensive application in the hydrogenation of CO_2 to ethanol and HA (Table 1). However, it is noteworthy that Co inherently exhibits low activity in the RWGS reaction but possesses strong CO_2 methanation capabilities [130,131]. Utilizing the optimized $Co_{0.52}Ni_{0.48}AlO_x$ catalyst [115], an impressive ethanol STY of 15.8 mmol·g_{cat}^{-1}·h^{-1} was achieved in a batch reactor (Fig. 8).

This catalyst exhibited a remarkable ethanol selectivity of 85.7 % under the operating conditions of 200 °C for a duration of 12 h. The $CoAlO_x$-600 catalyst, composed of cobalt-aluminum oxides calcinated at 600 °C, was synthesized and examined by the same research group [118]. Their findings revealed an impressive 92.1 % selectivity towards ethanol, coupled with a substantial STY of 0.444 mmol·g_{cat}^{-1}·h^{-1} under operating conditions of 140 °C and 40 bar (Fig. 9). This led to the conclusion that reducing the extent of reduction had a notable impact on both the STY and ethanol selectivity, highlighting a significant aspect of catalyst performance.

In a batch reactor operating at temperatures ranging from 135 to 200 °C, with a liquid 1,4-dioxane solvent, the CO_2 hydrogenation process was examined using Mo_2C-supported metal catalysts (Cu, Pd, Co, and Fe) by Chen and colleagues [116]. The inclusion of Cu and Pd in the catalyst composition was found to augment the methanol production, whereas the presence of Co and Fe contributed to an increased chain-

Table 1
The catalytic performance and reaction conditions of heterogenous catalysts in CO_2 thermocatalytic hydrogenation to EtOH and/or $C_{2+}OH$ in a batch reactor.

Catalyst	Catalytic performance			Reaction conditions					Ref.
	STY_{EtOH} mmol·g_{cat}^{-1}·h^{-1}	X_{CO2} (%)	S_{EtOH} or $C_{2+}OH$(%)	T (°C)	P (bar)	Solvent	H_2/CO_2	TOS (h)	
Zr_{12}-bpdc-CuCs	87.9	96	>99.0	100	20	THF	3	10	[111]
	728	52		85	350				
1.23Pd_2Cu NPs/P25	41.5	N.A.	92.0	200	24	H_2O	3	5	[112]
CoCu	10	N.A.	60.0	200	40	N.A.	3	12	[113]
CoCu/MCM-41	0.229 mmol/g_{metal}/h	N.A.	85.3	200	40	H_2O	3	34	[114]
$Co_{0.52}Ni_{0.48}AlO_x$	15.8	N.A.	85.7	200	40	H_2O	3	12	[115]
Co/Mo_2C	4.4	N.A.	25	200	40	1,4-dioxane	3	2	[116]
$CoMoC_x$	0.528	N.A.	97.4	180	15	DMF	3	6	[117]
$CoAlO_x$	0.444	N.A.	92.1	140	40	H_2O	3	15	[118]
1Pt/Co_3O_4	0.509	N.A.	82.5	200	80	H_2O/DMI (15/85)	3	15	[119]
Au/a-TiO_2	942.8 mmol/g_{Au}/h	N.A.	99.0	200	45	DMF	3	10	[120]
Rh_1/$CeTiO_x$	5.8 mmol/g_{Rh}/h	6.3	99.1	250	30	H_2O	3	5	[121]
Rh/CNP	3.68 mmol/g_{Rh}/h	4.9	81.8	250	30	H_2O	3	5	[122]
Ir_1-In_2O_3	0.99	N.A.	99.0	200	60	H_2O	5	5	[123]
$[Au_{11}(PPh_3)_8Cl_2]Cl$	N.A.	1.42	80.0	120	30	H_2O	3	14	[124]
$K_{0.2}Rh_{0.2}$/β-Mo_2C	33.7 μmol/g_{cat}/h	N.A.	72.1	150	60	1,4-dioxane	N.A.	10	[125]
$Ru_3(CO)_{12}$/$Co_4(CO)_{12}$/ PPNCl	29.5 mmol/L_{cat}/h	N.A.	90.8	200	60	DMI	2	12	[126]

N.A. means that the data is not available in the reference·THF – tetrahydrofuran; DMF − N,N-dimethylformamide; DMI − 1,3-dimethyl-2-imidazolidinone.

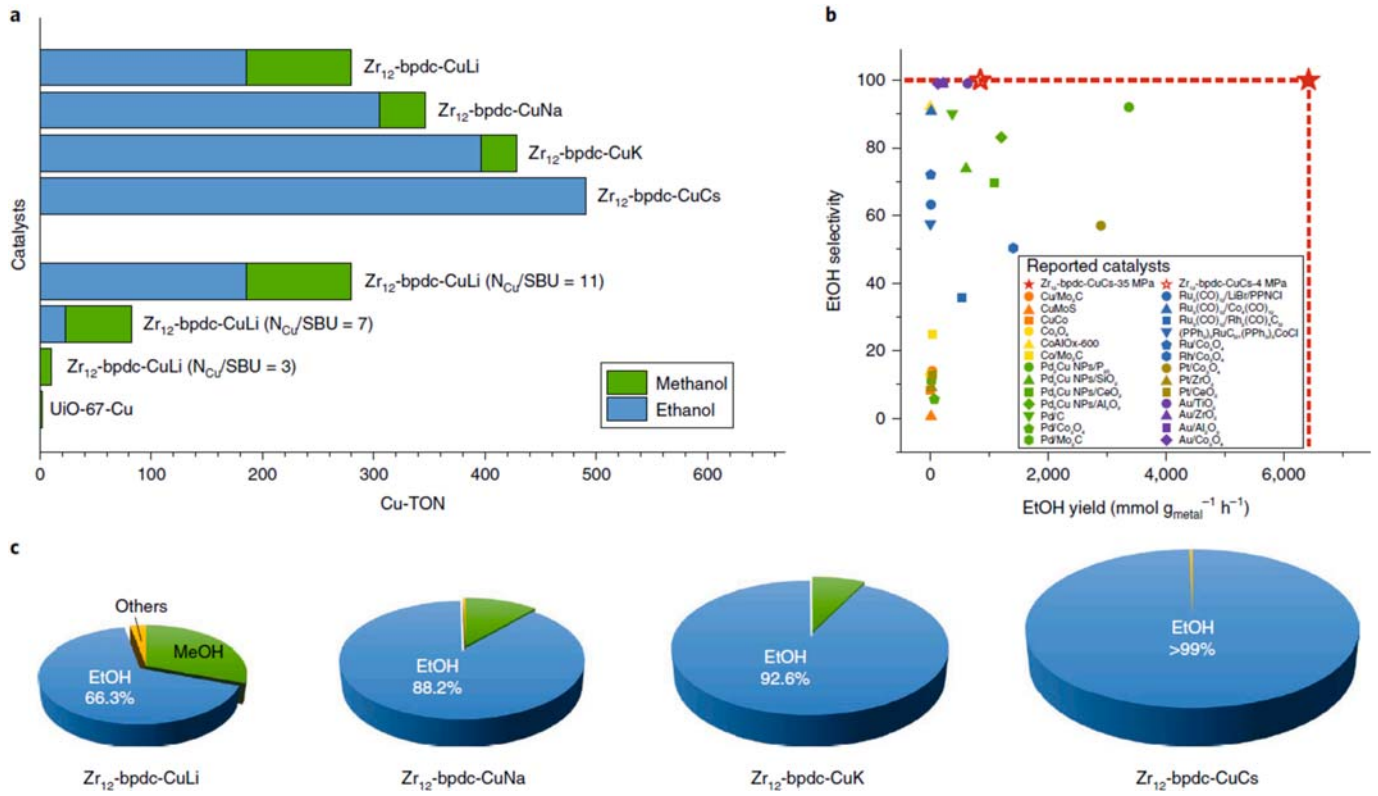

Fig. 6. Catalytic efficiency in the hydrogenation of CO_2: (a) – Alcohol production rates on diverse catalysts, expressed as the number of alcohol molecules produced per copper atom in a 10 h span. (b) – Comparative activity of different catalysts: ethanol yield calculated as CO_2 converted to ethanol per hour per gram of active metal. Conditions indicated by open red stars: H_2/CO_2 ratio of 3, pressure at 2 MPa, temperature set at 100 °C; filled red stars indicate conditions of 30 MPa CO_2, 5 MPa H_2, and temperature at 85 °C. (c) – Catalyst selectivity influenced by alkali metals: investigation into how catalyst selectivity changes when modified with various alkali metals. Reaction parameters include 10 mg of catalyst, H_2/CO_2 ratio of 3, pressure at 2 MPa, temperature of 100 °C, duration of 10 h, and 10 ml of anhydrous THF. Reprinted with permission from Ref. [111]. (For interpretation of the references to colour in this figure legend, the reader is referred to the web version of this article.)

growth capability, thereby enhancing the formation of ethanol within this specific reactor setup. In a recent study, Zhang et al. [117] investigated the synthesis of ethanol from CO_2 utilizing a range of $CoMoC_x$ catalysts. Among these, $CoMoC_x$-800 exhibited notable characteristics, demonstrating a high ethanol selectivity of 97.4 %. However, STY was relatively modest, reaching 0.528 mmol·g_{cat}^{-1}·h^{-1}. The experiments were conducted at 180 °C in dimethylformamide (DMF) solvent under a pressure of 20 bar. The solvent selection plays a critical role in influencing the catalytic performance within a batch reactor configuration. He et al. [119] conducted a study on CO_2 hydrogenation aiming to generate HA (C_2–C_4) using a 1 %Pt/Co_3O_4 catalyst, achieving a STY of 0.509 mmol·g_{cat}^{-1}·h^{-1} and a selectivity of 82.5 % at 140 °C, employing various solvents. They observed that polar solvents such as water, 1,3-dimethyl-2-imidazolidinone (DMI), and N-methyl-2-pyrrolidone (NMP) exhibited superior performance in alcohol synthesis. This enhanced performance could be attributed to solvent stabilization, potentially involving hydrogen bonding with alcoholic species.

Liu et al. [132] developed a series of Co-based catalysts derived from CoAl-CO_3^{2-} layered double hydroxides (LDHs) by tuning precipitation pH and reduction temperature, using water as the solvent to achieve varied reduction degrees and dispersions. By introducing the descriptor "fraction of reduced and surface-exposed Co ($F_{Co,r,s}$)", the authors successfully quantified the Co^0–Co^{2+} synergy, which is crucial for CO_2 hydrogenation to methane, methanol, and ethanol. They observed a volcano-shaped relationship between $F_{Co,r,s}$ and turnover frequencies (TOF), with the optimized catalyst (pH 8.5, 750 °C reduction) achieving a high CO_2 conversion rate of 26.8 mmol $g_{cat}^{-1}h^{-1}$ at 180 °C. Additionally, the same group [133] investigated the impact of Co-metal oxide interactions on CO_2 hydrogenation by calcining mixed CoAl hydroxide at various temperatures, using water as the reaction media. They found that a moderate Co-metal oxide interaction promotes a balanced Co^0–Co^{2+} synergy, enhancing CO_2 conversion via the HCOO intermediate at the Co^0–Co^{2+} interface. This optimized synergy results in high TOF for CO_2 conversion, with CH_4 selectivity exceeding 98 %, while methanol and ethanol are produced as minor byproducts.

2.3. *Nobel-metal catalysts with different promoters, supports, and solvents*

Noble metal catalysts such as Au, Rh, Pt, Ir, and Ru demonstrate superior catalytic performance in CO_2 hydrogenation to produce ethanol and HA. Table 1 provides a summary of the reported catalysts and their corresponding catalytic results. Rh-based catalysts garnered considerable attention for their ability to selectively synthesize ethanol from syngas [134–137]. Research suggests that these catalysts can facilitate both CO dissociation and CO insertion simultaneously through their atomically adjacent Rh^0 – Rh^{n+} species, leading to the generation of C_2 oxygenates such as ethanol, acetaldehyde, and acetic acid from syngas. Consequently, it is advisable to prioritize the investigation of Rh-based catalysts, known for their relatively high catalytic performance in ethanol and HA production via syngas, for CO_2 hydrogenation processes. Zheng et al. [121] reported on the remarkable performance of a Rh_1/$CeTiO_x$ single-atom catalyst, engineered by embedding monoatomic Rh onto a Ti-doped CeO_2 support (Fig. 10**I**). This catalyst exhibited exceptionally high ethanol selectivity (99.1 %) with a STY of 5.8 mmol·g_{cat}^{-1}·h^{-1} in a water solvent within a batch reactor. The outstanding catalytic efficacy is attributed to synergistic effects between Ti-doping and monoatomic Rh. Firstly, these effects facilitate the formation of

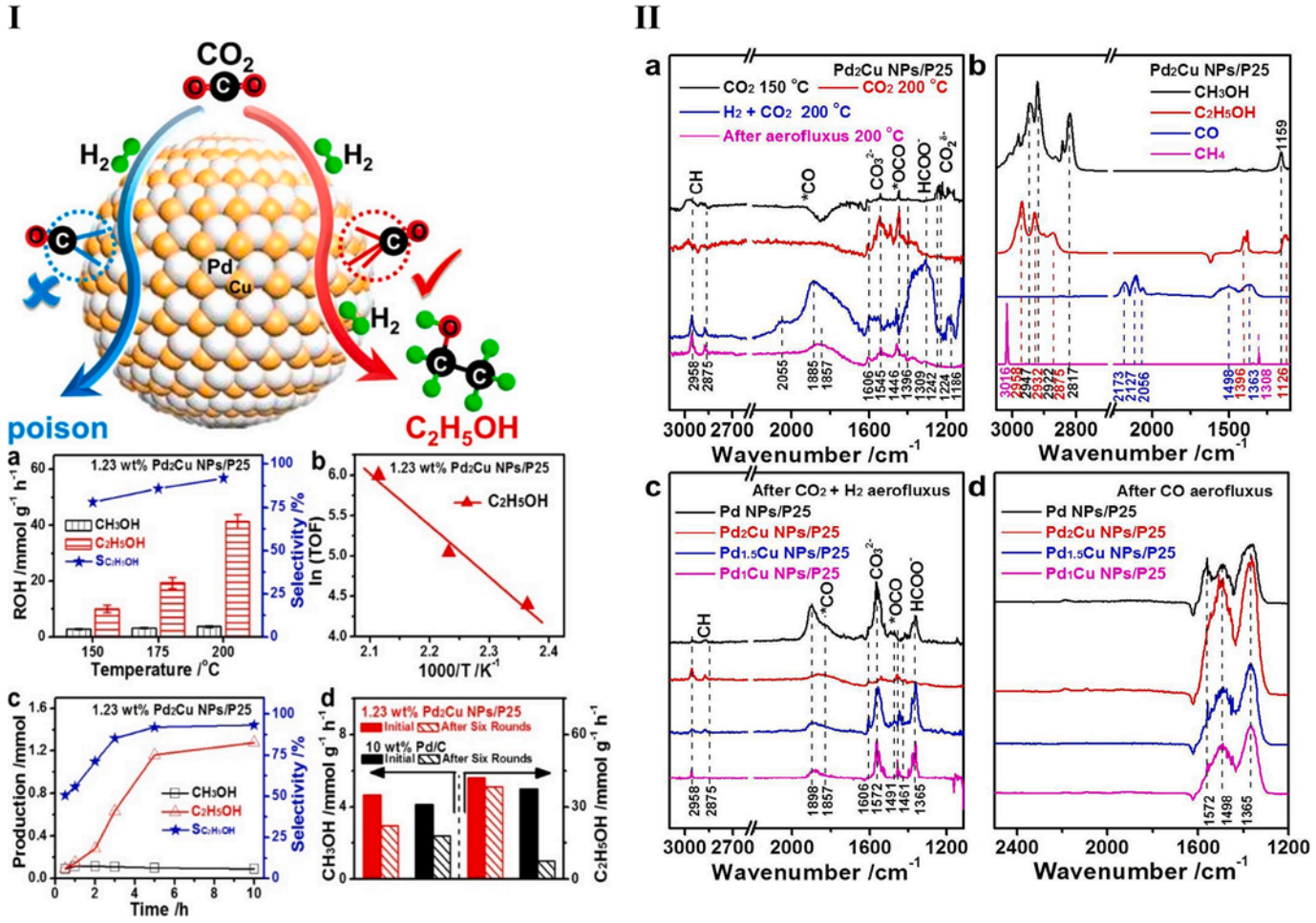

Fig. 7. I. (a) Achieved yields of ROHs and selectivity towards C_2H_5OH. (b) Arrhenius plot depicting C_2H_5OH production by 1.23 wt%Pd2Cu NPs/P25 at various temperatures over 5 h. (c) Time-course analysis of CO_2 hydrogenation catalyzed by 1.23 wt%Pd2Cu NPs/P25 at 200 °C. (d) Product yields obtained with 1.23 wt% Pd_2Cu NPs/P25 and 10 wt%Pd/C across six successive reaction cycles. II. (a) DRIFTS spectra of Pd2Cu NPs/P25 following exposure to CO_2 + Ar at 150 °C, and subsequent exposures to CO_2 + Ar, CO_2 + H_2 + Ar, and aeroflux with Ar at 200 °C. (b) Adsorption spectra post-exposure to CH_3OH, C_2H_5OH, CO, and CH_4 on Pd_2Cu NPs/P25. (c) DRIFTS spectra of Pd-based NPs/P25 after exposure to CO_2 + H_2 + Ar at 200 °C. (d) DRIFTS spectra of Pd-based NPs/P25 after exposure to CO + Ar aeroflux at 200 °C. Adapted with permission from Ref. [112].

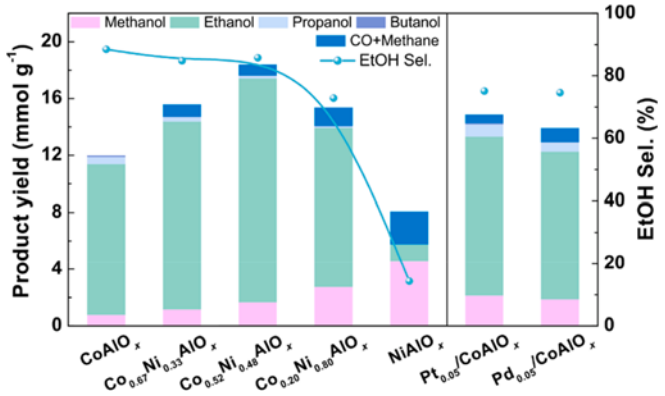

Fig. 8. The catalytic efficiency of $Co_mNi_nAlO_x$ catalysts in the hydrogenation of CO_2. Reaction parameters include: catalyst amount (25 mg), water volume (2 mL), initial pressure of 40 bar (H_2/CO_2 ratio of 3:1), reaction duration of 12 h, and temperature set at 200 °C. Adapted with permission from Ref. [115].

oxygen vacancies, generating oxygen-vacancy-Rh Lewis-acid-base pairs which enhance CO_2 adsorption and activation, cleavage of C − O bonds in CH_xOH* and COOH* into CH_x* and CO* species, followed by C − C coupling and hydrogenation into ethanol. Secondly, Ti-doping-induced crystal reconstruction generates strong Rh − O bonds, enhancing stability. Very recently, Zheng et al. [122] prepared a Rh/CN catalyst featuring Rh-N_4 sites via the pyrolysis of Rh-containing MOFs. Additionally, the authors designed the Rh/CNP catalyst with Rh-N_3P_1 sites by substituting phosphorus atoms into the atomically dispersed Rh-N_4 sites. These catalysts displayed distinct catalytic behaviors in CO_2 hydrogenation. The Rh/CN catalyst exhibited high selectivity towards methanol (91.3 %), while the Rh/CNP catalyst promoted ethanol production with a selectivity of 81.8 % and a TOF of 420.7 h^{-1} (Fig. 10**II**). This enhancement in ethanol formation and CO_2 conversion was attributed to the effective electron donation from the phosphorus atom, which weakened the C − O bond in CH_3OH*, facilitating its cleavage into CH_3*, and enabling the coupling between CO* and CH_3*.

Ye et al. [123] examined the impact of varying Ir content in the Ir − In_2O_3 catalyst, ranging from 0.2 to 1 wt%, under conditions of T = 200 °C, t = 5h, and an H_2/CO_2 ratio of 5. As the Ir content increased, both ethanol selectivity and STY experienced a consistent decrease, declining from 85.3 % (0.99 mmol·g_{cat}^{-1}·h^{-1}) to 5.7 % (0.13 mmol·g_{cat}^{-1}·h^{-1}) within the 0.2–1 wt% range. The increase in Ir loading led to the suppression of ethanol synthesis while promoting methanol production. Moreover, the transition from small-sized to agglomerated nanoparticles occurred as Ir loading increased from 0.5 to 1 wt%, resulting in reduced specific surface area and active sites, ultimately

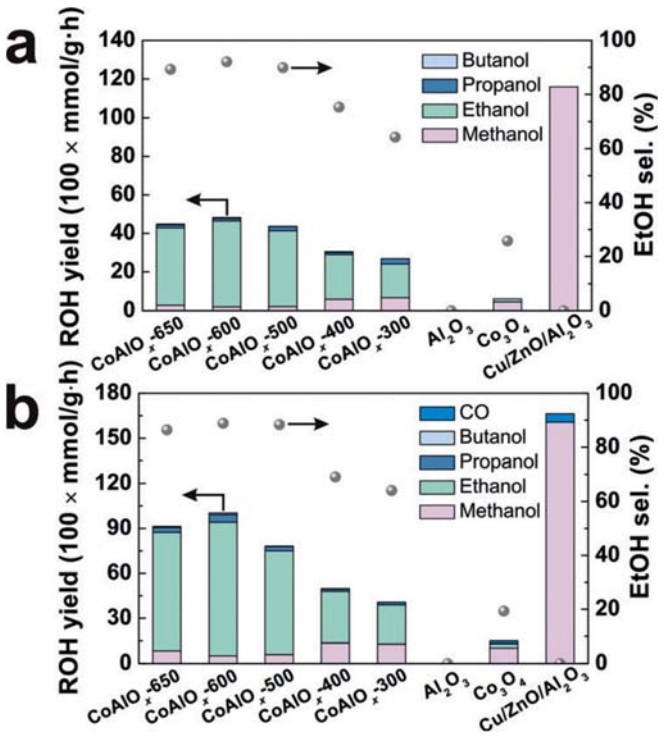

Fig. 9. The efficacy of different catalysts in the hydrogenation of CO_2. Reaction conditions are as follows: catalyst amount of 20 mg, water volume of 2 mL, initial pressure of 40 bar with a H_2/CO_2 ratio of 3:1, and reaction durations of 15 h at either 140 °C (a) or 200 °C (b). Adapted with permission from Ref. [118].

causing a decline in ethanol yield. This phenomenon was corroborated through SEM-EDX and TEM analysis. Wang et al. [120] conducted a study on the direct conversion of CO_2 to ethanol using Au nanoclusters supported on titania. Under the conditions of 200 °C temperature, 45 bar pressure for 10 h, they achieved an exceptional ethanol selectivity exceeding 99 %, along with a remarkable STY of 942.8 mmol $g_{Au}^{-1}h^{-1}$. This outstanding performance was attributed to the synergistic interaction between the Au nanoclusters and anatase-TiO_2 support. Various experiments were conducted to explore the factors influencing CO_2 hydrogenation, including solvent type, reaction temperature, H_2/CO_2 ratio, and Au loading. Among the different titania polymorphs tested – such as anatase (a), rutile (r), brookite (b), and amorphous (am), where anatase-TiO_2 emerged as the most effective support. This preference was rationalized based on the abundance of oxygen vacancies in the support, with anatase-TiO_2 exhibiting the highest number. Notably, solvent choice played a significant role in the direct synthesis of ethanol catalyzed by Au/a-TiO_2. Among the solvents tested, including NMP, cyclohexane, THF, water, and DMF, where DMF stood out as the most suitable solvent. Its superiority was attributed to unique advantages in facilitating CO_2 dissolution and enhancing interaction between CO_2 and the catalyst.

Yang et al. [124] delved into the catalytic properties of non-metallic gold clusters, namely $[Au_9(PPh_3)_8](NO_3)_3$ (referred to as Au_9), $[Au_{11}(PPh_3)_8Cl_2]Cl$ (referred to as Au_{11}), and $Au_{36}(TBBT)_{24}$ (referred to as Au_{36}; TBBT = 4-tert-butylbenzenethiol), showcasing their atomicity-dependent behavior in CO_2 hydrogenation processes. These clusters exhibit a remarkable capability to dictate the reaction pathways, steering towards either C_1 or C_2 products. Specifically, methane is predominantly produced on Au_9, ethanol on Au_{11}, and formic acid on Au_{36}. Au_{11} displays a selectivity of over 80 % for ethanol, a highly valued chemical, while Au_{36} achieves a selectivity of over 80 % for formic acid. Notably, the catalytic activity of these non-metallic gold clusters surpasses that of metallic nanoparticles by a factor of 10 to 70. Ye and colleagues [125] synthesized a bifunctional single-atom catalyst (SAC) designated as $K_{0.2}Rh_{0.2}/\beta$-Mo_2C. This catalyst exhibited an impressive ethanol selectivity of up to 72.1 % and STY of 33.7 μmol/g/h at a temperature of 150 °C. The study revealed that atomically dispersed Rh played a crucial role in forming bifunctional active sites when combined with the active carrier β-Mo_2C nanowires, thereby inducing synergistic effects that facilitated highly specific controlled C–C coupling reactions. Furthermore, the introduction of K was observed to enhance CO_2 adsorption and activation, effectively regulating the balanced performance of the two active centers and thereby improving hydrogenation selectivity. Finally, Cui et al. [126] conducted a study to investigate the synthesis of $C_{2+}OH$ from CO_2 hydrogenation using a $Ru_3(CO)_{12}$–$Co_4(CO)_{12}$ bimetallic catalyst along with bis(triphenylphosphoranylidene)ammonium chloride (PPNCl) as the cocatalyst and LiBr as the promoter in a 16 mL Teflon-lined stainless steel reactor. The authors explored the efficiency of this system in producing methanol, ethanol (STY = 29.5 mmol/L/h), propanol, and isobutanol under mild conditions. Through experimentation, they found that the combination of PPNCl and LiBr significantly improved the overall performance of the catalytic system compared to previously reported iodide-promoted systems. They observed that LiBr enhanced the activity of the catalyst while PPNCl improved selectivity, resulting in high levels of both activity and selectivity when used together. Additionally, it was demonstrated that the catalyst could be reused for at least five cycles without a noticeable decline in performance.

3. Catalysts in fixed-bed reactors

This section meticulously analyzes the previously mentioned catalytic formulations, offering valuable insights into how the choice of supports and catalyst structure influences performance in a fixed-bed reactor. As a result, CO_2-to-ethanol and HA catalysts are systematically classified into four groups: Cu-based catalysts, Co-based catalysts, Fe-based catalysts, and noble-metal-based catalysts (Ru, Rh, Pd, and Pt), each contributing unique advancements in catalytic efficiency. These encompass transition-based systems including Cu, Co, Fe, and bimetallic configurations, mono-metallic, multimetallic/multifunctional catalysts, as well as perovskite- and zeolite-based catalysts.

3.1. Cu-based catalysts with different promoters and supports

Catalysts based on modified copper found extensive application in HA synthesis from syngas within fixed-bed reactors [108,138–141]. Copper-based catalysts, including Cu-ZnO [72], Cu-ZrO_2 [142], and Cu-ZnO-ZrO_2 [143] are commonly employed for methanol synthesis. The Cu-ZnO-ZrO_2 catalyst demonstrates enhanced catalytic activity relative to Cu-ZnO and Cu-ZrO_2 catalysts, particularly at lower temperatures (180 to 240 °C), attributed to the ZrO_2 support's weak hydrophilic nature, which helps alleviate the poisoning effect of water on active sites during methanol synthesis [144]. Cu is acknowledged to favour non-dissociative hydrogenation of the $C(H_x)O$ bond, yielding alcohols, but with the introduction of other sites or promoters facilitating CH_x species formation, C_{2+} alcohols may form via CH_x–$C(H_x)O$ coupling through direct C–O dissociation or H-assisted C–O dissociation [108,145]. According to extensive research (Table 2), the approaches can be categorized into two strategies: (1) utilizing alkali-modified Cu-based catalysts featuring an H_xCO–H_xCO coupling chain-growth mechanism, and (2) employing FTS (Fe and Co) elements-modified Cu-based catalysts operating with an H_xC–H_xC coupling chain-growth mechanism [5].

Takagawa et al. [146] discovered 26 years ago that a K/Cu-Zn-Fe oxide catalyst is highly effective for synthesizing ethanol through the catalytic hydrogenation of CO_2. Under specific conditions of 7.0 MPa pressure, a GHSV of 5 000, and a H_2/CO_2 ratio of 3 in the feed, the catalyst exhibited an ethanol selectivity of 20 %, coupled with a CO_2 conversion rate of 44 %. Notably, an ethanol STY of 290 $g/L_{cat}/h$ was achieved at a GHSV of 20 000. Additionally, the introduction of Cr

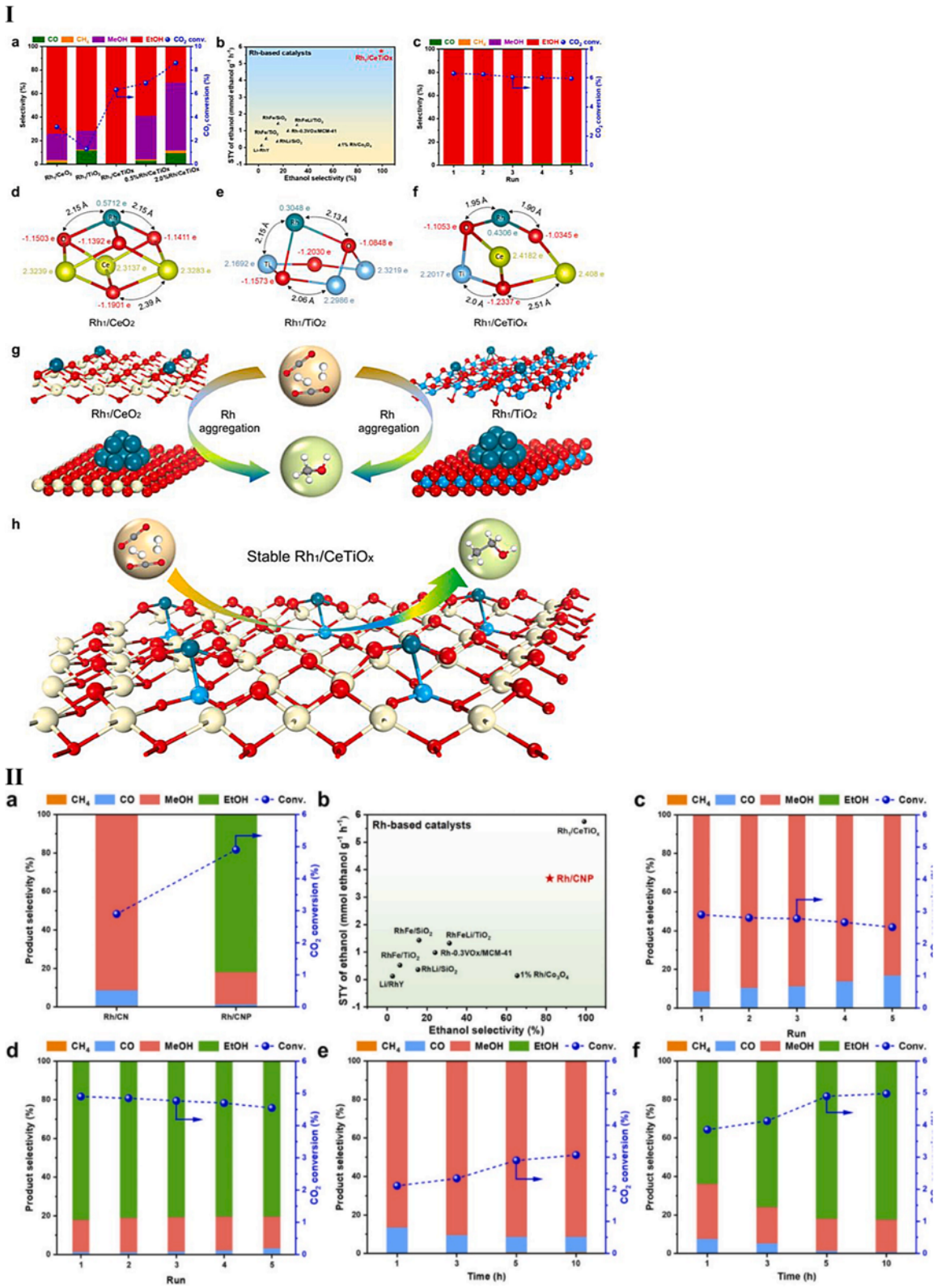

Fig. 10. I – a) Comparative analysis of activity and selectivity (based on carbon mole numbers) among various catalysts. Reaction conditions: catalyst mass of 30 mg, water volume of 20 mL, temperature at 250 °C, initial pressure of 3.0 MPa (H_2/CO_2 = 3), duration of 5 h, stirring at 400 rpm. b) Comparison of the STY of ethanol achieved in this study with other Rh-based catalysts reported in the literature. c) Recycling test of synthesized $Rh_1/CeTiO_x$ catalyst over five 5 h runs under conditions described in (a). d-f) Optimized structures depicting Rh atom dispersion on CeO_2 (d), TiO_2 (e), and $CeTiO_x$ (f) surfaces. g-h) Schematic representation of the reaction process for long-term stability testing in CO_2 hydrogenation to ethanol using single-atom Rh supported on CeO_2 (g), TiO_2 (h). Adapted with permission from Ref. [121]. II – a) Comparative analysis of activity and selectivity between Rh/CN and Rh/CNP catalysts. Reaction conditions: catalyst amount of 30 mg, water volume of 20 mL, temperature of 250 °C, initial pressure of 3.0 MPa (H_2/CO_2 = 3/1), duration of 5 h, stirring at 400 rpm. b) Comparison of the STY of ethanol achieved in this study with other Rh-based catalysts reported in the literature. c-d) Recycling tests of Rh/CN (c) and Rh/CNP (d) catalysts over five 5 h runs, examining product selectivity and CO_2 conversion over time. Reaction conditions are identical to those described in (a). Adapted with permission from Ref. [122].

Table 2
The catalytic performance and reaction conditions of heterogenous Cu-based catalysts in CO_2 thermocatalytic hydrogenation to EtOH and/or $C_{2+}OH$ in a continuous fixed-bed reactor.

Catalyst	Catalytic performance			Reaction conditions					Ref.
	STY_{EtOH} or $C_{2+}OH$ $mmol{\cdot}g_{cat}^{-1}{\cdot}h^{-1}$	X_{CO2} (%)	S_{EtOH} or $C_{2+}OH$(%)	T (°C)	P (bar)	GHSV (h^{-1})	H_2/CO_2	TOS (h)	
Cu@Na − Beta	8.64	14.0	100	300	21	12,000	3	100	[147]
CuZnAl/K-CuMgZnFe	2.24	42.3	90.0	320	50	N.A.	3	60	[148]
Cs-$Cu_{0.8}Fe_{1.0}Zn_{1.0}$	1.47	36.6	19.8	330	50	N.A.	3	30	[149]
4.6 K-CuMgZnFe	1.47	30.4	15.7	320	50	N.A.	3	N.A.	[150]
Cu-CoGa-0.4	1.35	17.8	23.8	220	30	6000 mL/g/h	3	3	[151]
CuFeZn-0.7PDA	1.26	10.6	N.A.	310	40	7200	3	96	[152]
$CuZnFe_{0.5}K_{0.15}$	2.84 mmol/mL	32.4	11.8	350	60	5000	3	N.A.	[153]
Cu	0.002	N.A.	84.0	190	1	9000	1	N.A.	[154]
K/Cu-Zn-Fe	290 $g/L_{cat}/h$	44	20.0	300	70	5000	3	500	[146]
CuNaFe	153 $mg/g_{cat}/h$	32.3	10	310	30	28800 mL/g/h	3	38	[155]
PDA/CuFeZn-N450	55.9 $mg/mL_{cat}/h$	7.2	39.8	320	40	N.A.	3	264	[156]
$(KP)_{0.1}$CuFeZn	53.8 $mg/mL_{cat}/h$	38.1	14.7	320	40	7200	3	N.A.	[157]
0.6S − KCuFeZn	50.7 $mg/g_{cat}/h$	36.1	22.9	320	50	3000 mL/g/h	3	35	[158]
0.6S-KCuFeZn/CuZnAlZr	173.9 $mg/g_{cat}/h$	36.6	18.2			12000 mL/g/h			

N.A. means that the data is not available in the reference.

significantly reduced catalyst deactivation, thereby enhancing its practical utility. Overall, the K/Cu-Zn-Fe-Cr oxide catalyst was deemed advantageous for industrial applications. Exceptionally high selectivity (100 % for EtOH) was reported by Ding et al. [147]. The authors utilized 8.24 wt% Cu modified Na-Beta zeolite in a fixed-bed reactor system.

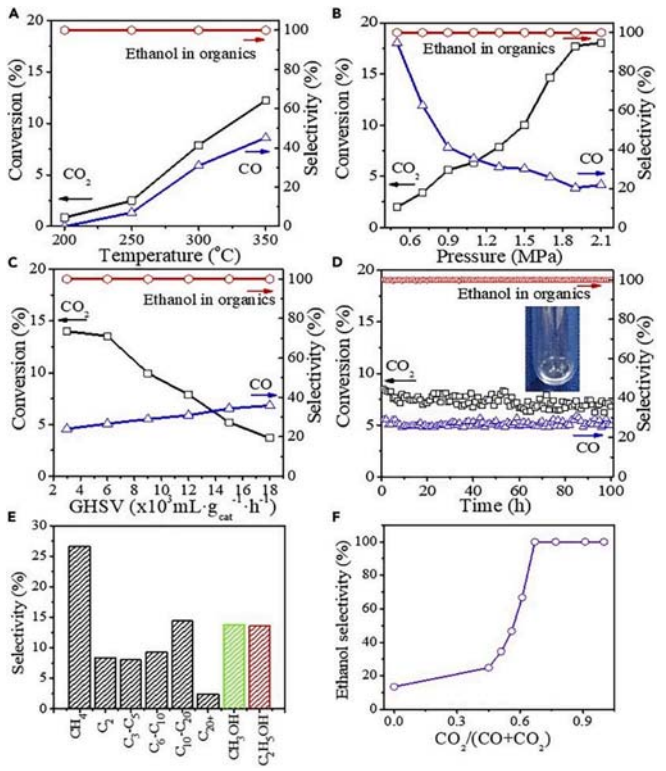

Fig. 11. Catalytic performance of the Cu@Na-Beta catalyst: (A) Evaluating the impact of varying reaction temperatures (12 000 $mL{\cdot}g_{cat}^{-1}{\cdot}h^{-1}$; 1.3 MPa; $CO_2 + 3H_2$). (B) Exploring the influence of different reaction pressures (12000 $mL{\cdot}g_{cat}^{-1}{\cdot}h^{-1}$; 300 °C; $CO_2 + 3H_2$). (C) Investigating the effect of space velocity (1.3 MPa; 300 °C; $CO_2 + 3H_2$) (D) Long-term reaction stability test (300 °C; 1.3 MPa; 12000 $mL{\cdot}g_{cat}^{-1}{\cdot}h^{-1}$; $CO_2 + 3H_2$. Inset: collection of products by a condenser during the initial 24 h period. (E) Analysis of product selectivities for syngas conversion (1.5 MPa; 12000 $mL{\cdot}g_{cat}^{-1}{\cdot}h^{-1}$; 300 °C; $CO + 2H_2$). (F) Assessment of ethanol selectivity in organic products using a blend of CO, CO_2, and H_2 as reactants (1.5 MPa; 12 000 $mL{\cdot}g_{cat}^{-1}{\cdot}h^{-1}$; 300 °C). Reprinted with permission from Ref. [147].

They reported remarkable stability, even after 100 h of time on stream (Fig. 11**D**). The selectivity remained at 100 % even if the feed stream contained up to 30 % of carbon monoxide. As the reaction temperature rises from 200 °C to 350 °C, the CO_2 conversion rate escalates from 0.85 % to 12.2 %. At 250 °C, CO emerges as a byproduct, with its selectivity increasing to 45.2 % as the temperature further climbs to 350 °C (Fig. 11**A**), while ethanol remains the sole organic product. The pressure significantly impacts catalyst performance. With pressure varying from 0.5 to 2.1 MPa (at 300 °C), CO_2 conversion notably surges from 2.0 % to 18 %, accompanied by a decrease in CO selectivity from 94.6 % to 21 % (Fig. 11**B**). Remarkably, ethanol remains the exclusive organic product observed during the reaction tests. As the space velocity escalates from 6000 to 18000, CO_2 conversion diminishes from 13.5 % to 3.7 %, while CO selectivity increases from 26.9 % to 35.9 % (Fig. 11**C**). The ethanol yield in a single pass was achieved ≈14 % at 300 °C, ≈12000 $mL/g_{cat}{\cdot}h$, and 21 bar, corresponding to a STY of ≈398 $mg/g_{cat}{\cdot}h$ or 8.64 $mmol{\cdot}g_{cat}^{-1}{\cdot}h^{-1}$.

Xu et al. [148] examined the impact of different reactor filling configurations of CuZnAl/K-CuMgZnFe catalysts on catalytic performance (Table 2). Their results indicated that utilizing the powder mixing mode resulted in the highest CO_2 conversion (42.3 %), HA selectivity (90 %), and STY (2.24 $mmol{\cdot}g_{cat}^{-1}{\cdot}h^{-1}$). Conversely, excessive proximity between the catalysts, as achieved through mortar mixing, led to decreased catalytic activity. This decline was attributed to the presence of the K promoter in the K-CuMgZnFe catalyst, which, when excessively close, could inhibit the CuZnAl oxide. Therefore, selecting an appropriate mixing mode is essential for optimizing the performance of both catalysts. The same group synthesized the Cs-$Cu_{0.8}Fe_{1.0}Zn_{1.0}$ [149] and 4.6 %K-CuMgZnFe [150] active catalysts with STY of 1.47 $mmol{\cdot}g_{cat}^{-1}{\cdot}h^{-1}$ in both cases. The authors [151] successfully fabricated a series of CuCo-based catalysts for the hydrogenation of CO_2 to ethanol using single-source CuCoGaAl layered double hydroxides precursors. Particularly, they found that the Cu-CoGa-0.4 catalyst with a Ga:Co molar ratio of 0.4 exhibited promising results, achieving a high ethanol selectivity of 23.8 % at a conversion rate of 17.8 %. Additionally, this catalyst showed a STY value of 1.35 $mmol_{EtOH}{\cdot}g_{cat}^{-1}{\cdot}h^{-1}$. The authors attributed these enhanced catalytic properties to the introduction of Ga, which strengthened the interaction between Cu and Co species and regulated the electronic structures of Cu and Co. This led to the formation of abundant interfacial structures like Cu-$CoGaO_x$ and Cu^+-$CoGaO_x$, ultimately improving the catalyst's performance in CO_2 hydrogenation to ethanol.

Yang et al. [152] successfully prepared N-doped CuFeZn catalysts using 2,6-pyridine dicarboxylic acid (PDA) as the organic ligand via a co-current co-precipitation method. The optimized catalyst, CuFeZn-

0.7PDA, demonstrated excellent catalytic performance, achieving a total alcohols selectivity of 34.8 % at a CO_2 conversion rate of 10.6 %. Furthermore, it exhibited a high $C_{2+}OH/ROH$ fraction of 95.3 % and a remarkable C_{2+} alcohols STY of 1.26 $mmol \cdot g_{cat}^{-1} \cdot h^{-1}$. Through the characterization of the catalysts and their catalytic performance for CO_2 hydrogenation, the authors discovered that the enhanced catalytic performance can be attributed to the coordination between PDA and active metal ions. This coordination facilitates electron transfer and the reduction of metallic oxides, leading to the uniform dispersion of active components within the catalyst.

The authors [153] developed a two-stage bed catalyst system for synthesizing HA from CO_2 hydrogenation. They investigated the roles of K_2O and ZnO promoters in Cu-based catalysts and found that K_2O improves the interaction between CuO and ZnO, while ZnO acts as a support for promoting the dispersion of copper species. It was optimized the loading mode and volume ratio of the catalyst combination system and identified the $CuZnK_{0.15}(1.5)//Cu_{25}Fe_{22}Co_3K_3(4.5)$ combination as effective for synthesizing HA from CO_2 hydrogenation, benefiting from thermal and product conversion coupling effects between the catalysts.

Recently, the authors [154] drawing inspiration from CO_2 electroreduction findings, demonstrated that ethanol synthesis can occur at atmospheric pressure using metallic Cu catalysts in CO_2 hydrogenation with water steam ($CO_2 + H_2 + H_2O$), achieving a selectivity of 84 % and a productivity of approximately 0.002 $mmol \cdot g_{cat}^{-1} \cdot h^{-1}$ at 190 °C. Interestingly, similar trends were observed even when only water steam (without H_2) was utilized. This study marks the first reported instance of ethanol synthesis at atmospheric pressure using only CO_2 and water as reactants in a thermocatalytic process. Despite the low ethanol productivity and catalyst stability observed, this research offers novel avenues for future investigations in CO_2 hydrogenation. The authors suggest that enhancing water content may lead to higher selectivity towards other HA. Additionally, they propose utilizing a feed gas mixture of CO_2, H_2, and H_2O over catalysts more resilient to water reduction, such as copper supported in oxides or multi-metallic materials, to achieve improved catalyst stability and simultaneous enhancement in carbon–metal strengthening through water enhancement.

Si et al. [155] achieved successful fabrication of a highly active CuNaFe catalyst using a self-made physical sputtering method for CO_2 hydrogenation. This catalyst demonstrates the ability to efficiently catalyze the reaction, resulting in the production of high-value olefins and ethanol. The sputtering of Cu onto NaFe facilitates a highly active Cu − Na − Fe coordination, leading to the formation of metallic Cu surrounding Fe_5C_2 active sites in a CO_2 hydrogenation environment. This sputtered Cu enhances CO_2 adsorption, promotes Fe reduction, and facilitates subsequent carbonization during CO_2 hydrogenation, ultimately resulting in the formation of more active Fe_5C_2 sites.

Jia and colleagues [156] investigated nitrogen-doped CuFeZn catalysts to address challenges in HA selectivity and catalyst stability, synthesizing them by calcination in a N_2 atmosphere using 2,6-pyridine dicarboxylic acid (PDA) as a nitrogen source. The optimal catalyst (PDA/CuFeZn-N450) demonstrated a high C_{2+} alcohol selectivity of 39.8 % and maintained stability for 264 h, with nitrogen doping and oxygen vacancies playing key roles in enhancing stability. However, potential deactivation due to metal sintering and migration of active species was noted as a limiting factor. Very recently, the same group [157] successfully modified CuFeZn catalysts with different amounts of K_3PO_4, achieving enhanced catalytic performance, with the $(KP)_{0.1}$CuFeZn catalyst demonstrating 15.8 % total alcohol selectivity at 38.1 % CO_2 conversion. They found a linear relationship between the proportions of Fe^{2+}, Cu^0, and medium base to the STY of $C_{2+}OH$, highlighting that the Cu^0 phase has the most significant impact. The introduction of K_3PO_4 reduces Fe^{2+} while increasing $Cu^+/(Cu^+ + Cu^0)$, thereby promoting C–C coupling and improving $C_{2+}OH$ synthesis, while Fe_3C or Fe_3O_4 formation negatively affects catalyst stability. At the same time, Wang et al. [158] conducted an investigation into the effects of sulfate modification on a CuFe-based catalyst for HA synthesis from CO_2 hydrogenation. Their research revealed that sulfate modification enhances the catalyst's CO_2 conversion activity, reaching peak HA activity when the KCuFeZn catalyst is modified with an optimal sulfate concentration (0.6 wt%). They observed that sulfate modification facilitates the reduction of CuFe oxides while also controlling the growth of Cu particles during the reduction process. Furthermore, they found that sulfate modification, when applied in the correct amount, can regulate the activation behavior of CO dissociation/nondissociation, thus improving hydrogenation capacity and enhancing the HA performance of CuFe-based catalysts.

3.2. Co-based catalysts with different promoters and supports

Co is a traditional component in Fischer-Tropsch synthesis and found extensive use in the conversion of CO or CO_2-based Fischer-Tropsch synthesis to hydrocarbons [128]. Despite its historically limited performance in the RWGS reaction, Co demonstrates robust hydrogenation capabilities (Table 3). Consequently, its primary role in CO_2 hydrogenation is often as a catalyst for methanation [5]. Okabe et al. [159] first reported and successfully synthesized highly dispersed Co-based catalysts supported on SiO_2 using acetate and utilized them for the hydrogenation of CO_2 to alcohols. By incorporating a small quantity of Ir into the catalyst, the authors significantly enhanced its catalytic activity. Remarkably, methanol was produced at a yield of approximately 20 %, which is higher compared to Co-based catalysts derived from nitrate precursors. Additionally, the selectivity towards ethanol was increased to 7.9 % by introducing Na salt into the Ir/Co-based catalyst supported on SiO_2. Witoon et al. [160] synthesized and examined K-Co supported on In_2O_3 catalysts for the CO_2 hydrogenation process to produce HA. They initially prepared pure In_2O_3 as a catalyst, observing its activity in transforming CO_2 to CO without CO dissociation. Following this, they decorated In_2O_3 with either K or Co separately, but found no significant improvement in HA formation. However, they proceeded to combine K and Co with In_2O_3, which resulted in a notable enhancement in HA production. The authors optimized the K-Co-In_2O_3 catalyst (Fig. 12**I**) and evaluated its catalytic performance, achieving the highest STY (3.73 $mmol \cdot g_{cat}^{-1} \cdot h^{-1}$) and distributions of HA (57.9 %) with exceptional stability over a prolonged period of operation (200 h). They attributed this improved performance to the formation of K-O-Co sites on the catalyst surface, which enhanced the interaction of H_2 with the catalyst and suppressed the hydrogenation of alkyl species, thus promoting the formation of HA from CO_2.

Lage et al. [161] synthesized a K-Co-Cu-Al catalyst via a coprecipitation method, exploring various Co to Cu ratios, reduction temperatures, and reaction conditions including temperature, space velocity, and H_2/CO_2 ratio to optimize its efficiency (Fig. 12**II**). They determined that the catalyst composition $Co_{1.8}Cu_{0.9}AlO_x$, containing 1 wt% K and reduced at 400 °C, exhibited outstanding performance. This specific catalyst configuration achieved a notable selectivity of 44.8 % for HA, with ethanol contributing 20.8 % to the overall selectivity. Moreover, it displayed a significant STY of 3.08 $mmol \cdot g_{cat}^{-1} \cdot h^{-1}$ of ethanol under mild operating conditions. These findings establish the catalyst as one of the top performers among Co-based catalysts, showcasing its potential for enhanced alcohol synthesis.

Zhang and co-authors [168] conducted research on Co-catalyzed CO_2 hydrogenation, exploring various supports including Al_2O_3, ZnO, AC, TiO_2, SiO_2, and Si_3N_4. Their investigation revealed that inert supports such as SiO_2 and Si_3N_4 effectively stabilized Co_2C in environments containing carbon, thereby providing active sites for ethanol and HA. Notably, Na–Co/SiO_2 demonstrated relatively high catalytic activity, achieving a CO_2 conversion rate of 18.8 %, a selectivity of 8.7 % towards C_{2+} alcohols, and an 87.5 % fraction of $C_{2+}OH$. Later, the same authors [163] achieved stable Na–Co_2C active sites by fine-tuning the interaction between Na and Co species. By enhancing the interaction of Na with Co_2C, resulting in the formation of Na–Co bonds, the authors facilitated the dispersion of Co_2C and reduction of particle size. This adjustment

Table 3
The catalytic performance and reaction conditions of heterogenous Co-based catalysts in CO_2 thermocatalytic hydrogenation to EtOH and/or $C_{2+}OH$ in a continuous fixed-bed reactor.

Catalyst	Catalytic performance			Reaction conditions					Ref.
	STY_{EtOH} or $C_{2+}OH$ $mmol \cdot g_{cat}^{-1} \cdot h^{-1}$	X_{CO2} (%)	S_{EtOH} or $C_{2+}OH$(%)	T (°C)	P (bar)	GHSV (h^{-1})	H_2/CO_2	TOS (h)	
$2.5K5Co\text{-}In_2O_3$	3.73	36.6	57.9	380	40	N.A.	3	200	[160]
1 $K/Co_{1.8}Cu_{0.9}AlO_x$	3.08 (5.54)	12.2	20.8 (44.8)	250	30	14,200	1.5	6	[161]
Co_2C and CuZnAl	2.2	21.2	18.3	250	50	12,000	3	N.A.	[82]
Cu/Co_3O_4	1.87	13.9	15.2	250	30	N.A.	3	N.A.	[162]
$2Na\text{-}Co/SiO_2$	1.1	53.2	6.8	310	50	N.A.	3	N.A.	[163]
CoMoS	0.6	28.0	4.2	310	104	0.6 kg/kg/h	3	N.A.	[164]
Na-CuCo-9	80.8 $mg/g_{cat}/h$	20.1	26.8	330	40	5000 mL/g/h	1	48	[165]
$CoGa_{1.0}Al_{1.0}O_4/SiO_2$	N.A.	4.8	20.1	270	30	3000	3	N.A.	[166]
$Co/La_4Ga_2O_9$	N.A.	4.6	35.0	270	35	3000	3	45	[167]
$Na\text{-}Co/SiO_2$	N.A.	18	62.8	250	50	4000	3	300	[168]
$Mo_1Co_1K_{0.8}$-S	N.A.	12.6	10.9	320	120	3000 mL/g/h	3	20	[169,170]
$Ir/Co(A)\text{–}Na_2O/SiO_2$	7.9 $g \cdot dm^{-3} \cdot h^{-1}$	7.6	8.0	220	21	2000	3	6	[159]

N.A. means that the data is not available in the reference.

notably enhanced the rate of the RWGS reaction and the selectivity to ethanol, leading to a significant increase in the ethanol STY. Optimal results were attained with a moderate interaction achieved at 2 wt% Na, where the ethanol STY reached an impressive 1.1 $mmol \cdot g_{cat}^{-1} \cdot h^{-1}$, representing a tenfold increase compared to the catalyst without Na. The same group [82] recently investigated the intricate reaction pathways occurring on Co_2C and CuZnAl multifunctional tandem catalysts by strategically designing surface adsorption – desorption reactions, conducting in situ chemical transient kinetics experiments, and employing theoretical calculations. These multifunctional tandem catalysts demonstrated a notable STY of $C_{2+}OH$, reaching 2.2 $mmol \cdot g_{cat}^{-1} \cdot h^{-1}$. Besides, Yang et al. [162] successfully synthesized Co_3O_4 nanorods characterized by low reducibility and high activity in the RWGS reaction. Catalysts consisting of Cu supported on Co_3O_4 nanorods exhibited a CO_2 conversion rate of 13.9 %, accompanied by an ethanol yield of 1.87 $mmol \cdot g_{cat}^{-1} \cdot h^{-1}$. Retaining the partial reduction of Co_3O_4 to Co is identified as a pivotal characteristic of the catalyst for yielding HA. Moreover, leveraging the strong metal-support interaction between Co and its supports to prevent excessive reduction and stabilize active Co centers represents a promising strategy in catalyst design. Nieskens et al. [164] reported a relatively modest ethanol selectivity of 4.2 % and a STY of 0.6 $mmol \cdot g_{cat}^{-1} \cdot h^{-1}$ over CoMoS catalysts at 340 °C under a pressure of 10.4 MPa.

Very recently Irshad and co-authors [165] demonstrated that a Na-promoted Co–Cu bimetallic tandem catalyst can achieve an unprecedentedly high STY (80.8 $mg \cdot g_{cat}^{-1} \cdot h^{-1}$) of $C_{3+}OH$. The initial restructuring of the catalyst morphology during the initial period of CO_2 hydrogenation led to the migration of Co nanoparticles to the outermost surface of the dendritic Cu substrate. Furthermore, the Cu–Co catalyst exhibited exceptional stability up to 1000 h by effectively suppressing re-oxidation and carbon deposition. The authors observed a process of segregation where Cu and Co domains separated, with Co migrating towards the periphery and accumulating at the outer surface throughout CO_2 hydrogenation, as illustrated in Fig. 13. This restructuring of the catalyst persisted until Co particles became adorned on stabilized Cu domains, leading to an increase in Co particle size from 6 nm after 36 h to 15–20 nm after 200 h. Interestingly, the size of Co particles remained stable for up to 1000 h. The initial 200 h period of CO_2 hydrogenation exhibited a restructuring phase, akin to an "induction" period, during which the catalyst underwent significant changes. Consequently, the initial decline in CO_2 conversion rates can be attributed to the reduction in active catalytic surface area due to sintering. Upon close examination of the spent catalyst after 1000 h, both Cu^0 and Cu_2O phases were observed within the Cu phase.

An et al. [166] developed a Co-based catalyst supported with Ga, derived from a Co-Al-O spinel precursor, aimed at enhancing synergistic catalysis for the conversion of CO_2 to ethanol. By adjusting the ratio of Ga to Al in the catalysts, they found that $Co^0 - Co^{\delta+}$ active sites were preferentially formed with an optimal $Co^0/Co^{\delta+}$ ratio due to variations in the interaction between Co-Ga and Co-Al species. The selectivity of ethanol reached 20.1 % over the reduced $CoGa_{1.0}Al_{1.0}O_4/SiO_2$ catalyst at 270 °C and 3.0 MPa. Characterization results indicate that the strong interaction between Ga oxide and cobalt induced the formation of $Co^0 - Co^{\delta+}$ active pairs, thereby promoting the process of ethanol synthesis. A series of composite materials based on Mo–Co–K sulfide were successfully synthesized via a straightforward co-precipitation and stepwise impregnation techniques [169,170]. By optimizing the K/Mo molar ratio within the range of 0.3–1.2, maintaining a Co/Mo molar ratio of 1.0, and controlling reaction conditions appropriately, the $Mo_1Co_xK_y$ sulfide catalyst demonstrated promising potential for producing C_{2+} alcohols through CO_2 hydrogenation. Activated carbon was identified as a potent promoter for $Mo_1Co_xK_y$, surpassing the effects of SiO_2, Al_2O_3, and TiO_2. The inclusion of activated carbon enhanced the interaction between Mo and Co, elevated the Mo^{4+} content on the catalyst's surface, and influenced its adsorption capacity and strength for CO_2 and H_2.

3.3. Fe-based catalysts with different promoters and supports

Fe-based catalysts are recognized for their efficiency in CO_2 conversion and the formation of C–C bonds [1,36]. Notably, FeK oxides employed in Fischer-Tropsch synthesis were effective in converting CO_2 into hydrocarbons, CO, and alcohols [171–180]. Therefore, incorporating Fe into a CuZnK catalyst is expected to enhance the production of ethanol and HA (Table 4). Indeed, Li and colleagues [181] shown that incorporating Fe promoter into the K/Cu–Zn catalyst has a significant impact on both its microstructure and performance in the synthesis of HA from CO_2 hydrogenation. By adding a moderate concentration of Fe promoter to the K/Cu–Zn catalyst, the interaction between Cu and Fe is improved, which aids in the dispersion and reduction of CuO and $CuFe_2O_4$ spinel. This facilitates the production of CO through the RWGS reaction. Moreover, it enhances the interaction between Zn and Fe, resulting in the dispersion and reduction of $ZnFe_2O_4$ spinel, thus promoting the conversion of CO through CO hydrogenation. The combined effect of Cu–Fe and Zn–Fe interactions improves the catalyst reduction process, leading to an increase in the amount of dispersed Cu and Fe carbide species. Consequently, this enhances the selectivity towards HA and boosts the catalytic activity of CO_2 hydrogenation.

A recent breakthrough by Zhang et al. [182] introduces a novel K-CuZnAl/Zr(0.03)-CuFe composite catalyst, showcasing exceptional performance in converting CO_2 into ethanol and HA. Operating at 320 °C, 4 MPa, and a space velocity of 6000 mL $g_{cat}^{-1}h^{-1}$, the catalyst achieves a CO_2 conversion of 40.6 % and a $C_{2+}OH$ selectivity of 22.4 %, with CO selectivity as low as 10.3 % and sustained for at least 200 h (Fig. 14**I**). Scaling up the space velocity to 24000 mL $g_{cat}^{-1}h^{-1}$ raises the

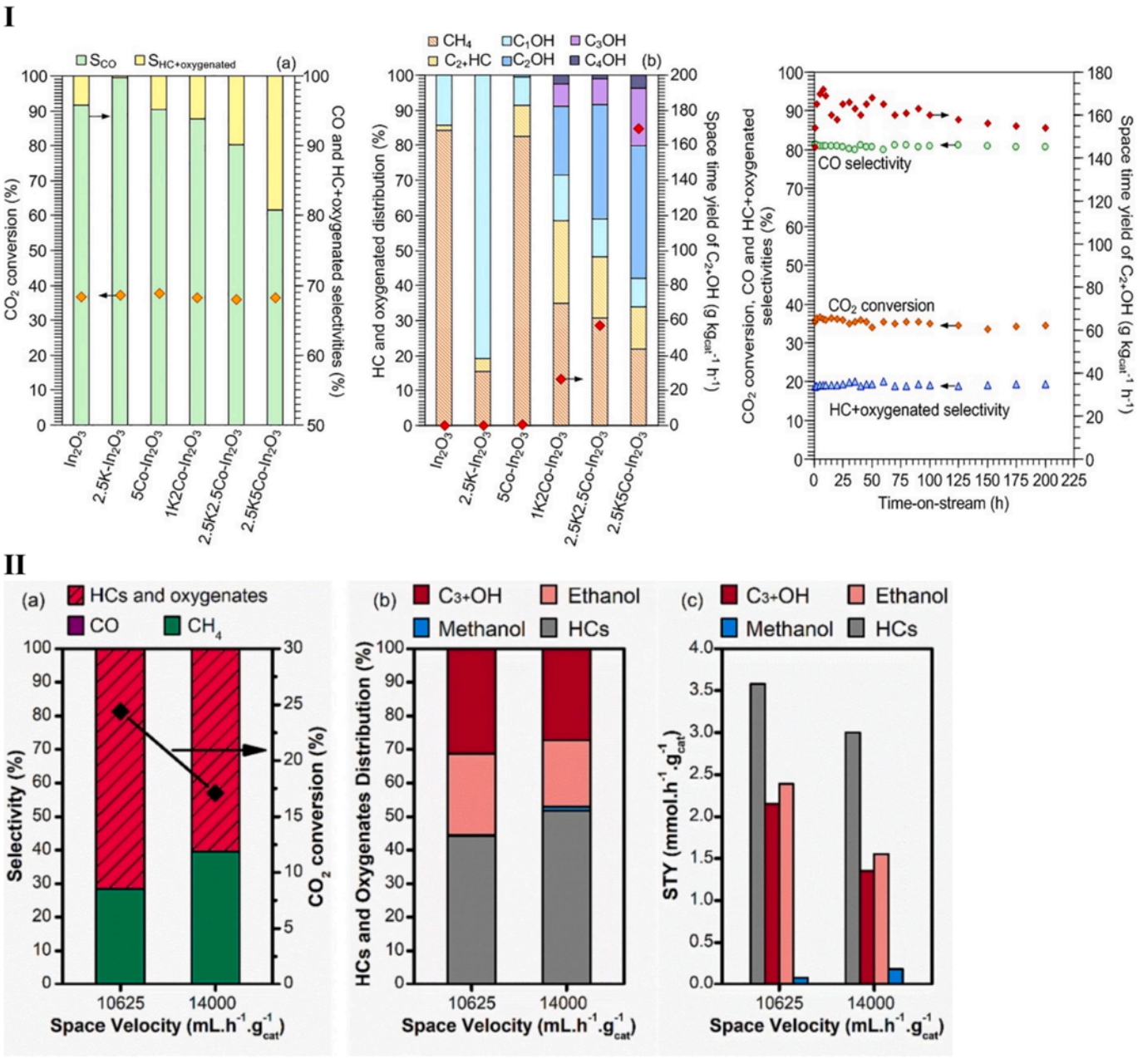

Fig. 12. I – CO_2 conversion and products selectivity: (a) distribution of hydrocarbon and oxygenated products, and STY of $C_{2+}OH$ over various catalysts; (b) STY of $C_{2+}OH$ across different catalysts; (c) – CO_2 conversion, product selectivities, and STY of $C_{2+}OH$ over time-on-stream of the 2.5K5Co-In_2O_3 catalyst reduced at 380 °C. Adapted with permission from Ref. [160]. II – Effect of the H_2/CO_2 ratio on the selectivity and CO_2 conversion: (a) variation in selectivity and CO_2 conversion; (b) distribution of hydrocarbons (HCs) and oxygenates; (c) analysis of STY of $Co_{1.8}Cu_{0.9}AlO_x$ reduced at 400 °C. Adapted with permission from Ref. [161].

$C_{2+}OH$ STY to 195.1 mg $g_{cat}^{-1}h^{-1}$, surpassing that of most reported Fe-based catalysts. The introduction of K-CuZnAl has been verified to facilitate the formation of a greater quantity of non-dissociative CO* species. Additionally, by controlling its proximity to Zr-CuFe, the interaction between CH_x species and CO* is enhanced, resulting in the generation of a higher quantity of HA.

Liu and colleagues [183] shown that the creation of interfaces between K and ZrO_2 significantly enhances the activity of HA production in the direct conversion of CO_2 over FeCu-based catalysts (Fig. 14**II**). The KFeCu/a-ZrO_2 catalyst, after optimization, exhibits a HA production rate 4.6 times higher than that of KFeCu/SiO_2. Under the optimal conditions of 320 °C, 4 MPa, and 12 $L{\cdot}g_{cat}^{-1}{\cdot}h^{-1}$, the most effective catalyst achieves a HA STY of 125.0 $mg{\cdot}g_{cat}^{-1}{\cdot}h^{-1}$. The combined findings from in situ spectroscopy and chemisorption indicate that the presence of K – ZrO_2 interfaces prompts the generation of oxygen defects on the amorphous ZrO_2 support. This process leads to a surplus of exposed Zr sites functioning as Lewis acid sites, facilitating the nondissociative adsorption and activation of CO. Zhang and co-authors [184] conducted a study on various Cr-modified CuFe catalysts. The authors found that the addition of small amounts of Cr enhances the interaction between Cu and Fe species, thereby mitigating CO over-dissociation and suppressing the formation of iron carbides. The CO_2 conversion rate, as well as the selectivity and STY of $C_{2+}OH$ over the 1 %Cr-CuFe catalyst, reached 38.4 %, 29.2 %, and 104.1 $mg{\cdot}g_{cat}^{-1}{\cdot}h^{-1}$, respectively, at operating conditions of 320 °C, 4.0 MPa, and 6000 $mL{\cdot}g_{cat}^{-1}{\cdot}h^{-1}$. Moreover, with a higher space velocity of 48000 $mL{\cdot}g_{cat}^{-1}{\cdot}h^{-1}$, the STY of $C_{2+}OH$ could be further increased to 268.5 $mg{\cdot}g_{cat}^{-1}{\cdot}h^{-1}$, surpassing that of most Fe-based catalysts reported in the literature (Table 4).

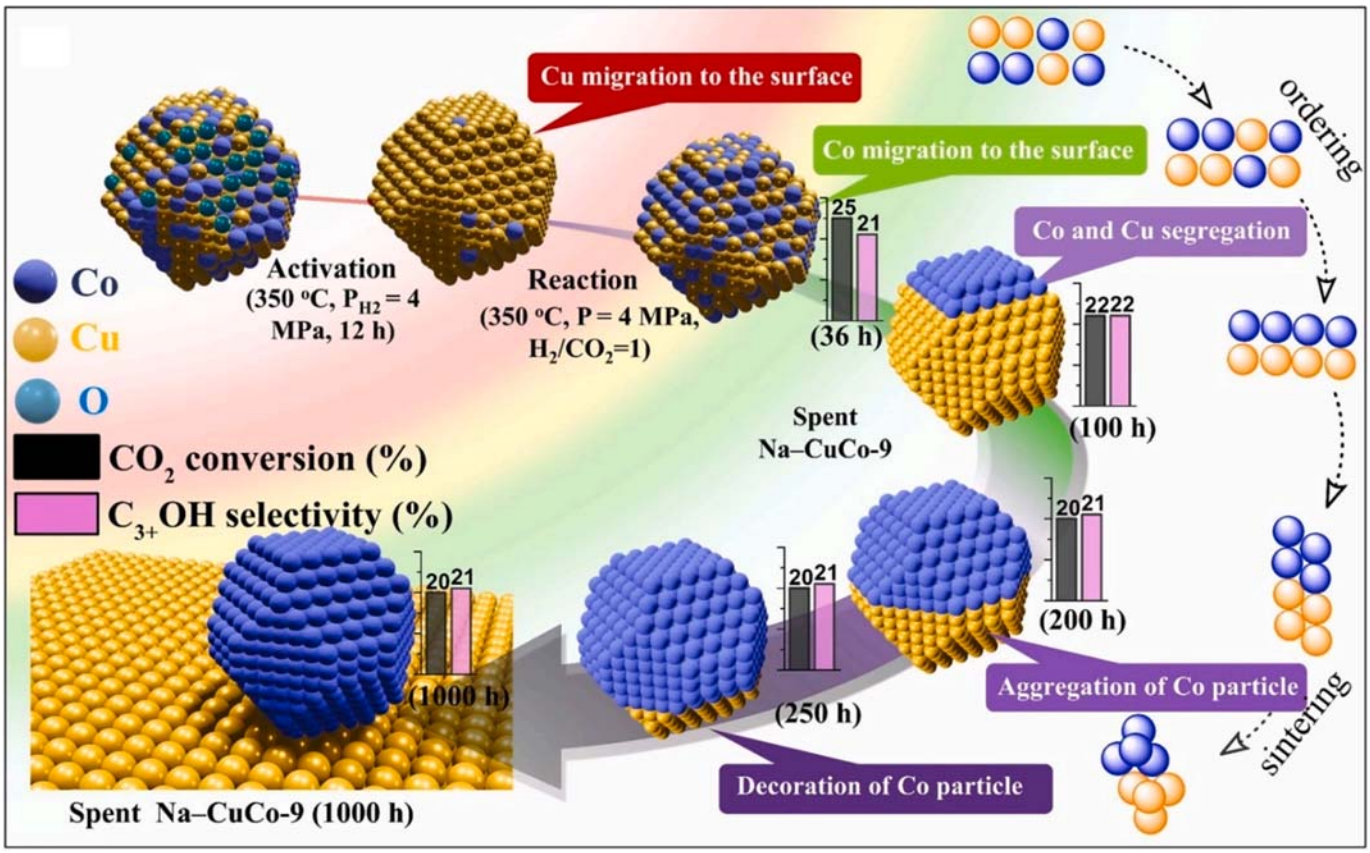

Fig. 13. Diagram illustrating the morphological reconstruction of the Na–CuCo-9 catalyst throughout calcination, reduction, induction, and long-term hydrogenation processes. Adapted with permission from Ref. [165].

Table 4
The catalytic performance and reaction conditions of heterogenous Fe-based catalysts in CO_2 thermocatalytic hydrogenation to EtOH and/or $C_{2+}OH$ in a continuous fixed-bed reactor.

Catalyst	Catalytic performance			Reaction conditions					Ref.
	STY_{EtOH} or $C_{2+}OH$ $mmol \cdot g_{cat}^{-1} \cdot h^{-1}$	X_{CO2} (%)	S_{EtOH} or $C_{2+}OH$(%)	T (°C)	P (bar)	GHSV (h^{-1})	H_2/CO_2	TOS (h)	
$CuZnFe_{0.5}K_{0.15}$	0.17 $g/mL_{cat}/h$ + MeOH	42.3	36.7	300	60	5000	3	N.A.	[181]
K-CuZnAl/Zr-CuFe	195.1 $mg/g_{cat}/h$	40.6	22.4	320	40	24000 mL/g/h	3	200	[182]
KFeCu/a-ZrO_2	125.0 $mg/g_{cat}/h$	25.7	26.1	320	40	12,000	3	80	[183]
1Cr-CuFe	104.1 (268.5) $mg/g_{cat}/h$	38.4	29.2	320	40	6000	3	120	[184]
PdFe alloy-Fe_5C_2	87.8 $mg/g_{cat}/h$	35.6	18.2	320	50	6000 mL/g/h	3	3	[185]
0.3K1Pd/Fe_2O_3	48 $mg/g_{cat}/h$	30.0	13.4	320	50	6000 mL/g/h	3	3	[186]
10Mn1K-FeC	N.A.	40.5	10.5	300	30	6000	3	N.A.	[187]
Na-Fe@C/CuZnAl	N.A.	39.2	35.0	320	50	N.A.	3	8	[77]
$K_{0.82}$FeIn/Ce-ZrO_2	N.A.	29.6	28.7	300	100	4500	3	100	[188]
FeIn/K-Al_2O_3	N.A.	36.7	42.0	300	20	4000 mL/g/h	3	20	[189]
5Rh-Fe(1:2)/SiO_2	N.A.	26.7	16.0	260	50	6000 mL/g/h	3	N.A.	[190]

N.A. means that the data is not available in the reference.

Recently, Wang and colleagues [185] demonstrated a novel method for fabricating PdFe alloy-Fe_5C_2 interfaces in situ, serving as active sites for highly efficient and stable production of HA from CO_2 hydrogenation. The PdFe alloy plays a crucial role in regulating the adsorptive activation of H_2 and CO_2, leading to the complete transformation of Fe species into Fe_5C_2 and the formation of abundant PdFe alloy-Fe_5C_2 interfacial sites. The authors achieved an HA yield of 86.5 $mg \cdot g_{cat}^{-1} \cdot h^{-1}$ with a selectivity of 26.5 % at operating conditions of 300 °C, 5 MPa, and a space velocity of 6000 mL $g_{cat}^{-1} \cdot h^{-1}$. Additionally, the same group [186] synthesized the 0.3 K-1Pd/Fe_2O_3 catalyst, which exhibited superior catalytic performance, with an HA STY of 48 mg $g_{cat}^{-1} \cdot h^{-1}$ at 320 °C, 5 MPa, and a space velocity of 6 L $g_{cat}^{-1} \cdot h^{-1}$. This STY was 3.5 times higher than that of 1Pd/Fe_2O_3 and 35 times higher than that of the 0.3 K/Fe_2O_3 catalyst. The authors observed that the in situ generated PdFe alloy and K synergistically stabilize the iron carbide phase, responsible for CO dissociation and alkyl formation, while the PdFe alloy serves as an active site for CO non-dissociative activation and CO insertion.

Huang et al. [187] presented findings on a catalyst composed of iron carbide modified with Mn and K. This catalyst demonstrates a CO_2 conversion rate exceeding 40 % and a selectivity towards HA exceeding 10 %. Moreover, the proportion of propanol and butanol in the alcohol products exceeds 30 %. In contrast, unpromoted iron carbide exhibits a strong tendency for hydrocarbon chain growth, leading to rapid formation of hydrocarbon products rather than HA. However, on the Mn-

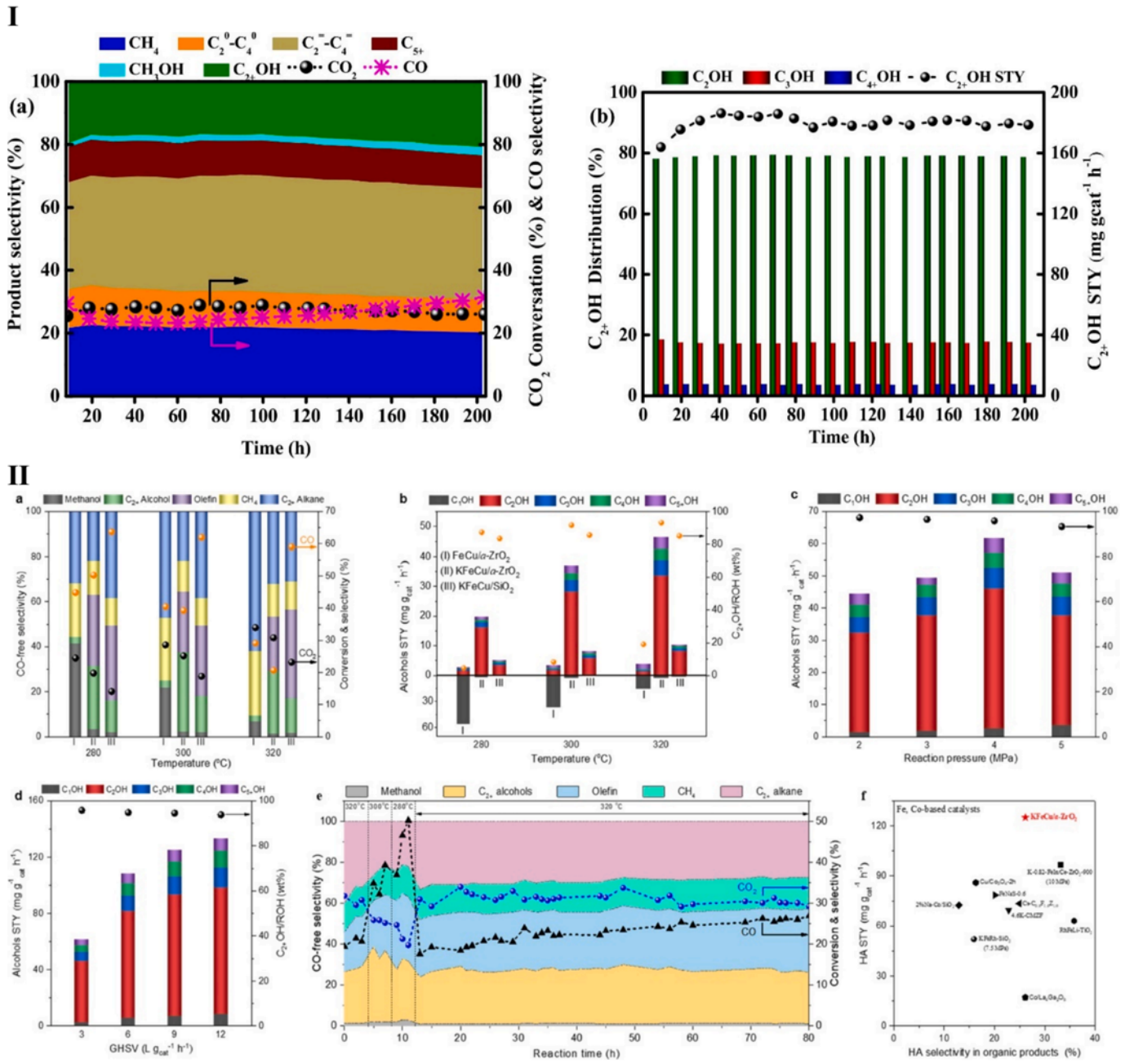

Fig. 14. I – Catalytic results of K-CuZnAl/Zr-CuFe composite within 200 h in CO_2 hydrogenation to $C_{2+}OH$ at 320 °C, 4 MPa and GHSV of 24000 mL $g_{cat}^{-1}h^{-1}$. Adapted with permission from Ref. [182]. II – Catalytic performance of the KFeCu/a-ZrO_2 catalyst. (a) CO_2 conversion and product distribution and (b) alcohol distribution at 280–320 °C, 5 MPa, and 3 L·g_{cat}^{-1}·h^{-1}; (c) effect of reaction pressure (2–5 MPa) on the STY of alcohols at 320 °C, 3 L·g_{cat}^{-1}·h^{-1}; (d) effect of GHSV on the STY of alcohols at 320 °C, 4.0 MPa; (e) TOS test at 5 MPa and 3 L·g_{cat}^{-1}·h^{-1}; (f) comparison of HA STY/selectivity of the KFeCu/a-ZrO_2 catalyst with other reports. Adapted with permission from Ref. [183].

and K-modified iron carbide catalyst, K serves to increase the surface C/H ratio of the catalyst by enhancing the adsorption of CO_2 on the catalytic surface. This increased C/H ratio is crucial for the formation of HA, and the addition of manganese promoter significantly enhances the production of HA, particularly the formation of propanol and butanol. Xi et al. [188] investigated a new type of catalyst composed of K-promoted bimetallic Fe and In on a Ce – ZrO_2 support. They prepared and examined FeIn/Ce – ZrO_2 precursors with varying Fe contents, providing detailed characterization of the catalysts. The analysis revealed well-dispersed Fe_2O_3 and In_2O_3 phases with oxygen vacancies. The most promising performance, featuring a CO_2 conversion rate of 29.6 % and a selectivity towards HA of 28.7 %, coupled with excellent stability (100 h), was achieved with the $K_{0.82}$FeIn/Ce – ZrO_2 catalyst after activation under a CO atmosphere. The authors attributed these results to the influence of individual catalyst components (K, Fe, and In) on the overall catalyst performance. Wang and colleagues [77] employed a novel approach involving the combination of an alkene synthesis Na-Fe@C catalyst with a potassium-doped methanol synthesis CuZnAl catalyst to achieve the selective direct conversion of CO_2 to ethanol, achieving a CO_2 conversion rate of 39.2 % and ethanol selectivity of 35.0 %. Further in-depth in situ characterizations and DFT calculations were conducted, revealing the crucial roles played by unique catalytic interfaces, intimate modes of interaction among multifunctional catalysts, and the presence of aldehyde species intermediates in facilitating the higher conversion rate of CO_2 to ethanol.

Goud et al. [189] pioneered the development of a novel catalyst by

incorporating In into Fe_2O_3. Through optimal substitution of In into Fe_2O_3 supported on Al_2O_3, and subsequent promotion with K, they achieved impressive activity, boasting a CO_2 conversion rate of 36.7 % and HA selectivity of 42 %, resulting in a corresponding yield of 15.4 %. This superior performance is attributed to the heightened strain induced by In substitution, surpassing that of Fe due to its larger size. Furthermore, the strain was further manipulated with K promotion, favoring increased CO_2 conversion and setting a new record value for HA selectivity. Kusama et al. [190] investigated the synthesis of ethanol through the catalytic hydrogenation of CO_2 using Rh-Fe/SiO_2 catalysts prepared via co-impregnation. The authors observed that the amount of added Fe influenced both ethanol selectivity and CO_2 conversion within the range of Fe/Rh = 0 − 3. The product selectivity was found to correlate with the percentage of Fe evaluated by X-ray photoelectron spectroscopy. It was suggested that Fe altered the electronic states of Rh and that elemental iron promoted methanation while hindering the formation of ethanol, as well as CO and methanol. Ultimately, the study achieved an ethanol selectivity of 16.0 % and a CO_2 conversion of 26.7 %.

3.4. Nobel-metal catalysts with different promoters and supports

Table 5 provides a summary of the catalytic performances observed for noble-metal (Ru, Rh, Pd, and Pt) catalysts in the continuous fixed-bed reactor for the hydrogenation of CO_2 to ethanol and HA. Rh-based catalysts promoted by metal oxides found extensive application in CO_2 hydrogenation, particularly in ethanol synthesis. Nonetheless, this process often encounters challenges such as low CO_2 conversion, alcohol selectivity and poor catalyst stability, primarily attributed to the formation of byproducts methane and CO [191–193].

Ver recently, Ji et al. [193] successfully demonstrated that the 2Rh0.5Fe0.5Na/CeO_2 catalyst exhibits high catalytic activity for CO_2 conversion, particularly in ethanol production. By systematically varying the reaction temperature and space velocity, they identified the optimal conditions – 250 °C, 3 MPa pressure, and a space velocity of 4000 mL·g^{-1}·h^{-1} under which the catalyst achieved a CO_2 conversion of 13.0 % and a notable ethanol selectivity of 29.8 % (Fig. 15**I**). The study highlighted that while higher temperatures improve CO_2 conversion, they also reduce oxygenate selectivity, with ethanol production peaking at 250 °C. Additionally, lower space velocities were found to favor ethanol formation, despite generally reducing CO_2 conversion. The catalyst's ethanol productivity of 116.7 mmol·g_{Rh}^{-1}·h^{-1} or 2.33 mmol·g_{cat}^{-1}·h^{-1} surpassed that of previously reported Rh-based catalysts and was comparable to or even exceeded the performance of the best non-Rh-based catalysts, underscoring its potential for efficient CO_2-to-ethanol conversion.

A highly effective catalyst was introduced, comprising vanadium oxide-promoted Rh-based catalysts confined within the mesopores of MCM-41 [192]. The Rh-0.3VO_x/MCM-41 catalyst demonstrates outstanding performance (STY = 47.9 g·kg_{cat}^{-1}·h^{-1}) with approximately 12 % CO_2 conversion and ethanol selectivity reaching around 24 % in CO_2 hydrogenation. This enhanced performance can be ascribed to the synergistic effects of the high dispersion of Rh facilitated by the confinement effect of MCM-41 and the formation of VO_x-Rh interface sites. Oyang et al. [194] investigated the utilization of two types of Co_3O_4 with distinct morphologies (nanorods and nanoplates) as supports for Pt nanoparticles in the preparation of Pt/Co_3O_4 catalysts. The synergistic effect arising from Pt, Co nanoparticles, and oxygen vacancies within Co_3O_4-x enhanced the adsorption of H_2 and CO_2, resulting in the highest yield of C_{2+}OH at 0.56 mmol·g_{cat}^{-1}·h^{-1} achieved at 200 °C and 2 MPa.

Zhang et al. [191] reported that zeolite silicalite-1 embedded Na-promoted Rh nanoparticles (Na-Rh@S-1) exhibit remarkable productivity and stability (100 h) for CO_2 hydrogenation to EtOH. The Na-Rh@S-1 catalyst achieved an ethanol selectivity of 24 % at a CO_2 conversion of 10 %, and a STY of ethanol reaching 72 mmol·g_{Rh}^{-1}·h^{-1} (Fig. 15**II**). The Na^+ modifier plays a crucial role in enhancing CO_2 conversion and ethanol selectivity by suppressing methane formation. Characterization results suggest that the presence of Na^+ enables the coexistence of Rh^0 and Rh^+ species, enhancing CO_2 adsorption and thereby boosting ethanol formation. Lou and colleagues [195] showed that CeO_2-supported Pd dimers efficiently convert CO_2 to ethanol, achieving a selectivity of 99.2 % to ethanol with a STY of 45.6 g·g_{Pd}^{-1}·h^{-1}. The unique Pd_2O_4 configuration and high homogeneity of the Pd dimers allow for the direct dissociation of CO_2 to CO, triggering C–C coupling while appropriately inhibiting further C_{2+} coupling, thereby favoring selective ethanol formation. The Pd_2O_4 configuration strongly binds CO on Pd_2/CeO_2, preventing CO desorption and promoting coupling between CO and CH_3 intermediates to form ethanol precursors. Goryachev and colleagues [196] synthesized and tested a series of SiO_2-supported Rh-based catalysts. Through high-throughput screening, they identified an optimal catalyst composition. Systems containing 2 wt% K, 20 wt% Fe, and 5 wt% Rh demonstrated the lowest selectivity of CH_4 at 46 %, with selectivity of ethanol at 15.9 % and CO_2 conversion at 18.4 %. The authors found that the presence of Fe is essential for alcohol formation, while K promotion plays a crucial role in reducing the undesired direct methanation of CO_2. Fe facilitates chain growth, while K promotion enhances CO dissociation, leading to higher ethanol selectivity. Despite the exceptional activity of Rh-based catalysts (with proper oxidation states) in CO_2 hydrogenation, their industrial application is constrained by their lack of economic feasibility. Consequently, there is a need for further research aimed at the development of catalysts based on non-noble metals.

Yang et al. [198] conducted the synthesis of a catalyst termed RhFeLi/TiO_2 NR, where TiO_2 nanorods (TiO_2 NR) served as the support material. The presence of TiO_2 NR facilitated the dispersion of Rh nanoparticles, while the abundant hydroxyl groups on the TiO_2 NR

Table 5
The catalytic performance and reaction conditions of heterogenous noble-metal-based catalysts in CO_2 thermocatalytic hydrogenation to EtOH and/or C_{2+}OH in a continuous fixed-bed reactor.

Catalyst	Catalytic performance			Reaction conditions					Ref.
	STY_{EtOH} or C_{2+}OH mmol·g_{cat}^{-1}·h^{-1}	X_{CO2} (%)	S_{EtOH} or C_{2+}OH(%)	T (°C)	P (bar)	GHSV (h^{-1})	H_2/CO_2	TOS (h)	
2Rh0.5Fe0.5Na/CeO_2	2.33	13.0	29.8	250	30	4000 mL/g/h	3	N.A.	[193]
Rh-0.3VO_x/MCM-41	47.9 g/kg/h	12.1	24.1	250	30	6000	3	N.A.	[192]
Pt/Co_3O_4	0.56	28.0	26.7	200	20	6000 mL/g/h	3	50	[194]
Na-Rh@S-1	72 mmol/g_{Rh}/h	10.0	24.0	250	50	N.A.	3	20	[191]
Pd/CeO_2	45.6 g_{EtOH}/g_{Pd}/h	9.0	99.2	240	30	3000	3	1	[195]
2K20Fe5Rh/SiO_2	21.4 mL/g/h	18.4	15.9	250	50	7000	3	6	[196]
Ru/In_2O_3-ZrO_2	130 mg_{EtOH}/g_{Ru}/h	1.0	70.0	225	6	1333 mL/g/h	3	24	[197]
RhFeLi/TiO_2	N.A.	15.0	32.0	250	30	6000	3	7	[198]
Li/RhY	0.12	13.1	2.7	250	30	6000 mL/g/h	3	N.A.	[199]
Rh-Li/SiO_2	N.A.	15.5	7.0	240	50	6000 mL/g/h	3	N.A.	[200]

N.A. means that the data is not available in the reference.

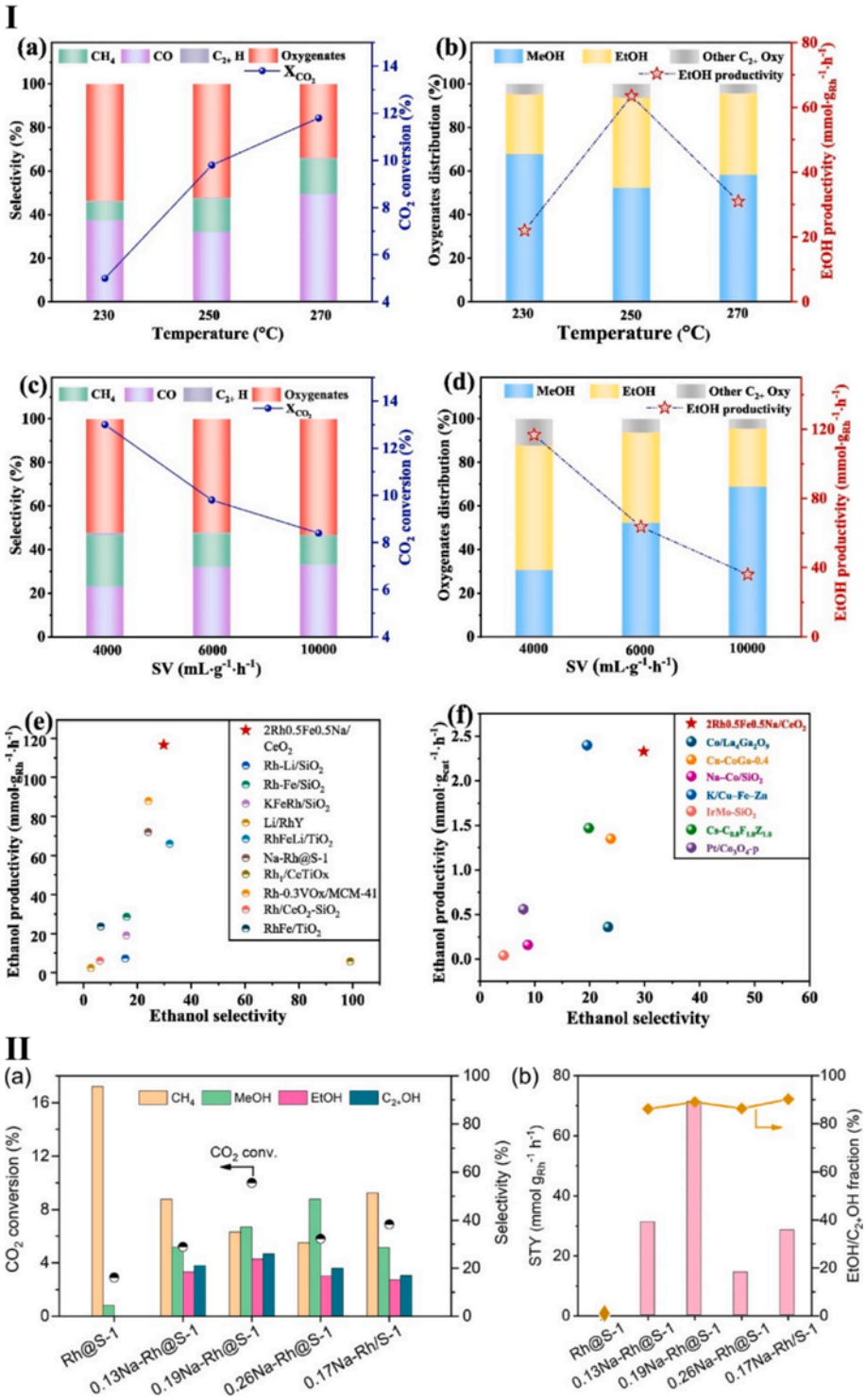

Fig. 15. I – The effect of transition metal promoters (a) and alkali metals (b) on the catalytic performance of Rh/CeO_2, including CO_2 conversion, selectivity, oxygenate distribution, and ethanol productivity, was examined for both non-promoted and Fe and/or Na-promoted Rh/CeO_2 catalysts in CO_2 hydrogenation (c and d). The reaction conditions were as follows: 0.3 g of catalyst, 250 °C, 3 MPa, H_2/CO_2 molar ratio of 3, and a space velocity of 6000 $mL{\cdot}g^{-1}{\cdot}h^{-1}$. Adapted with permission from Ref. [193]. II – Performance of Rh-based catalysts in CO_2 hydrogenation: (a) CO_2 conversion and product selectivity; (b) STY of C_2H_5OH and the fraction of C_2H_5OH in C_{2+} oxygenates. Adapted with permission from Ref. [191].

played a pivotal role in the production of HA through CO_2 hydrogenation. Consequently, the authors achieved a CO_2 conversion rate of 15 % and a HA selectivity of 32 % under conditions of 250 °C, 3 MPa, and 6000 $mL{\cdot}g_{cat}^{-1}{\cdot}h^{-1}$. It was observed that as the hydroxyl density on the surface-treated TiO_2 nanorods increased, the selectivity towards methane and ethanol also increased. These hydroxyl groups were found to stabilize formate species and protonate methanol, which then underwent dissociation into $*CH_x$. Subsequently, CO generated from the RWGS reacted with $*CH_x$ to form CH_3CO*, followed by hydrogenation of CH_3CO* to produce ethanol. Bando et al. [199] investigated the CO_2 hydrogenation reaction using Li-promoted Rh ion-exchanged zeolite catalysts (Li/RhY). They found that as the amount of added Li increased,

the main product of the reaction shifted from methane to CO. Additionally, they observed increased production of ethanol and methanol. Furthermore, when 1.8 % of CO was added to the reactant gas, the selectivity for ethanol significantly increased up to 13 % on Li/RhY catalyst, while no such influence was observed on undoped Rh ion-exchanged zeolite catalyst. Kusama et al. [200] conducted hydrogenation of CO_2 to ethanol using Rh/SiO_2-based catalysts. Initially, methane was the primary product over the unpromoted catalysts. However, upon adding various metal oxide promoters, both CO_2 conversion and selectivity to alcohols (methanol and ethanol) increased. Notably, Li salts demonstrated the most significant effect on ethanol production among the 30 promoters tested. Through optimization of reaction conditions, the authors achieved the highest ethanol selectivity of 15.5 % with a CO_2 conversion rate of 7.0 %.

4. Mechanistic aspects

4.1. Co-mediated pathway

The reaction mechanism for ethanol and HA from CO_2 hydrogenation remains controversial due to the coexistence of a diverse array of surface species at varying concentrations, necessitating further in situ or operando studies for clarity [5]. Accepted mechanisms for activating CO_2 in catalysts for ethanol and HA synthesis typically involve two pathways (Fig. 16**I**): (I) the CO-mediated pathway, which consists of two steps: firstly, the conversion of CO_2 to CO, followed by the subsequent hydrogenation and/or dissociation of CO; (II) the formate/methoxy-mediated pathway, wherein CO_2 reacts with hydrogen to yield C_1 intermediates such as formate (HCOO*) and/or methoxy (CH_3O*) species [49]. Among the available studies, the CO-mediated mechanism proposed by Kusama et al. [200] is widely accepted. This mechanism can be understood as a combination of CO_2 conversion to CO and syngas conversion to ethanol and HA. Thus, the CO_2-to-ethanol (HA) reaction involves the RWGS to produce CO, followed by the formation of dissociated CO and H_2 to aid carbon-chain growth, resulting in the formation of C_xH_y intermediates. Subsequently, undissociated CO insertion occurs (either through CO insertion into alkyl groups or alkyl groups reacting with CO), followed by hydrogenation to form ethanol and HA. On oxide surfaces with plentiful oxygen vacancies, direct CO_2 dissociation is a prevalent occurrence. These vacancies readily accommodate oxygen species (O*) generated during dissociation. Subsequently, the resulting CO* species undergo hydrogenation to form CH*.

For instance, Liu and colleagues [113] investigated how moderate surface segregation influences the promotion of CO_2 hydrogenation to ethanol on CoCu catalysts using DFT analysis. The authors verified that CO_2 was hydrogenated to produce CO through the RWGS reaction on these catalysts. Additionally, a variety of CH_x species were identified as participants in the coupling process with CO (Fig. 16**II**). This suggests that the generation of CO and its subsequent dissociation to form CH_x species play crucial roles. The pathway from adsorbed *CO to ethanol production involves several steps: *CO conversion to *CH_2O, electron transfer from CO to *CH_2O, and the splitting of *CH_2O into *CH_2. The energy required for methanation was found to be higher compared to the energy needed for CO insertion. This energy difference favored the formation of *CH_2CO ethanol intermediates. Ye and colleagues [123] conducted DFT calculations, which elucidated the direct dissociation of CO_2 to CO* on both pristine and Ir-promoted In_2O_3 catalysts in the context of CO_2 hydrogenation to ethanol. It is noteworthy that the presence of Ir dopants in In_2O_3 not only facilitates CO_2 dissociation but also enhances CO_2 chemisorption through the formation of distinctive active site configurations (Fig. 16**III**). Initially, CO_2 is adsorbed onto the In metal site as CO_2*, followed by CO_2 activation initiated by its conversion into CO on the Ir metal site. The intermediate $Ir^{\delta+}$–CO* plays a crucial role in ethanol generation. The Lewis acid-base interaction between the monatomic Ir and nearby oxygen abundance on In_2O_3 is significant for CO_2 activation. Theoretical calculations and infrared spectra suggest the formation of a Lewis acid-base pair between monatomic Ir and nearby oxygen abundance on In_2O_3, resulting in the creation of two distinct catalytic sites that facilitate the reduction of CO_2 to active intermediates and promote C–C coupling, ultimately leading to ethanol generation. Under hydrogenation conditions, CHO* is formed from CO, while CO_2 undergoes hydrogenation to form the crucial CH_3O* intermediate. Further hydrogenation yields the C_2H_5O* species on Ir metal sites. Eventually, ethanol is produced as the final product through the hydrogenation of this species.

4.2. Formate/methoxy-mediated pathway

The formate/methoxy-mediated pathway is another prevalent route for ethanol and HA synthesis [49]. Unlike the CO pathway, which involves the direct cleavage of the C–O bond in CO_2 or cleavage via the formation of a COOH* intermediate, the formate/methoxy-mediated pathway occurs on catalysts that exhibit a higher propensity for hydrogenating carbon atoms. These catalysts often feature Lewis-acid-base pair sites. As illustrated in Fig. 17**I**, when single-atom Rh catalysts are supported on Ti-doped CeO_2, CO_2* attaches to a Lewis acid-base pair arrangement, where the carbon atom is bound to a Lewis acid site (Rh) and the oxygen atom is bound to the neighbouring oxygen vacancy (Ov) [121]. When CO_2 is adsorbed in this configuration, it adopts a bent structure, facilitating accessibility to the carbon center for hydrogenation into HCOO*. Subsequently, HCOO* undergoes further hydrogenation and deoxygenation, leading to the formation of C_1 building blocks like CH_xOH*, CH_x*, and CO*. These intermediates are crucial for ethanol and HA formation through C–C coupling reactions.

The formate/methoxy pathway over the Pt/Co_3O_4 catalyst was first suggested by researchers [119] based on experimental evidence gathered in a batch reactor. The authors conducted a $^{13}CH_3OH$-labeling experiment to probe the reaction mechanism. Upon adding $^{13}CH_3OH$ into the reactor before the reaction, they observed peaks at m/z = 47, in addition to the expected peak at m/z = 46, which corresponds to ethanol. The presence of the m/z = 47 peak suggests the formation of either $^{13}CH_3CH_2OH$ or $CH_3{}^{13}CH_2OH$, indicating that the carbon atom in ethanol might originate from methanol.

Lately, the same viewpoint was claimed by Yang et al. [198] over the RhFeLi–TiO_2 NR catalyst in a fixed-bed reactor. As depicted in Fig. 17**II**, the presence of surface hydroxyl groups is beneficial for stabilizing formate intermediates and facilitating the cleavage of C–O bonds in methoxy species. The authors assert that the *CH_3 species originates from the formate/methoxy pathway. Additionally, they highlight a linear correlation between the total amount of *CH_3 and the density of hydroxyl groups on the supporting TiO_2. Therefore, hydroxyl groups are believed to protonate methoxy, serving a similar function to using water as a solvent.

A reaction mechanism for transforming CO_2 into ethanol was introduced by researchers [122] in a recent study. They employed a batch reactor and the Rh/CNP catalyst, and their proposal was backed by DFT calculations (Fig. 17**III**). The process begins with the adsorption and activation of CO_2, where the most favorable pathway for CO formation involves the RWGS reaction through a COOH* intermediate, followed by its dissociation. Additionally, adsorbed CO_2 can undergo hydrogenation to form HCOO*, a crucial intermediate that can further transform into H_2COO* and HCOOH* over the Rh/CNP model. The production of ethanol is attributed to the coupling between CO* and CH_3* species generated from the dissociation of CH_3OH*. These findings highlight that Rh-N_3P_1 and Rh-N_4 sites display distinct catalytic behaviors due to their varying abilities to activate the dissociation of CH_3OH*. Specifically, Rh-N_4 sites may be deficient in facilitating the coupling between CH_3* and CO*, thus rendering them less favorable for ethanol production.

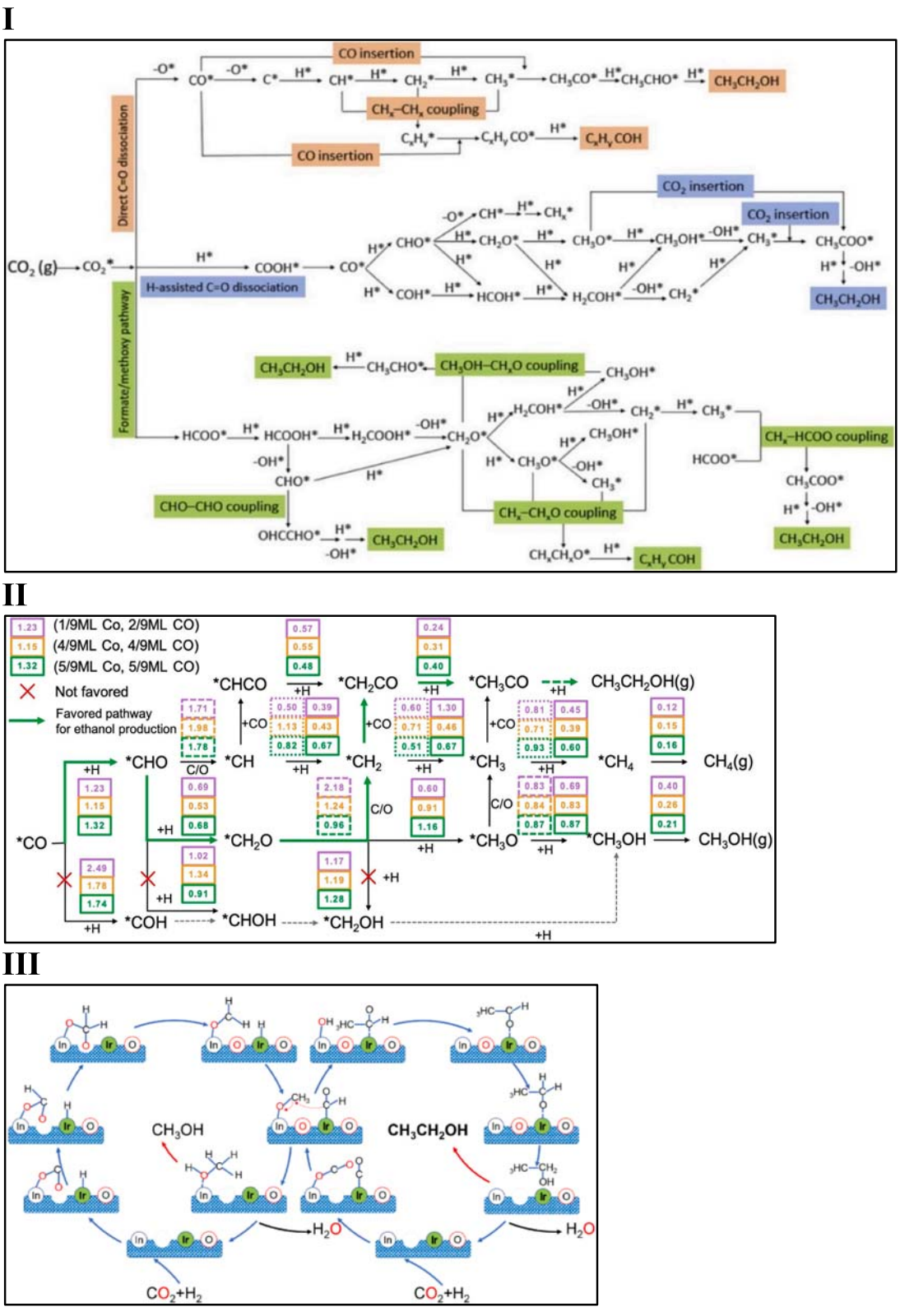

Fig. 16. I – Overview of potential pathways for CO_2 hydrogenation to HA. In the text, * denotes adsorbed species. Adapted with permission from Ref. [49]. II – DFT-calculated reaction networks of *CO hydrogenation towards methanol, methane and ethanol. Barriers of hydrogenation are in boxes with a solid line, barriers of C–O scission are in boxes with along dashed line, and barriers of CO insertion are in boxes with a short dashed line. All values are in eV. The barrier values are as follows: 1/9ML Co, 2/9ML CO (purple), 4/9ML Co, 4/9ML CO (orange) and 5/9ML Co, 5/9ML CO (green). The most favored pathway towards ethanol is highlighted with green arrows. Adapted with permission from Ref. [113]. III – Proposed catalytic mechanism of CO_2 hydrogenation to ethanol on the Ir_1-In_2O_3 catalyst. Adapted with permission from Ref. [123]. (For interpretation of the references to colour in this figure legend, the reader is referred to the web version of this article.)

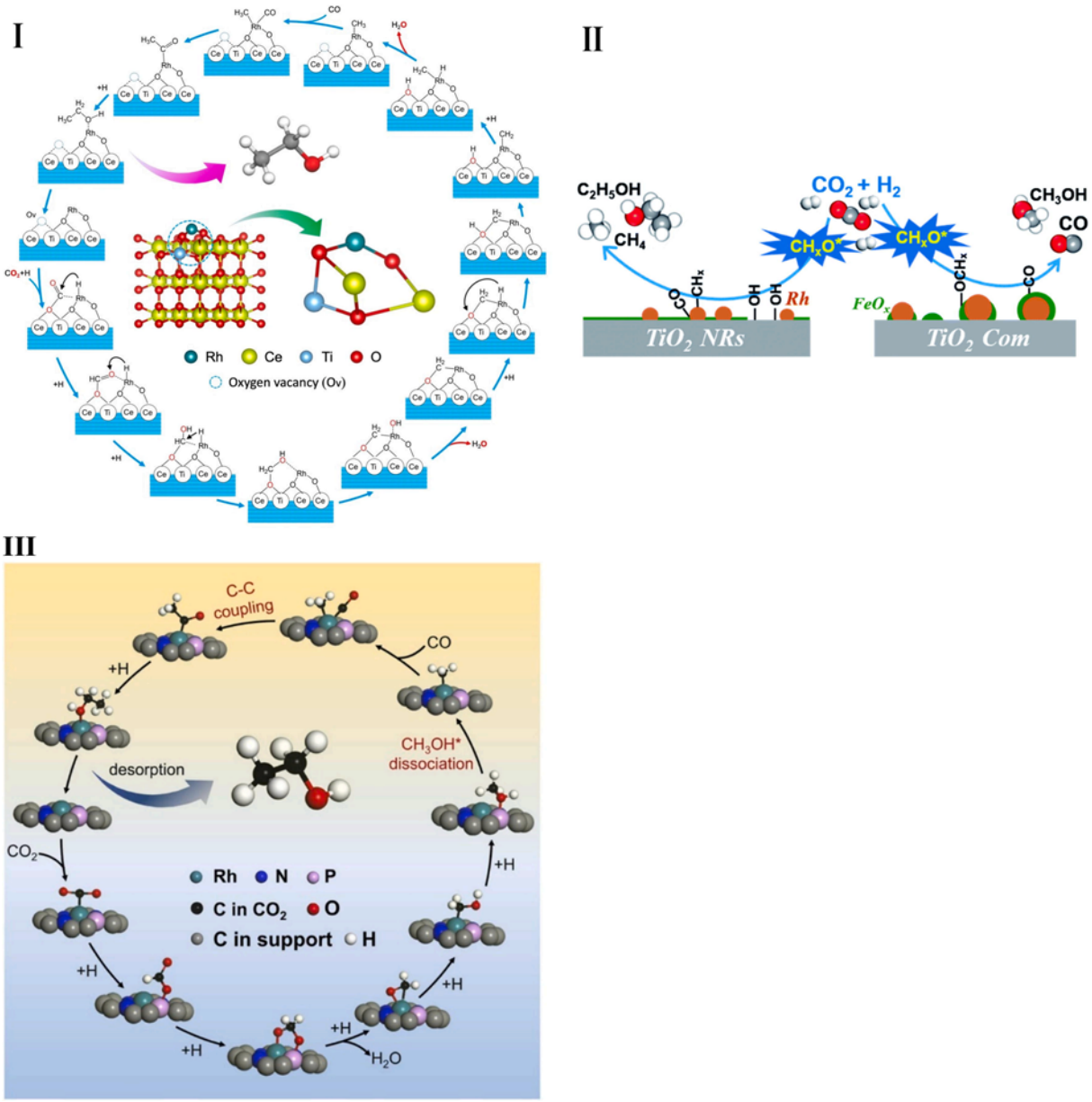

Fig. 17. I – Catalytic cycle illustrating ethanol formation from CO2 hydrogenation on the $Rh_1/CeTiO_x$ catalyst. Adapted with permission from Ref. [121]. II – Diagram depicting the CO_2 hydrogenation process over the Rh-based catalyst with and without hydroxyl groups on TiO_2. Hydroxyl groups are pivotal in expediting the CH_x–O* scission and enhancing ethanol formation. Adapted with permission from Ref. [198]. III – Proposed reaction mechanism for ethanol production from CO_2 hydrogenation over Rh/CNP catalyst. Adapted with permission from Ref. [122].

4.3. C–C coupling pathways

CO_2 activation can yield various C_1 intermediates such as CO, CH_xO, and CH_x, which are capable of undergoing C–C coupling reactions to generate C_{2+} intermediates, thereby facilitating the formation of ethanol and/or HA. The stability of these C_1 intermediates, determined by their adsorption strength and the abundance and activity of surface hydrogen, influences their composition on the surface and, consequently, the mechanism of C–C coupling. Accepted mechanisms for C–C coupling include CO insertion, CO_2 insertion, CH_x–CH_xO/CH_x coupling, and CH_x–HCOO coupling [49]. In addition to HA synthesis, C–C coupling can result in the production of alkanes, olefins, aldehydes, and other byproducts. The widely accepted CO insertion mechanism facilitates HA synthesis via CO_2 hydrogenation on catalysts such as Cu-based and noble metals, entailing the reaction of CO* with alkyl species (CH_x*) followed by the hydrogenation of C_{2+} intermediates into ethanol and HA. The CO insertion mechanism for HA synthesis necessitates a delicate equilibrium between surface CH_x* and CO* species, achieved by regulating dissociative CO activation (alkylation) and nondissociative CO activation rates on the catalyst. Xu and colleagues [149] have proposed an integrated reaction mechanism with CO insertion for CO_2 hydrogenation over Cs-CuFeZn catalysts, illustrated in Fig. 18**I**. The synthesis of methanol follows a direct pathway from CO_2 to methanol via HCOO* intermediates, facilitated by Cu-ZnO interfaces. The promotion of methanol formation is impeded by the presence of the Cs promoter. Moreover, at elevated temperatures, particularly above 300 °C, thermodynamic constraints limit the equilibrium of the reaction, causing methanol to revert back to CO_2 and H_2, with a concurrent acceleration in CO formation. Conversely, HA synthesis is observed to be more favorable over this catalyst at elevated temperatures. This is attributed to Cu-ZnO catalyzing the RWGS reaction to produce CO, while copper-iron carbide facilitates the insertion of C(H)O* intermediates into surface

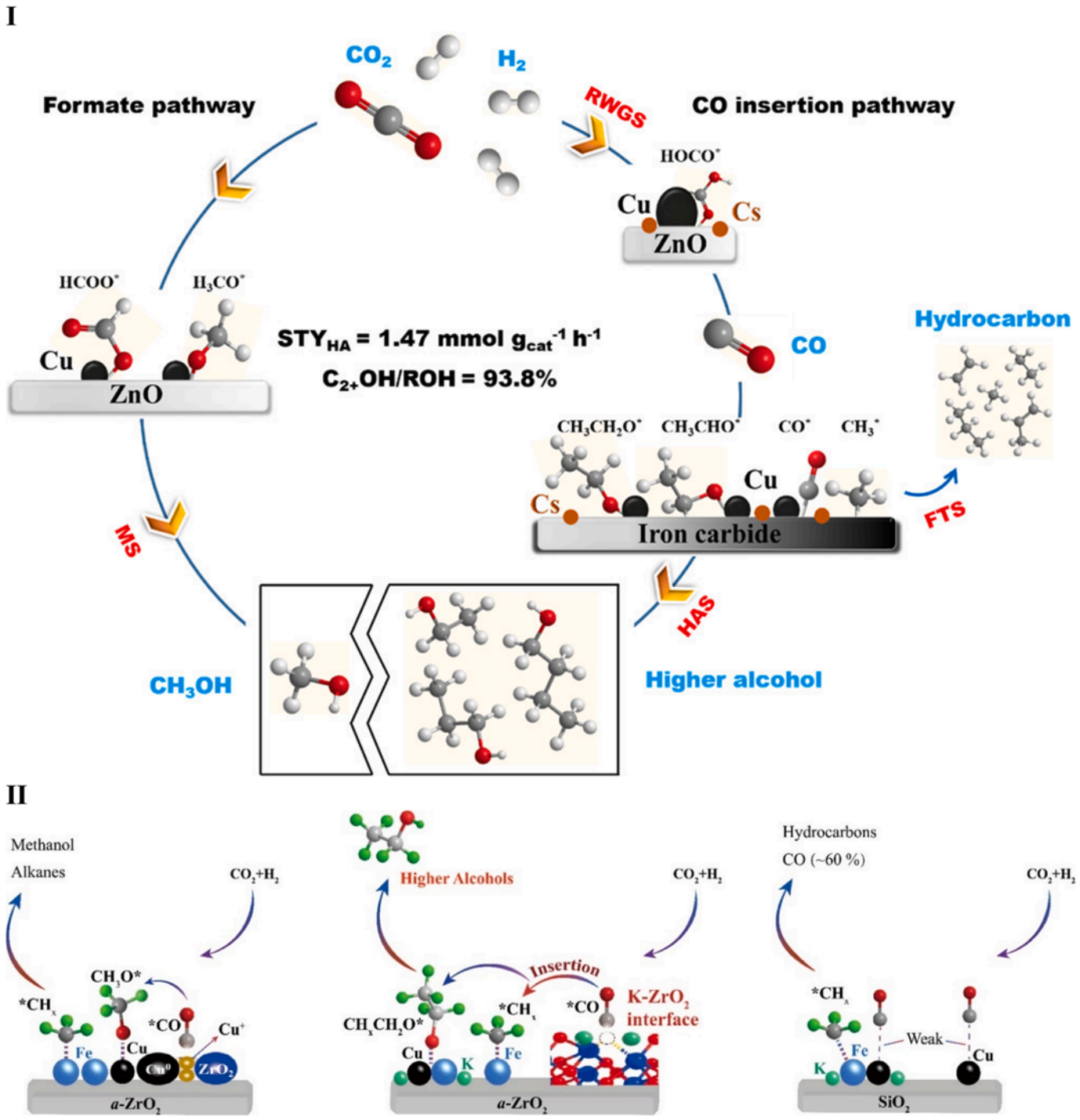

Fig. 18. I – Illustration of reaction pathways of CO_2 hydrogenation over the Cs-CuFeZn catalyst. Adapted with permission from Ref. [149]. II – Illustration for the contribution of K – ZrO_2 interfaces to HA over supported FeCu-based catalysts. Adapted with permission from Ref. [183].

hydrocarbon species, resulting in the formation of HA at a comparable rate.

Throughout the CO_2-to-HA conversion process, the Cs promoter plays a crucial role in enhancing the CO insertion reaction by modulating the hydrogenation capability of the CuFeZn catalysts. Liu and co-authors [183] demonstrated the significant influence of K promoters in their research on K-Cu-Fe catalysts, which were supported on amorphous ZrO_2. As depicted in Fig. 18**II**, the $Zr^{\delta+}$ sites and oxygen vacancies on the surface of K-ZrO_2 interfaces provided unoccupied 4d orbitals capable of accepting lone pair electrons from the carbon atom of CO, thereby enhancing non-dissociative CO adsorption. Consequently, a heightened surface coverage of CO* promoted the CO insertion reaction (CH_x* + CO* → CH_x*–CO) at Cu-Fe_5C_2 interfaces, consequently augmenting the productivity of HA.

4.4. Other C–C coupling pathways

In addition to the previously mentioned CO and formate/methoxy-mediated mechanisms, in batch reactors with solvent have also proposed alkyl-formate-coupling and formyl-methanol-coupling mechanisms. For instance, An et al. [111] presented a fresh catalytic cycle for CO_2 hydrogenation to methanol and ethanol, observing that C–C

coupling occurs between methanol and formyl species over diatomic Cu^{I}_{2} centers, enhanced by alkali metals such as Cs or Li, on Zr_{12}-bpdc-Cu catalysts (Fig. 19**I**). The process initiates with H_2 activation on bimetallic Cu^{+} sites, leading to the formation of $(Cu^{2+}–H^{-})^{2}$ species, followed by CO_2 hydrogenation to methanol and formyl species. The C–C coupling proceeds through nucleophilic attack, facilitated by electron-rich formyl species stabilized by Cu^{2+} and Cs^{+}, onto the methyl group in methanol activated by neighbouring Cu^{2+}. The resulting CH_3CHO species undergoes stepwise hydrogenation to ethanol.

The coupling of CH_x and CH_xO species has been widely recognized as a significant C–C coupling process, supported by numerous observations [201–206]. In catalyst systems where the adsorption of CH_x and CH_xO species prevails over that of CO, the CH_x–CH_xO coupling pathway is considered more plausible for C–C bond formation than CO insertion. Zhang and colleagues [82] employed DFT to investigate a reaction pathway, delineating the growth of carbon chains and the formation of HA over $Cu_6/ZnAl_2O_4(110)$, identified as the most stable structure (Fig. 19**IIa)**. Calculation of ΔG and E_a indicated that only the ΔG of CO insertion into CH_2 or CH_3 exceeded zero, corroborating the unfavorable nature of the CO insertion mechanism (Fig. 19**IIb,c**). Conversely, the coupling between CH_2 and CHO exhibited the lowest ΔG (−1.60 eV) and Ea (0.35 eV) compared to other couplings such as $CH_2 - CH_2O$, $CH_3 - CHO$, and $CH_3 - CH_2O$. These findings strongly indicate that the most advantageous mechanism for C–C coupling entails $CH_2 - CHO$ coupling on multifunctional tandem $Co_2C||CuZnAl$ catalyst. During the reaction, $R - CH_2CHO$ can undergo successive hydrogenation steps, ultimately leading to the production of $C_{2+}OH$.

Apart from the CO insertion pathways outlined previously, another avenue for $C - C$ coupling involves the coupling of CO_2 with CH_3*. This process entails initial hydrogenation of a fraction of adsorbed CO_2* to CH_3* on metallic sites, followed by its reaction with an adjacent non-hydrogenated CO_2* molecule, resulting in the formation of CH_3COO*. Subsequently, CH_3COO* undergoes hydrogenation to yield ethanol. Ding et al. [147] presented a groundbreaking perspective, highlighting the importance of the CO_2 insertion mechanism ($*CH_3 - *CO_2$) from the isotopic-labeling experiments and DFT calculations conducted on a Cu@Na-Beta zeolite catalyst in a fix-bed continuous flow reactor. As depicted in Fig. 20**I**, three types of surfaces – perfect, Cu vacancy, or O-doped – specifically at the edge Cu (221) models, were compared based on their DFT calculations. The researchers discovered that the barrier/reaction heat for the breaking of the C–O bond in $*CH_3O$ is higher than that of $*CH_3OH$ for the O-doped Cu (221) surface. This suggests that methyl formation via the cleavage of the C–O bond in CH_3OH is more favorable in this scenario, while the synchronous variation of the $^{12}CH_3^{13}CH_2OH$ signal with the $^{13}CO_2$ feed indicates the ready reaction of gaseous $^{13}CO_2$ with surface $^{12}CH_3$* to yield $^{12}CH_3^{13}CH_2OH$ on the step sites of the zeolite-entrapped Cu nanoparticles.

The coupling of CH_xO–CH_x, widely recognized as a compelling mechanism for C–C coupling, is supported by extensive observational evidence, and notably enables the formation of C_{3+} alcohols. Irshad and colleagues [165] have proposed a viable mechanism for n-butanol formation in a fixed-bed reactor, as shown in Fig. 20**II.** While the precise mechanism of the RWGS reaction over CuCo-based surfaces remains ambiguous, the presence of Cu^0 and O_v in the NAP-XPS profiles suggests that H_2-assisted CO_2 dissociation might be the primary RWGS pathway over the Na–CuCo-9 catalyst. Maintaining a delicate balance between dissociated and non-dissociated C–O bonds is crucial to enhance the activity for forming $C_{3+}OH$ species, which are pivotal for favorable $C_{3+}OH$ production kinetics. The generated CO can undergo concurrent transformation with CH_3O* and CH_3* species on Cu and Co sites, respectively, due to their differing intrinsic activities. CH_3* interacts with *CO to yield a C_{2+} oxygenate intermediate, eventually hydrogenating into acetaldehyde. The inhibition of CH_x to CH_4 over the Co surface, which competes with the crucial CO insertion for generating the aldehydic intermediate necessary for n-butanol formation, presents a challenge. Subsequently, the acetaldehyde intermediate re-adsorbs and activates as $CH_3CHOH* + CH_2CHO*$ on the Cu surface. The facilitated C–O bond dissociation of CH_3CHOH* over the Co site produces CH_3CH*, initiating a subsequent C–C coupling reaction between CH_3CH* and CH_2CHO* to yield C_4 oxygenates as precursors for n-butanol formation in a tandem reaction. Hence, the formation of n-butanol critically hinges on the kinetics of several key elementary steps, including C–C coupling, C–O dissociation, and C–H formation.

5. Challenges and future perspectives

Given the challenges posed by global warming, it is crucial to take immediate and resolute actions to reduce and ultimately eliminate CO_2 emissions. In the past decade, there has been a significant shift in public opinion, driven by evolving governmental policies that vary across regions and evolve over time. This shift has catalyzed rigorous research efforts not only towards developing more efficient CO_2 capture technologies but also towards exploring methods to utilize carbon-containing resources more effectively. Among these methods, the hydrogenation of CO_2 into C_{2+} alcohols emerges as a compelling technology for transforming CO_2 into valuable chemicals and fuels, receiving extensive study and attention over recent decades.

Currently, the direct hydrogenation of CO_2 to C_{2+} alcohols faces challenges such as low CO_2 conversion rates, insufficient selectivity towards ethanol/HA, and intense competition from side reactions and catalyst stability. The detailed description of challenges that must be addressed for further advancement of CO_2 hydrogenation into ethanol/HA (1. Catalyst performance in different reactor types; 2. Effect of solvents; 3. Role of supports; 4. Comprehensive characterization and mechanistic investigations; 5. Engineering next-generation catalysts) is presented in **the Support Information file**. Various promising catalyst categories have been explored, ranging from noble-metal catalysts to those based on Cu, Co, and Fe, often in conjunction with alkali metals. This research has investigated the impact of catalyst structure, promoters, supports, precursor materials, and reaction conditions on catalytic performance. Additionally, there have been suggestions regarding correlations between structure and performance, as well as proposed reaction mechanisms. This review provides a comprehensive overview and analysis of recent advancements in diverse catalyst formulations, the impacts of promoters and supports, as well as potential reaction mechanisms in both batch and fixed-bed reactors.

The efficiency of producing C_{2+} alcohols is largely determined by the kinetic rates governing critical processes, such as C–C coupling, C–O dissociation and insertion, and C–H formation. This insight stems from the detailed mechanistic analysis mentioned earlier. To attain peak C_{2+} alcohols selectivity, it's essential to maintain a precise equilibrium between non-dissociated and dissociated activations of C–O bonds. This equilibrium plays a pivotal role in augmenting C_{2+} alcohols production. Boosting selectivity towards C_{2+} alcohols requires a kinetic suppression of undesirable competitive reactions, notably the formation of CO, methanol and hydrocarbons. As a result, increasing ethanol selectivity may require either raising the energy barrier for $*CH_3$ hydrogenation or lowering the activation energy of the CO-insertion reaction. Adjusting *CO levels or *H coverage on distinct metal surfaces could also be pivotal in achieving high C_{2+} alcohols selectivity. This highlights the significance of maintaining an optimal $*CH_3$ coverage to minimize selectivity towards CO or methanol. In summary, fine-tuning the adsorption strengths of these surface species through electronic promoters to alter their fundamental adsorption behaviors and lifetimes could greatly influence the selectivity towards C_{2+} alcohols. Moreover, there is a need to develop new catalysts with bifunctional active sites, as both carbon chain propagation and alcohol formation are crucial aspects of C_{2+} alcohols synthesis. An efficient catalyst for C_{2+} alcohols synthesis should possess dual sites capable of providing both functions.

Fig. 21 presents a summary of the catalytic performance of the most active catalysts in both batch and fixed-bed reactors. In batch (tank) reactors, the ethanol/HA STY of the catalysts is ranked as follows: Cu-

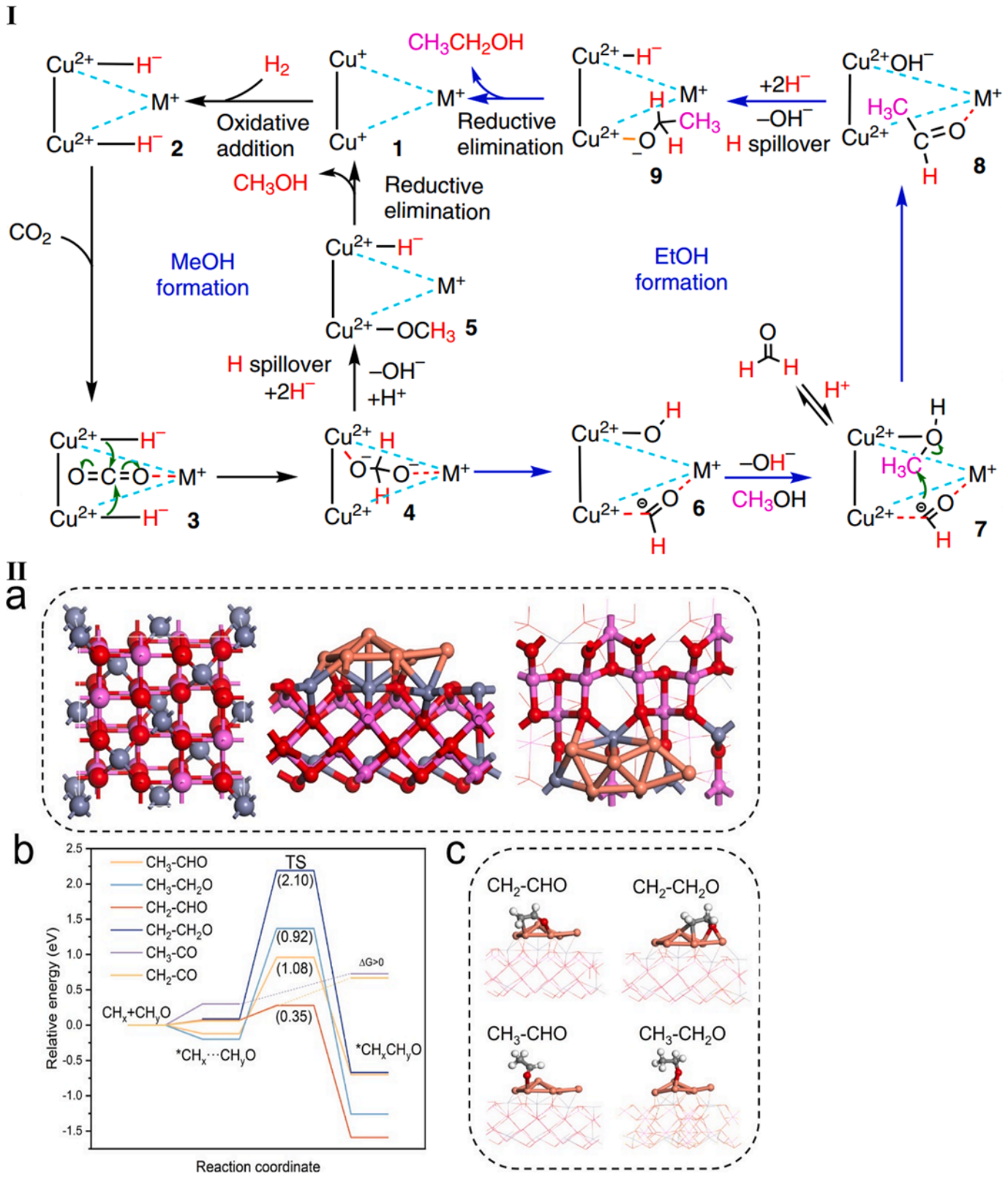

Fig. 19. I – Proposed mechanism of methanol and ethanol synthesis from CO_2 hydrogenation over Zr_{12}-bpdc-Cu catalysts. Adapted with permission from Ref. [111]. II – (a) Structure model of $Cu_6/ZnAl_2O_4(110)$ (gray: Al atom; red: O atom; pink: Zn atom; and orange: Cu atom); (b) energy profiles for the different C–C coupling paths; and (c) final adsorption form of CH_xCH_yO on $Cu_6/ZnAl_2O_4(110)$. Adapted with permission from Ref. [82]. (For interpretation of the references to colour in this figure legend, the reader is referred to the web version of this article.)

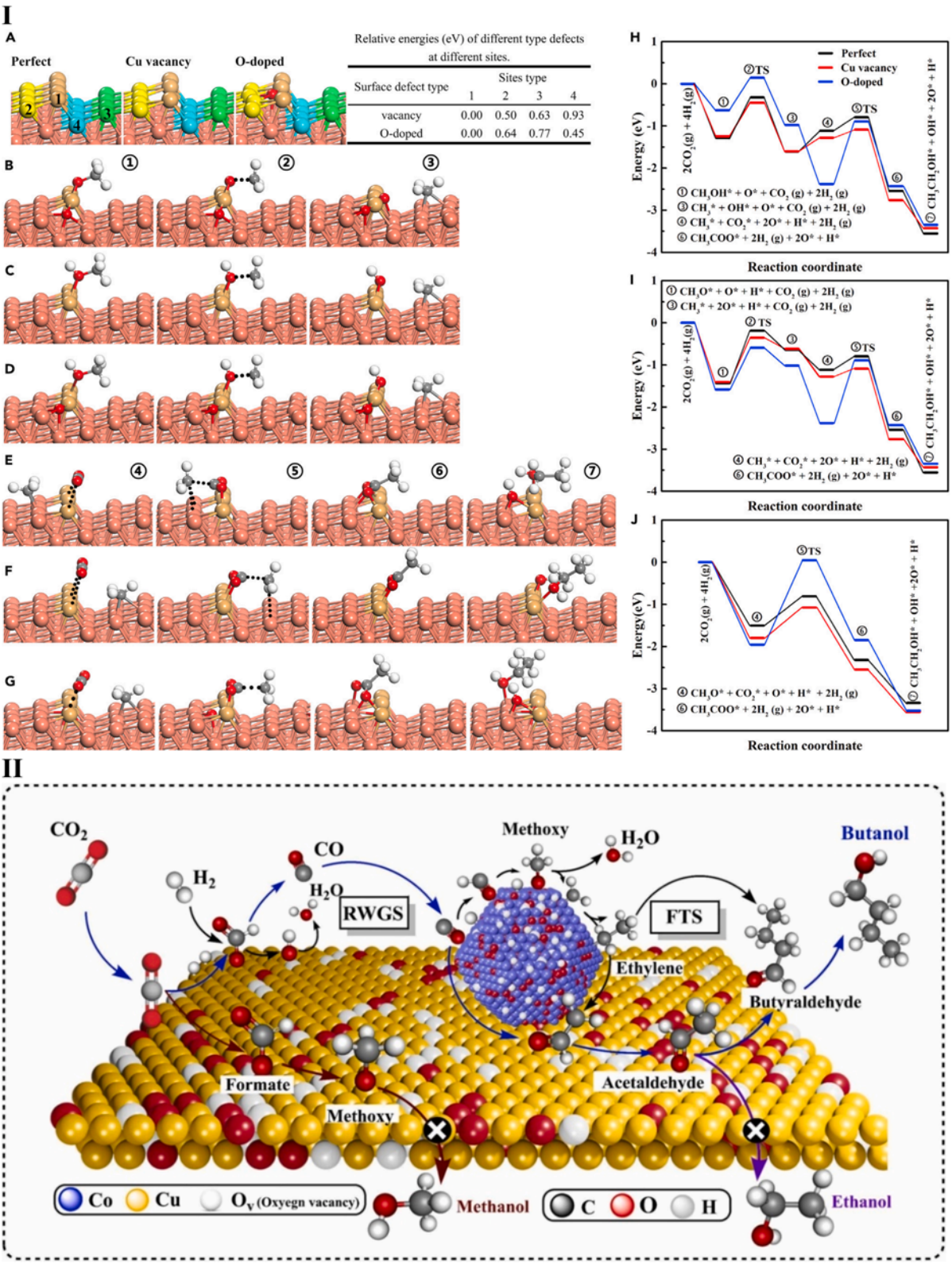

Fig. 20. I – Reaction pathway of CO_2 to ethanol and reaction energetics calculated by DFT. (A) Illustrations of perfect, Cu vacancy, and O-doped surfaces on the edges. The differently colored atoms represent different sites on first layer (yellowish-brown for site type 1, yellow for site type 2, green for site type 3, and blue for site type 4. Dark brown sphere is for Cu at lower layers). (B–D) Illustrations of the initial state, transition state, and final state of methyl formation fromCH_3O^* on (B) O-doped Cu(221) and fromCH_3OH on (C) Cu vacancy defect surface and (D) O-doped surface. (E–J) Illustrations of the initial state, transition state, and final state of $CO_2 + CH_3$ reaction paths on (E) Cu vacancy defect surface, (F) perfect surface, (G) O-doped surface and potential energy surfaces for the reaction of (H) $CO_2 + CH_3OH \rightarrow CO_2 + CH_3 \rightarrow CH_3CH_2OH$, (I) $CO_2 + CH_3O \rightarrow CO_2 + CH_3 \rightarrow CH_3CH_2OH$, and (J) $CO_2 + CH_3O \rightarrow CH_3CH_2OH$. Dark brown sphere, Cu; red sphere, O; gray sphere, C; white sphere, H; yellowish-brown, Cu on edge. Adapted with permission from Ref. [147]. II – Schematic depicting a plausible reaction mechanism and intermediates for the synthesis of n-butanol from CO_2 hydrogenation over the Na–CuCo-9 catalyst. Adapted with permission from Ref. [165]. (For interpretation of the references to colour in this figure legend, the reader is referred to the web version of this article.)

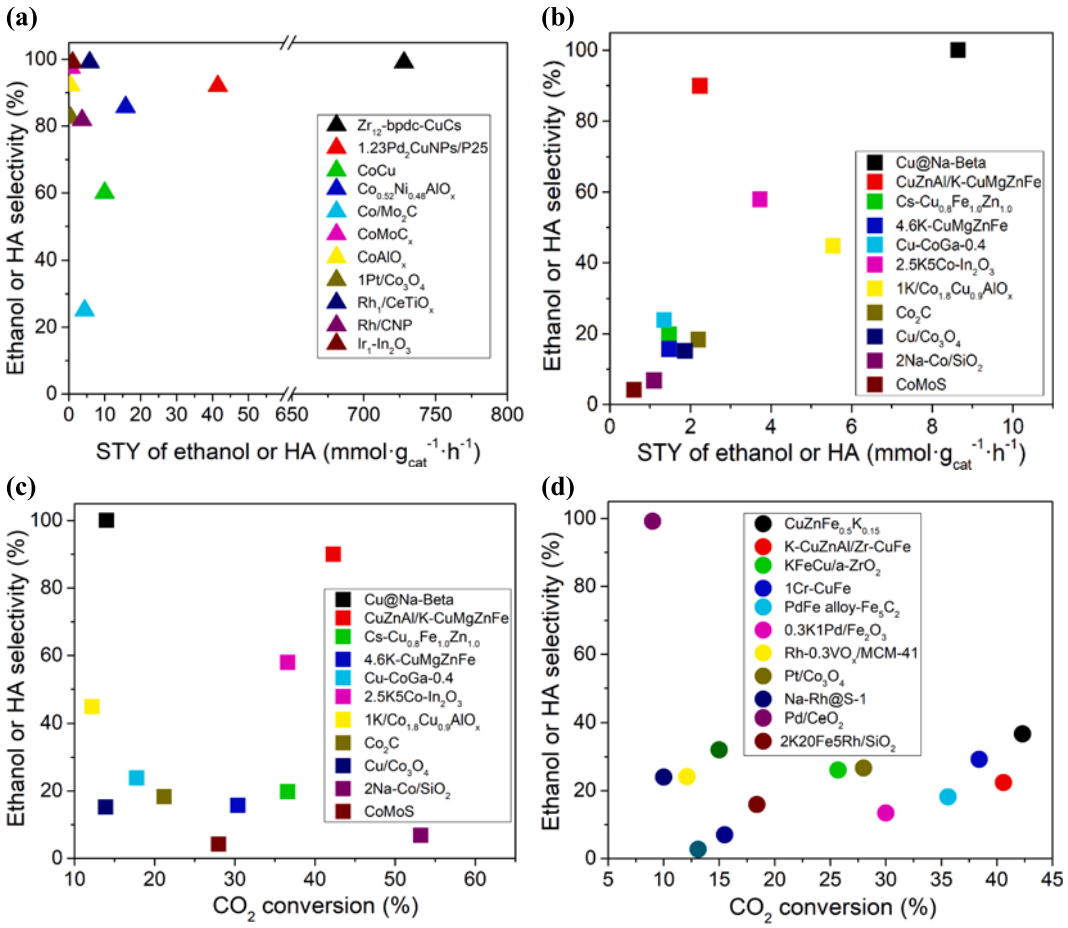

Fig. 21. Comparison of ethanol and HA production from CO_2 hydrogenation in batch (a) and fixed-bed reactors (b–d).

based catalysts > noble-metal catalysts > Co-based catalysts (Fig. 21**a**). While most catalysts were tested in continuous flow fixed-bed reactors, intriguingly, the highest catalytic performances were observed in batch reactors, particularly when various solvents were present. One explanation for the high STY of ethanol and HA in batch reactors is the "solvent entrapment effect." Polar solvents, in particular, have been shown to significantly enhance ethanol and HA selectivity by participating in specific elementary reactions and increasing the solubility of CO_2. Mechanistically, these solvents likely stabilize polar intermediates on the catalyst surface, promoting reaction pathways such as the formate/methoxy mechanism, alkyl-formate coupling, formyl-methanol coupling, and alkyl-CO_2 coupling [5]. These pathways are less commonly observed in fixed-bed continuous flow reactors where solvents are typically absent. Through careful catalyst design, both noble and non-noble metal catalysts can achieve remarkable ethanol (or HA) selectivity (greater than 90 %) and STY, often surpassing the performance of fixed-bed reactors by several times. This optimization of catalyst structure enables enhanced interaction with reactants, contributing to superior catalytic efficiency. For example, the Zr_{12}-bpdc-CuCs catalyst in a batch reactor achieved an impressive STY of 728 mmol·g_{cat}^{-1}·h^{-1} (Fig. 21**a**), which is significantly higher than that of most fixed-bed reactors. This underscores the importance of solvent effects and the potential for optimizing catalytic performance through careful catalyst design, irrespective of whether noble or non-noble metals are used.

However, it is also important to note that while batch reactors may offer enhanced selectivity and STY due to solvent interactions, they face inherent limitations such as the inability to operate continuously, a key advantage of fixed-bed reactors for industrial-scale applications. Furthermore, cost-effective catalysts based on Cu, Co, and Fe provide additional advantages in terms of scalability due to their simpler preparation methods and lower costs compared to more complex MOF-based catalysts, making them more suitable for large-scale industrial processes. In summary, the primary reasons for the clear differences in catalytic performance between batch and fixed-bed reactors are the presence of solvents, reaction mechanisms facilitated by solvent interactions, and the differences in contact time and reaction environment between the two reactor types. These factors significantly influence the selectivity and yield of ethanol and highlight the importance of tailoring catalysts specifically to the operating conditions of each reactor system.

In fixed-bed continuous flow reactors, the catalyst families rank as Cu-based > Co-based > noble-metal > Fe-based catalysts in terms of their C_{2+} alcohols STY (Fig. 21**b**). In fixed-bed reactors, the selectivity and STY towards C_{2+} alcohols are typically low. This is attributed to the limited contact duration between the feed gas and catalyst, potentially leading to the destabilization of crucial surface species. It is hypothesized that prolonging the contact time can increase the chances of $CH_x - C(H)O_x$ coupling, consequently resulting in enhanced selectivity towards C_{2+} alcohols. Notably, the Cu@Na-Beta catalyst displayed exceptional catalytic activity in a fixed-bed reactor, achieving 100 % ethanol selectivity and STY of 8.64 mmol·g_{cat}^{-1}·h^{-1}, despite its relatively low CO_2 conversion (Fig. 21**b,c**). Similarly, noble-metal catalysts, such as Pd/CeO_2, exhibited high ethanol selectivity but even lower CO_2 conversion compared to the Cu@Na-Beta catalyst (Fig. 21**d**).

Considering both catalyst activity and cost considerations, Cu-based catalysts warrant increased attention in future explorations in both batch and fixed-bed reactors. Recent significant findings have highlighted the use of porous supports for accommodating small metal catalysts and tailoring the active sites at an atomic scale, particularly in enhancing selectivity towards C_{2+} alcohols. Further exploration is

warranted due to indications that the surface properties and confinement effects of porous supports play a role in influencing the stability of crucial surface species of trapped metals, similar to solvents. Moreover, it is crucial to further explore the capability of supports to transport adsorbed species to the enclosed active surface, thereby enhancing the collaborative synthesis of C_{2+} alcohols. This necessitates conducting more rigorous experiments, including $^{13}C/^{2}H$ labeled experiments and *in situ* infrared spectroscopy under high pressure, alongside theoretical calculations. The integration of these methods with *in situ* X-ray photoelectron spectroscopy, *in situ* X-ray absorption spectroscopy, *in situ* X-ray powder diffraction, and *in situ* transmission electron microscopy is paramount for future studies aimed at achieving an advanced understanding of the reaction mechanism at the atomic level. In conclusion, we anticipate that through improved/optimized catalyst preparation, comprehensive characterization, and thorough mechanistic investigations, customized non-noble metal-based catalysts, potentially trimetallic ones with alkali metal promotion, could be engineered as next-generation catalytic systems for CO_2 hydrogenation, facilitating the synthesis of ethanol and/or HA. Finally, we are optimistic that these breakthroughs will soon yield advanced catalysts for synthesizing ethanol and/or HA, meeting the urgent demand for economically viable CO_2 conversion technologies suitable for widespread implementation.

6. Conclusions

In light of the pressing need to combat global warming, immediate action to reduce and ultimately eliminate CO_2 emissions is crucial. Over the past decade, evolving governmental policies and a shift in public opinion have driven extensive research efforts, not only to develop more efficient CO_2 capture technologies but also to explore methods for utilizing carbon-containing resources more effectively. One promising approach is the hydrogenation of CO_2 into C_{2+} alcohols, which holds potential as a viable technology for converting CO_2 into valuable chemicals and fuels. However, significant challenges remain, including low CO_2 conversion rates, insufficient selectivity for ethanol/HA, and issues related to catalyst stability. This review has provided a comprehensive analysis of the current progress in catalyst development for CO_2 hydrogenation to C_{2+} alcohols, with a focus on noble-metal and non-noble metal catalysts, such as Cu, Co, and Fe. Through detailed mechanistic studies, the kinetic limitations that govern the critical processes, such as C–C coupling, C–O dissociation, and C–H formation, have been identified as key factors influencing C_{2+} alcohol production. Achieving high selectivity towards C_{2+} alcohols requires the delicate balancing of adsorption behaviors and reaction pathways, which can be manipulated through careful catalyst design and the use of electronic promoters. The use of batch reactors, particularly in the presence of polar solvents, has demonstrated superior catalytic performances, largely attributed to the "solvent entrapment effect" that stabilizes polar intermediates and promotes key reaction mechanisms. However, batch reactors also face inherent limitations in terms of scalability and continuous operation, making fixed-bed reactors more suitable for industrial applications. Nevertheless, fixed-bed reactors still struggle with lower selectivity and STY due to limited interaction between the feed gas and catalyst, suggesting that strategies to enhance contact duration and improve catalyst stability could lead to better outcomes. In conclusion, Cu-based catalysts, particularly trimetallic ones with alkali metal promotion, emerge as promising candidates for future research due to their favorable activity, cost-effectiveness, and potential for enhanced C_{2+} alcohol selectivity. These catalysts hold significant promise for overcoming current challenges in CO_2 hydrogenation and advancing towards economically viable and scalable CO_2 conversion technologies. The exploration of porous supports and bifunctional catalysts, along with advanced *in situ* characterization techniques, will be crucial for developing next-generation catalysts. These advancements are expected to overcome current limitations and enable the efficient synthesis of C_{2+} alcohols, such as ethanol, thereby contributing to sustainable and economically viable CO_2 conversion technologies for widespread application.

CRediT authorship contribution statement

Andrii Kostyniuk: Writing – review & editing, Writing – original draft, Visualization, Validation, Software, Project administration, Methodology, Investigation, Data curation, Conceptualization. **Blaž Likozar:** Supervision, Resources, Project administration, Conceptualization.

Declaration of competing interest

The authors declare that they have no known competing financial interests or personal relationships that could have appeared to influence the work reported in this paper.

Acknowledgements

The authors express their gratitude for the financial support provided by the Slovenian Research Agency (ARIS) through the research Grant J7-4638 (Unlocking the selective catalytic conversion processes of CO_2 to ethanol – UliSess).

Appendix A. Supplementary data

Supplementary data to this article can be found online at https://doi.org/10.1016/j.cej.2024.158467.

Data availability

No data was used for the research described in the article.

References

[1] F. Zeng, C. Mebrahtu, X. Xi, L. Liao, J. Ren, J. Xie, H.J. Heeres, R. Palkovits, Catalysts design for higher alcohols synthesis by CO2 hydrogenation: Trends and future perspectives, Appl. Catal. B Environ. 291 (2021) 120073, https://doi.org/10.1016/j.apcatb.2021.120073.

[2] S. De, A. Dokania, A. Ramirez, J. Gascon, Advances in the Design of Heterogeneous Catalysts and Thermocatalytic Processes for CO2 Utilization, ACS Catal. 10 (2020) 14147–14185, https://doi.org/10.1021/acscatal.0c04273.

[3] I.C. Have, J.J.G. Kromwijk, M. Monai, F. Meirer, B.M. Weckhuysen, E.B. Sterk, Uncovering the reaction mechanism behind CoO as active phase for CO2 hydrogenation, Nat. Commun. 13 (2022), https://doi.org/10.1038/s41467-022-27981-x.

[4] S. Saeidi, S. Najari, V. Hessel, K. Wilson, F.J. Keil, P. Concepción, S.L. Suib, A. E. Rodrigues, Recent advances in CO2 hydrogenation to value-added products — Current challenges and future directions, Prog. Energy Combust. Sci. 85 (2021) 100905, https://doi.org/10.1016/j.pecs.2021.100905.

[5] D. Xu, Y. Wang, M. Ding, X. Hong, G. Liu, S.C.E. Tsang, Advances in higher alcohol synthesis from CO2 hydrogenation, Chem 7 (2021) 849–881, https://doi.org/10.1016/j.chempr.2020.10.019.

[6] X. Jiang, X. Nie, X. Guo, C. Song, J.G. Chen, Recent Advances in Carbon Dioxide Hydrogenation to Methanol via Heterogeneous Catalysis, Chem. Rev. 120 (2020) 7984–8034, https://doi.org/10.1021/acs.chemrev.9b00723.

[7] A. Ramirez, X. Gong, M. Caglayan, S.A.F. Nastase, E. Abou-Hamad, L. Gevers, L. Cavallo, A. Dutta Chowdhury, J. Gascon, Selectivity descriptors for the direct hydrogenation of CO2 to hydrocarbons during zeolite-mediated bifunctional catalysis, Nat. Commun. 12 (2021) 1–13, https://doi.org/10.1038/s41467-021-26090-5.

[8] K.Y. Kim, H. Lee, W.Y. Noh, J. Shin, S.J. Han, S.K. Kim, K. An, J.S. Lee, Cobalt Ferrite Nanoparticles to Form a Catalytic Co-Fe Alloy Carbide Phase for Selective CO2 Hydrogenation to Light Olefins, ACS Catal. 10 (2020) 8660–8671, https://doi.org/10.1021/acscatal.0c01417.

[9] H. Zhao, C. Zeng, N. Tsubaki, A mini review on recent advances in thermocatalytic hydrogenation of carbon dioxide to value-added chemicals and fuels, Resour, Chem. Mater. 1 (2022) 230–248, https://doi.org/10.1016/j.recm.2022.07.002.

[10] J.I. Orege, N. Liu, C.C. Amoo, J. Wei, Q. Ge, J. Sun, Boosting CO2 Hydrogenation to High-Value Olefins with Highly Stable Performance over Ba and Na Co-Modified Fe Catalyst ACS Paragon Plus Environment, J. Energy Chem. 80 (2023) 614–624, https://doi.org/10.1016/j.jechem.2023.02.007.

[11] L. Wang, Y. Han, J. Wei, Q. Ge, S. Lu, Y. Mao, J. Sun, Dynamic confinement catalysis in Fe-based CO2 hydrogenation to light olefins, Appl. Catal. B Environ. 328 (2023) 122506, https://doi.org/10.1016/j.apcatb.2023.122506.

[12] S. Wang, L. Zhang, W. Zhang, P. Wang, Z. Qin, W. Yan, M. Dong, J. Li, J. Wang, L. He, U. Olsbye, W. Fan, Selective Conversion of CO2 into Propene and Butene, Chem 6 (2020) 3344–3363, https://doi.org/10.1016/j.chempr.2020.09.025.
[13] A. Dokania, A. Dutta Chowdhury, A. Ramirez, S. Telalovic, E. Abou-Hamad, L. Gevers, J. Ruiz-Martinez, J. Gascon, Acidity modification of ZSM-5 for enhanced production of light olefins from CO2, J. Catal. 381 (2020) 347–354, https://doi.org/10.1016/j.jcat.2019.11.015.
[14] C.G. Visconti, M. Martinelli, L. Falbo, A. Infantes-Molina, L. Lietti, P. Forzatti, G. Iaquaniello, E. Palo, B. Picutti, F. Brignoli, CO2 hydrogenation to lower olefins on a high surface area K-promoted bulk Fe-catalyst, Appl. Catal. B Environ. 200 (2017) 530–542, https://doi.org/10.1016/j.apcatb.2016.07.047.
[15] Y. Xu, P. Zhai, Y. Deng, J. Xie, X. Liu, S. Wang, D. Ma, Highly Selective Olefin Production from CO2 Hydrogenation on Iron Catalysts: A Subtle Synergy between Manganese and Sodium Additives, Angew, Chemie. 132 (2020) 21920–21928, https://doi.org/10.1002/ange.202009620.
[16] X. Liu, M. Xu, C. Cao, Z. Yang, J. Xu, Effects of Zinc on χ-Fe5C2 for Carbon Dioxide Hydrogenation to Olefins: Insights from Experimental and Density Function Theory Calculations, Chinese, J. Chem. Eng. 54 (2022) 206–214, https://doi.org/10.1016/j.cjche.2022.03.027.
[17] S. Tada, D. Li, M. Okazaki, H. Kinoshita, M. Nishijima, N. Yamauchi, Y. Kobayashi, K. Iyoki, Influence of Si/Al ratio of MOR type zeolites for bifunctional catalysts specific to the one-pass synthesis of lower olefins via CO2 hydrogenation, Catal. Today. (2022), https://doi.org/10.1016/j.cattod.2022.06.043.
[18] J. Bao, G. Yang, Y. Yoneyama, N. Tsubaki, Significant Advances in C1 Catalysis: Highly Efficient Catalysts and Catalytic Reactions, ACS Catal. 9 (2019) 3026–3053, https://doi.org/10.1021/acscatal.8b03924.
[19] L. Jie, W. Xin-yu, G.A.O. Xin-hua, T. Ju-mei, D. Bin, Z. Wei, J. Yong-jun, P. Reubroycharoen, Z. Jian-li, Z. Tian-sheng, Effect of Na promoter and reducing atmosphere on phase evolution of Fe-based catalyst and its CO2 hydrogenation performance, J. Fuel Chem. Technol. 50 (2022) 1573–1580, https://doi.org/10.1016/S1872-5813(22)60060-4.
[20] W. Gao, L. Guo, Q. Wu, C. Wang, X. Guo, Y. He, P. Zhang, G. Yang, G. Liu, J. Wu, N. Tsubaki, Capsule-like zeolite catalyst fabricated by solvent-free strategy for para-Xylene formation from CO2 hydrogenation, Appl. Catal. B Environ. 303 (2022) 120906, https://doi.org/10.1016/j.apcatb.2021.120906.
[21] L. Zhang, W. Gao, F. Wang, C. Wang, J. Liang, X. Guo, Y. He, G. Yang, N. Tsubaki, Highly selective synthesis of light aromatics from CO2 by chromium-doped ZrO2 aerogels in tandem with HZSM-5@SiO2 catalyst, Appl. Catal. B Environ. 328 (2023) 122535, https://doi.org/10.1016/j.apcatb.2023.122535.
[22] I. Nezam, W. Zhou, G.S. Gusmão, M.J. Realff, Y. Wang, A.J. Medford, C.W. Jones, Direct aromatization of CO2 via combined CO2 hydrogenation and zeolite-based acid catalysis, J. CO2 Util. 45 (2021), https://doi.org/10.1016/j.jcou.2020.101405.
[23] Y. Ni, Z. Chen, Y. Fu, Y. Liu, W. Zhu, Z. Liu, Selective conversion of CO2 and H2 into aromatics, Nat. Commun. 9 (2018) 1–7, https://doi.org/10.1038/s41467-018-05880-4.
[24] Y. Wang, W. Gao, S. Kazumi, H. Li, G. Yang, N. Tsubaki, Direct and Oriented Conversion of CO2 into Value-Added Aromatics, Chem. - A Eur. J. 25 (2019) 5149–5153, https://doi.org/10.1002/chem.201806165.
[25] Y. Wang, L. Tan, M. Tan, P. Zhang, Y. Fang, Y. Yoneyama, G. Yang, N. Tsubaki, Rationally Designing Bifunctional Catalysts as an Efficient Strategy to Boost CO2 Hydrogenation Producing Value-Added Aromatics, ACS Catal. 9 (2019) 895–901, https://doi.org/10.1021/acscatal.8b01344.
[26] Y. Wang, S. Kazumi, W. Gao, X. Gao, H. Li, X. Guo, Y. Yoneyama, G. Yang, N. Tsubaki, Direct conversion of CO2 to aromatics with high yield via a modified Fischer-Tropsch synthesis pathway, Appl. Catal. B Environ. 269 (2020) 118792, https://doi.org/10.1016/j.apcatb.2020.118792.
[27] J. Mertens, C. Breyer, K. Arning, R. Belmans, A. Dibenedetto, S. Erkman, J. Gripekoven, Carbon capture and utilization: More than hiding CO2 for some time, Joule. (2023) 1–8, https://doi.org/10.1016/j.joule.2023.01.005.
[28] A. Álvarez, A. Bansode, A. Urakawa, A.V. Bavykina, T.A. Wezendonk, M. Makkee, J. Gascon, F. Kapteijn, Challenges in the Greener Production of Formates/Formic Acid, Methanol, and DME by Heterogeneously Catalyzed CO2 Hydrogenation Processes, Chem. Rev. 117 (2017) 9804–9838, https://doi.org/10.1021/acs.chemrev.6b00816.
[29] A.A. Al-Qadri, G.A. Nasser, H. Adamu, O. Muraza, T.A. Saleh, CO2 utilization in syngas conversion to dimethyl ether and aromatics: roles and challenges of zeolites-based catalysts, J. Energy Chem. 79 (2023) 418–449, https://doi.org/10.1016/j.jechem.2022.12.037.
[30] A. Ramirez, A. Dutta Chowdhury, M. Caglayan, A. Rodriguez-Gomez, N. Wehbe, E. Abou-Hamad, L. Gevers, S. Ould-Chikh, J. Gascon, Coated sulfated zirconia/SAPO-34 for the direct conversion of CO2 to light olefins, Catal. Sci. Technol. 10 (2020) 1507–1517, https://doi.org/10.1039/c9cy02532d.
[31] L. Guo, J. Sun, X. Ji, J. Wei, Z. Wen, R. Yao, H. Xu, Q. Ge, Directly converting carbon dioxide to linear α-olefins on bio-promoted catalysts, Commun. Chem. 1 (2018) 1–8, https://doi.org/10.1038/s42004-018-0012-4.
[32] C. Zhu, C. Huang, M. Zhang, K. Fang, Design of ZSM-5 encapsulating FeMnK nanocatalysts for light olefins synthesis with enhanced carbon utilization efficiency, Fuel 335 (2023) 126745, https://doi.org/10.1016/j.fuel.2022.126745.
[33] T. Numpilai, C. Wattanakit, M. Chareonpanich, J. Limtrakul, T. Witoon, Optimization of synthesis condition for CO2 hydrogenation to light olefins over In2O3 admixed with SAPO-34, Energy Convers. Manag. 180 (2019) 511–523, https://doi.org/10.1016/j.enconman.2018.11.011.
[34] R. Liu, D. Leshchev, E. Stavitski, M. Juneau, J.N. Agwara, M.D. Porosoff, Selective hydrogenation of CO2 and CO over potassium promoted Co/ZSM-5, Appl. Catal. B Environ. 284 (2021) 119787, https://doi.org/10.1016/j.apcatb.2020.119787.
[35] Z. Zhang, C. Wei, L. Jia, Y. Liu, C. Sun, P. Wang, W. Tu, Insights into the regulation of FeNa catalysts modified by Mn promoter and their tuning effect on the hydrogenation of CO2 to light olefins, J. Catal. 390 (2020) 12–22, https://doi.org/10.1016/j.jcat.2020.07.020.
[36] M. Albrecht, U. Rodemerck, M. Schneider, M. Bröring, D. Baabe, E. V. Kondratenko, Unexpectedly efficient CO2 hydrogenation to higher hydrocarbons over non-doped Fe2O3, Appl. Catal. B Environ. 204 (2017) 119–126, https://doi.org/10.1016/j.apcatb.2016.11.017.
[37] A.J. Barrios, D.V. Peron, A. Chakkingal, A.I. Dugulan, S. Moldovan, K. Nakouri, J. Thuriot-roukos, R. Wojcieszak, J.W. Thybaut, M. Virginie, A.Y. Khodakov, Efficient Promoters and Reaction Paths in the CO2 Hydrogenation to Light Olefins over Zirconia-Supported Iron Catalysts, ACS Catal. 12 (2022) 3211–3225, https://doi.org/10.1021/acscatal.1c05648.
[38] Z. Zhang, H. Yin, G. Yu, S. He, J. Kang, Z. Liu, K. Cheng, Q. Zhang, Y. Wang, Selective hydrogenation of CO2 and CO into olefins over Sodium- and Zinc-Promoted iron carbide catalysts, J. Catal. 395 (2021) 350–361, https://doi.org/10.1016/j.jcat.2021.01.036.
[39] W. Zhang, S. Wang, S. Guo, Z. Qin, M. Dong, J. Wang, W. Fan, Effective conversion of CO2 into light olefins along with generation of low amounts of CO, J. Catal. 413 (2022) 923–933, https://doi.org/10.1016/j.jcat.2022.07.041.
[40] J. Wei, R. Yao, Y. Han, Q. Ge, J. Sun, Towards the development of the emerging process of CO2 heterogenous hydrogenation into high-value unsaturated heavy hydrocarbons, Chem. Soc. Rev. 50 (2021) 10764–10805, https://doi.org/10.1039/d1cs00260k.
[41] T. Numpilai, N. Chanlek, Y. Poo-Arporn, S. Wannapaiboon, C.K. Cheng, N. Siri-Nguan, T. Sornchamni, P. Kongkachuichay, M. Chareonpanich, G. Rupprechter, J. Limtrakul, T. Witoon, Pore size effects on physicochemical properties of Fe-Co/K-Al2O3 catalysts and their catalytic activity in CO2 hydrogenation to light olefins, Appl. Surf. Sci. 483 (2019) 581–592, https://doi.org/10.1016/j.apsusc.2019.03.331.
[42] E.C. Ra, K.Y. Kim, E.H. Kim, H. Lee, K. An, J.S. Lee, Recycling Carbon Dioxide through Catalytic Hydrogenation: Recent Key Developments and Perspectives, ACS Catal. 10 (2020) 11318–11345, https://doi.org/10.1021/acscatal.0c02930.
[43] A. Dokania, A. Ramirez, A. Bavykina, J. Gascon, Heterogeneous Catalysis for the Valorization of CO2: Role of Bifunctional Processes in the Production of Chemicals, ACS Energy Lett. 4 (2019) 167–176, https://doi.org/10.1021/acsenergylett.8b01910.
[44] Z. Li, Y. Qu, J. Wang, H. Liu, M. Li, S. Miao, C. Li, Highly Selective Conversion of Carbon Dioxide to Aromatics over Tandem Catalysts, Joule. 3 (2019) 570–583, https://doi.org/10.1016/j.joule.2018.10.027.
[45] A. Ramirez, A. Dutta Chowdhury, A. Dokania, P. Cnudde, M. Caglayan, I. Yarulina, E. Abou-Hamad, L. Gevers, S. Ould-Chikh, K. De Wispelaere, V. Van Speybroeck, J. Gascon, Effect of Zeolite Topology and Reactor Configuration on the Direct Conversion of CO2 to Light Olefins and Aromatics, ACS Catal. 9 (2019) 6320–6334, https://doi.org/10.1021/acscatal.9b01466.
[46] W. Gao, L. Guo, Y. Cui, G. Yang, Y. He, C. Zeng, A. Taguchi, T. Abe, Q. Ma, Y. Yoneyama, N. Tsubaki, Selective Conversion of CO2 into para-Xylene over a ZnCr2O4-ZSM-5 Catalyst, ChemSusChem 13 (2020) 6541–6545, https://doi.org/10.1002/cssc.202002305.
[47] J. Zhang, M. Zhang, S. Chen, X. Wang, Z. Zhou, Y. Wu, T. Zhang, G. Yang, Y. Han, Y. Tan, Hydrogenation of CO2 into aromatics over a ZnCrOx-zeolite composite catalyst, Chem. Commun. 55 (2019) 973–976, https://doi.org/10.1039/c8cc09019j.
[48] Y. Li, L. Zeng, G. Pang, X. Wei, M. Wang, K. Cheng, J. Kang, J.M. Serra, Q. Zhang, Y. Wang, Direct conversion of carbon dioxide into liquid fuels and chemicals by coupling green hydrogen at high temperature, Appl. Catal. B Environ. 324 (2023) 122299, https://doi.org/10.1016/j.apcatb.2022.122299.
[49] Y. Sheng, M.V. Polynski, M.K. Eswaran, B. Zhang, A.M.H. Lim, L. Zhang, J. Jiang, W. Liu, S.M. Kozlov, A review of mechanistic insights into CO2 reduction to higher alcohols for rational catalyst design, Appl. Catal. B Environ. 343 (2024) 123550, https://doi.org/10.1016/j.apcatb.2023.123550.
[50] Y. He, F.H. Müller, R. Palkovits, F. Zeng, C. Mebrahtu, Tandem catalysis for CO2 conversion to higher alcohols: A review, Appl. Catal. B Environ. 345 (2024) 123663, https://doi.org/10.1016/j.apcatb.2023.123663.
[51] H. Huo, H. He, C. Huang, X. Guan, F. Wu, Y. Du, H. Xing, E. Kan, A. Li, Solar-driven CO2-to-ethanol conversion enabled by continuous CO2 transport via a superhydrophobic Cu2O nano fence, Chem. Sci. 15 (2023) 1638–1647, https://doi.org/10.1039/d3sc05702j.
[52] R. Das K. Das B. Ray C.P. Vinod S.C. Peter Green transformation of CO2 to ethanol using water and sunlight by the combined effect of naturally abundant red phosphorus and Bi2MoO6 Energy Environ. Sci. (2022) 1967–1976. 10.1039/d1ee02976b.
[53] H. Yu, C. Sun, Y. Xuan, K. Zhang, K. Chang, Full solar spectrum driven plasmonic-assisted efficient photocatalytic CO2 reduction to ethanol, Chem. Eng. J. 430 (2022) 132940, https://doi.org/10.1016/j.cej.2021.132940.
[54] B. Rhimi, M. Zhou, Z. Yan, X. Cai, Z. Jiang, Cu-Based Materials for Enhanced C2+ Product Selectivity in Photo-/Electro-Catalytic CO2 Reduction: Challenges and Prospects, Springer Nature Singapore (2024), https://doi.org/10.1007/s40820-023-01276-2.
[55] S. Hao, Y. Chen, C. Peng, H. Wang, Q. Wen, C. Hu, L. Zhang, Q. Han, G. Zheng, Photocatalytic Coupling of CH4 and CO2 to Ethanol on Asymmetric Ce−O−Zn Sites, Adv. Funct. Mater. 2314118 (2023) 1–7, https://doi.org/10.1002/adfm.202314118.

[56] S. Gong, B. Ni, X. He, J. Wang, K. Jiang, D. Wu, Y. Min, H. Li, Z. Chen, Electronic modulation of a single-atom-based tandem catalyst boosts CO2 photoreduction to ethanol, Energy Environ. Sci. 16 (2023) 5956–5969, https://doi.org/10.1039/d3ee02643d.
[57] S. Nitopi, E. Bertheussen, S.B. Scott, X. Liu, A.K. Engstfeld, S. Horch, B. Seger, I.E. L. Stephens, K. Chan, C. Hahn, J.K. Nørskov, T.F. Jaramillo, I. Chorkendorff, Progress and Perspectives of Electrochemical CO_2 Reduction on Copper in Aqueous Electrolyte, Chem. Rev. 119 (2019) 7610–7672, https://doi.org/10.1021/acs.chemrev.8b00705.
[58] W. Ma, S. Xie, T. Liu, Q. Fan, J. Ye, F. Sun, Z. Jiang, Q. Zhang, J. Cheng, Y. Wang, Electrocatalytic reduction of CO2 to ethylene and ethanol through hydrogen-assisted C–C coupling over fluorine-modified copper, Nat. Catal. 3 (2020) 478–487, https://doi.org/10.1038/s41929-020-0450-0.
[59] A. Dutta, I.Z. Montiel, R. Erni, K. Kiran, M. Rahaman, J. Drnec, P. Broekmann, Activation of bimetallic AgCu foam electrocatalysts for ethanol formation from CO_2 by selective Cu oxidation/reduction, Nano Energy 68 (2020) 104331, https://doi.org/10.1016/j.nanoen.2019.104331.
[60] H. Xu, D. Rebollar, H. He, L. Chong, Y. Liu, C. Liu, C.J. Sun, T. Li, J.V. Muntean, R. E. Winans, D.J. Liu, T. Xu, Highly selective electrocatalytic CO2 reduction to ethanol by metallic clusters dynamically formed from atomically dispersed copper, Nat. Energy. 5 (2020) 623–632, https://doi.org/10.1038/s41560-020-0666-x.
[61] R.E. Vos, K.E. Kolmeijer, T.S. Jacobs, W. Van Der Stam, B.M. Weckhuysen, M.T. M. Koper, How Temperature Affects the Selectivity of the Electrochemical CO2Reduction on Copper, ACS Catal. 13 (2023) 8080–8091, https://doi.org/10.1021/acscatal.3c00706.
[62] A. Singh, S. Barman, F.A. Rahimi, A. Dey, R. Jena, R. Kumar, N. Mathew, D. Bhattacharyya, T.K. Maji, Atomically dispersed Co2+ in a redox-active COF for electrochemical CO2 reduction to ethanol: unravelling mechanistic insight through operando studies, Energy Environ. Sci. (2024) 2315–2325, https://doi.org/10.1039/d3ee02946h.
[63] R. Purbia, S.Y. Choi, C.H. Woo, J. Jeon, C. Lim, D.K. Lee, J.Y. Choi, H.S. Oh, J. M. Baik, Highly selective and low-overpotential electrocatalytic CO2 reduction to ethanol by Cu-single atoms decorated N-doped carbon dots, Appl. Catal. B Environ. 345 (2024) 123694, https://doi.org/10.1016/j.apcatb.2024.123694.
[64] S. Das, J. Pérez-Ramírez, J. Gong, N. Dewangan, K. Hidajat, B.C. Gates, S. Kawi, Core-shell structured catalysts for thermocatalytic, photocatalytic, and electrocatalytic conversion of CO2, Chem. Soc. Rev. 49 (2020) 2937–3004, https://doi.org/10.1039/c9cs00713j.
[65] Basf, Process for the production of hydrocarbons and their derivatives, German Patent DE293787C (1913).
[66] A. Mittasch, M. Pier, K. Winkler, Implementation of Organic Catalyses, BASF, German Patent DE415686C (1923).
[67] A. Mittasch, K. Winkler, M. Pier, Process for the production of organic compounds through catalytic gas reactions, BASF, German Patent DE441433C (1927).
[68] Basf, Process for the production of oxygen-containing organic compounds from oxides of carbon through reduction, German Patent DE462837C (1928).
[69] A. Beck, M.A. Newton, L.G.A. van de Water, J.A. van Bokhoven, The Enigma of Methanol Synthesis by Cu/ZnO/Al2O3-based Catalysts, Chem. Rev. 124 (2024) 4543–4678, https://doi.org/10.1021/acs.chemrev.3c00148.
[70] S. Otto, U. Johannes, Manufacturing methanol synthetically, BASF, Canadian Patent, CA251486A (1925).
[71] L.H. Vieira, A.H.M. da Silva, C.S. Santana, E.M. Assaf, J.M. Assaf, J.F. Gomes, Recent Understanding of Water-Assisted CO2 Hydrogenation to Alcohols, ChemCatChem 202301390 (2024) e202301390, https://doi.org/10.1002/cctc.202301390.
[72] S. Kattel, P.J. Ramírez, J.G. Chen, J.A. Rodriguez, P. Liu, Active sites for CO2 hydrogenation to methanol on Cu/ZnO catalysts, Science (80-.). 355 (2017) 1296–1299. doi: 10.1126/science.aal3573.
[73] X. Wang, P.J. Ramírez, W. Liao, J.A. Rodriguez, P. Liu, Cesium-Induced Active Sites for C-C Coupling and Ethanol Synthesis from CO2 Hydrogenation on Cu/ZnO(0001) Surfaces, J. Am. Chem. Soc. 143 (2021) 13103–13112, https://doi.org/10.1021/jacs.1c03940.
[74] T. Tatsumi, A. Muramatsu, H. Tominaga, Alcohol synthesis from CO2/H2 on silica-supported molybdenum catalysts, Chem. Lett. 21 (1985) 162.
[75] C.H. Vo, J. Peréz-Ramírez, S. Farooq, I.A. Karimi, Prospects of Producing Higher Alcohols from Carbon Dioxide: A Process System Engineering Perspective, ACS Sustain. Chem. Eng. 10 (2022) 11875–11884, https://doi.org/10.1021/acssuschemeng.2c02810.
[76] A. Kostyniuk, D. Bajec, B. Likozar, One-step synthesis of ethanol from glycerol in a gas phase packed bed reactor over hierarchical alkali-treated zeolite catalyst materials, Green Chem. 22 (2020) 753–765, https://doi.org/10.1039/c9gc03262b.
[77] Y. Wang, K. Wang, B. Zhang, X. Peng, X. Gao, G. Yang, H. Hu, M. Wu, N. Tsubaki, Direct Conversion of CO2 to Ethanol Boosted by Intimacy-Sensitive Multifunctional Catalysts, ACS Catal. 11 (2021) 11742–11753, https://doi.org/10.1021/acscatal.1c01504.
[78] X. Luan, Z. Ren, X. Dai, X. Zhang, J. Yong, Y. Yang, H. Zhao, M. Cui, F. Nie, X. Huang, Selective Conversion of Syngas into Higher Alcohols via a Reaction-Coupling Strategy on Multifunctional Relay Catalysts, ACS Catal. 10 (2020) 2419–2430, https://doi.org/10.1021/acscatal.9b04111.
[79] A. Ramirez, P. Ticali, D. Salusso, T. Cordero-Lanzac, S. Ould-Chikh, C. Ahoba-Sam, A.L. Bugaev, E. Borfecchia, S. Morandi, M. Signorile, S. Bordiga, J. Gascon, U. Olsbye, Multifunctional Catalyst Combination for the Direct Conversion of CO2 to Propane, JACS Au (2021), https://doi.org/10.1021/jacsau.1c00302.
[80] C. Wang, T. Lin, X. Qi, F. Yu, Y. Lu, L. Zhong, Y. Sun, Direct Conversion of Syngas to Higher Alcohols over Multifunctional Catalyst: The Role of Copper-Based Component and Catalytic Mechanism, J. Phys. Chem. c. 125 (2021) 6137–6146, https://doi.org/10.1021/acs.jpcc.1c01006.
[81] A. Dokania, S. Ould-Chikh, A. Ramirez, J.L. Cerrillo, A. Aguilar, A. Russkikh, A. Alkhalaf, I. Hita, A. Bavykina, G. Shterk, N. Wehbe, A. Prat, E. Lahera, P. Castaño, E. Fonda, J.-L. Hazemann, J. Gascon, Designing a Multifunctional Catalyst for the Direct Production of Gasoline-Range Isoparaffins from CO2, JACS Au 1 (2021) 1961–1974, https://doi.org/10.1021/jacsau.1c00317.
[82] S. Zhang, C. Huang, Z. Shao, H. Zhou, J. Chen, L. Li, J. Lu, X. Liu, H. Luo, L. Xia, H. Wang, Y. Sun, Revealing and Regulating the Complex Reaction Mechanism of CO2 Hydrogenation to Higher Alcohols on Multifunctional Tandem Catalysts, ACS Catal. 13 (2023) 3055–3065, https://doi.org/10.1021/acscatal.2c06245.
[83] Y. He, S. Liu, W. Fu, C. Wang, C. Mebrahtu, R. Sun, F. Zeng, Thermodynamic Analysis of CO2 Hydrogenation to Higher Alcohols (C2−4OH): Effects of Isomers and Methane, ACS Omega 7 (2022) 16502–16514, https://doi.org/10.1021/acsomega.2c00502.
[84] Y. He, W. Fu, Z. Tang, S. Liu, J. Chen, Q. Zhong, X. Tan, R. Sun, C. Mebrahtu, F. Zeng, Thermodynamic analysis of ethanol synthesis by CO2 hydrogenation using Aspen Plus: effects of tail gas recycling and CO co-feeding, Chem. Eng. Commun. 211 (2024) 300–310, https://doi.org/10.1080/00986445.2023.2240709.
[85] Y. He, S. Liu, W. Fu, J. Chen, Y. Zhai, X. Bi, J. Ren, R. Sun, Z. Tang, C. Mebrahtu, F. Zeng, Assessing the efficiency of CO2 hydrogenation for emission reduction: Simulating ethanol synthesis process as a case study, Chem. Eng. Res. Des. 195 (2023) 106–115, https://doi.org/10.1016/j.cherd.2023.05.043.
[86] T. Fuels, C.H. Vo, C. Mondelli, H. Hamedi, P. Javier, S. Farooq, I.A. Karimi, Sustainability Assessment of Thermocatalytic Conversion of CO2 to Transportation Fuels, Methanol, and 1-Propanol, ACS Sustain. Chem. Eng. 9 (2021) 10591–10600, https://doi.org/10.1021/acssuschemeng.1c02805.
[87] W. Wang, C. Zeng, N. Tsubaki, Recent advancements and perspectives of the CO2 hydrogenation reaction, Green, Carbon 1 (2023) 133–145, https://doi.org/10.1016/j.greenca.2023.10.003.
[88] S. Liu, Y. He, W. Fu, J. Chen, J. Ren, L. Liao, R. Sun, Z. Tang, C. Mebrahtu, F. Zeng, Hetero-site cobalt catalysts for higher alcohols synthesis by CO2 hydrogenation: A review, J. CO2 Util. 67 (2023) 102322, https://doi.org/10.1016/j.jcou.2022.102322.
[89] Y.A. Alli, P.O. Oladoye, O. Ejeromedoghene, O.M. Bankole, O.A. Alimi, E. O. Omotola, C.A. Olanrewaju, K. Philippot, A.S. Adeleye, A.S. Ogunlaja, Nanomaterials as catalysts for CO2 transformation into value-added products: A review, Sci. Total Environ. 868 (2023) 161547, https://doi.org/10.1016/j.scitotenv.2023.161547.
[90] J. Gao, S. Choo Sze Shiong, Y. Liu, Reduction of CO2 to chemicals and Fuels: Thermocatalysis versus electrocatalysis, Chem. Eng. J. 472 (2023) 145033, https://doi.org/10.1016/j.cej.2023.145033.
[91] S. Schemme, J.L. Breuer, R.C. Samsun, R. Peters, D. Stolten, Promising catalytic synthesis pathways towards higher alcohols as suitable transport fuels based on H2 and CO2, J. CO2 Util. 27 (2018) 223–237, https://doi.org/10.1016/j.jcou.2018.07.013.
[92] G. Prieto, Carbon Dioxide Hydrogenation into Higher Hydrocarbons and Oxygenates: Thermodynamic and Kinetic Bounds and Progress with Heterogeneous and Homogeneous Catalysis, ChemSusChem 10 (2017) 1056–1070, https://doi.org/10.1002/cssc.201601591.
[93] R.P. Ye, J. Ding, W. Gong, M.D. Argyle, Q. Zhong, Y. Wang, C.K. Russell, Z. Xu, A. G. Russell, Q. Li, M. Fan, Y.G. Yao, CO2 hydrogenation to high-value products via heterogeneous catalysis, Nat. Commun. 10 (2019), https://doi.org/10.1038/s41467-019-13638-9.
[94] X. Li, M. Song, Y. Zhou, P. Zhou, D. Xu, T. Liu, X. Hong, Support-induced structural changes in CO2 hydrogenation to higher alcohols over metal/oxide catalysts, ChemCatChem (2024) e202301577, https://doi.org/10.1002/cctc.202301577.
[95] A.I. Latsiou, N.D. Charisiou, Z. Frontistis, A. Bansode, M.A. Goula, CO2 hydrogenation for the production of higher alcohols: Trends in catalyst developments, challenges and opportunities, Catal. Today. 420 (2023) 114179, https://doi.org/10.1016/j.cattod.2023.114179.
[96] X. Li, J. Ke, R. Li, P. Li, Q. Ma, T.S. Zhao, Research progress of hydrogenation of carbon dioxide to ethanol, Chem. Eng. Sci. 282 (2023) 119226, https://doi.org/10.1016/j.ces.2023.119226.
[97] S.S. Ali, S.S. Ali, N. Tabassum, A review on CO2 hydrogenation to ethanol: Reaction mechanism and experimental studies, J. Environ. Chem. Eng. 10 (2022) 106962, https://doi.org/10.1016/j.jece.2021.106962.
[98] Y.Z. Mao, F. Zha, H.F. Tian, X.H. Tang, Y. Chang, X.J. Guo, Progress in the thermo-catalytic hydrogenation of CO2 to ethanol, J. Fuel Chem. Technol. 51 (2023) 1515–1528, https://doi.org/10.1016/S1872-5813(22)60065-3.
[99] J. Zhong, X. Yang, Z. Wu, B. Liang, Y. Huang, T. Zhang, State of the art and perspectives in heterogeneous catalysis of CO2 hydrogenation to methanol, Chem. Soc. Rev. 49 (2020) 1385–1413, https://doi.org/10.1039/c9cs00614a.
[100] S.-N. Jaén, M. Virginie, J. Bonin, M. Robert, R. Wojcieszak, A.Y. Khodakov, Highlights and challenges in the selective reduction of carbon dioxide to methanol, Nat. Rev. Chem. 5 (2021).
[101] J. Zhu, Y. Su, J. Chai, V. Muravev, N. Kosinov, E.J.M. Hensen, Mechanism and Nature of Active Sites for Methanol Synthesis from CO/CO2on Cu/CeO2, ACS Catal. 10 (2020) 11532–11544, https://doi.org/10.1021/acscatal.0c02909.
[102] A. Velty, A. Corma, Advanced zeolite and ordered mesoporous silica-based catalysts for the conversion of CO2 to chemicals and fuels, Chem. Soc. Rev. 52 (2023) 1773–1946, https://doi.org/10.1039/d2cs00456a.

[103] W. Wang, Z. Qu, L. Song, Q. Fu, CO2 hydrogenation to methanol over Cu/CeO2 and Cu/ZrO2 catalysts: Tuning methanol selectivity via metal-support interaction, J. Energy Chem. 40 (2020) 22–30, https://doi.org/10.1016/j.jechem.2019.03.001.
[104] T. Witoon, J. Chalorngtham, P. Dumrongbunditkul, M. Chareonpanich, J. Limtrakul, CO2 hydrogenation to methanol over Cu/ZrO2 catalysts: Effects of zirconia phases, Chem. Eng. J. 293 (2016) 327–336, https://doi.org/10.1016/j.cej.2016.02.069.
[105] J. Niu, H. Liu, Y. Jin, B. Fan, W. Qi, J. Ran, Comprehensive review of Cu-based CO2 hydrogenation to CH3OH: Insights from experimental work and theoretical analysis, Int. J. Hydrogen Energy. 47 (2022) 9183–9200, https://doi.org/10.1016/j.ijhydene.2022.01.021.
[106] H. Liang, G. Zhang, Z. Li, Y. Zhang, P. Fu, Catalytic hydrogenation of CO2 to methanol over Cu-based catalysts: Active sites profiling and regulation strategy as well as reaction pathway exploration, Fuel Process. Technol. 252 (2023) 107995, https://doi.org/10.1016/j.fuproc.2023.107995.
[107] M. Ao, G.H. Pham, J. Sunarso, M.O. Tade, S. Liu, Active Centers of Catalysts for Higher Alcohol Synthesis from Syngas: A Review, ACS Catal. 8 (2018) 7025–7050, https://doi.org/10.1021/acscatal.8b01391.
[108] M. Gupta, M.L. Smith, J.J. Spivey, Heterogeneous catalytic conversion of dry syngas to ethanol and higher alcohols on Cu-based catalysts, ACS Catal. 1 (2011) 641–656, https://doi.org/10.1021/cs2001048.
[109] Z. Cao, T. Hu, J. Guo, J. Xie, N. Zhang, J. Zheng, L. Che, B.H. Chen, Stable and facile ethanol synthesis from syngas in one reactor by tandem combination CuZnAl-HZSM-5, modified-H-Mordenite with CuZnAl catalyst, Fuel 254 (2019) 115542, https://doi.org/10.1016/j.fuel.2019.05.125.
[110] T. Lin, X. Qi, X. Wang, L. Xia, C. Wang, F. Yu, H. Wang, S. Li, L. Zhong, Y. Sun, Direct Production of Higher Oxygenates by Syngas Conversion over a Multifunctional Catalyst, Angew. Chemie - Int. Ed. 58 (2019) 4627–4631, https://doi.org/10.1002/anie.201814611.
[111] B. An, Z. Li, Y. Song, J. Zhang, L. Zeng, C. Wang, W. Lin, Cooperative copper centres in a metal–organic framework for selective conversion of CO2 to ethanol, Nat. Catal. 2 (2019) 709–717, https://doi.org/10.1038/s41929-019-0308-5.
[112] S. Bai, Q. Shao, P. Wang, Q. Dai, X. Wang, X. Huang, Highly Active and Selective Hydrogenation of CO2 to Ethanol by Ordered Pd-Cu Nanoparticles, J. Am. Chem. Soc. 139 (2017) 6827–6830, https://doi.org/10.1021/jacs.7b03101.
[113] S. Liu, C. Yang, S. Zha, D. Sharapa, F. Studt, Z.J. Zhao, J. Gong, Moderate Surface Segregation Promotes Selective Ethanol Production in CO2 Hydrogenation Reaction over CoCu Catalysts, Angew. Chemie - Int. Ed. 61 (2022), https://doi.org/10.1002/anie.202109027.
[114] Z. Wang, C. Yang, X. Li, X. Song, C. Pei, Z.J. Zhao, J. Gong, The role of CO2 dissociation in CO2 hydrogenation to ethanol on CoCu/silica catalysts, Nano Res. 16 (2023) 6128–6133, https://doi.org/10.1007/s12274-022-5092-x.
[115] L. Wang, S. He, L. Wang, Y. Lei, X. Meng, F.S. Xiao, Cobalt-Nickel Catalysts for Selective Hydrogenation of Carbon Dioxide into Ethanol, ACS Catal. 9 (2019) 11335–11340, https://doi.org/10.1021/acscatal.9b04187.
[116] Y. Chen, S. Choi, L.T. Thompson, Low temperature CO2 hydrogenation to alcohols and hydrocarbons over Mo2C supported metal catalysts, J. Catal. 343 (2016) 147–156, https://doi.org/10.1016/j.jcat.2016.01.016.
[117] H. Zhang, H. Han, L. Xiao, W. Wu, Highly Selective Synthesis of Ethanol via CO2 Hydrogenation over CoMoCx Catalysts, ChemCatChem 13 (2021) 3333–3339, https://doi.org/10.1002/cctc.202100204.
[118] L. Wang, L. Wang, J. Zhang, X. Liu, H. Wang, W. Zhang, Q. Yang, J. Ma, X. Dong, S.J. Yoo, J.G. Kim, X. Meng, F.S. Xiao, Selective Hydrogenation of CO2 to Ethanol over Cobalt Catalysts, Angew. Chemie - Int. Ed. 57 (2018) 6104–6108, https://doi.org/10.1002/anie.201800729.
[119] Z. He, Q. Qian, J. Ma, Q. Meng, H. Zhou, J. Song, Z. Liu, B. Han, Water-Enhanced Synthesis of Higher Alcohols from CO2 Hydrogenation over a Pt/Co3O4 Catalyst under Milder Conditions, Angew. Chemie - Int. Ed. 55 (2016) 737–741, https://doi.org/10.1002/anie.201507585.
[120] D. Wang, Q. Bi, G. Yin, W. Zhao, F. Huang, X. Xie, M. Jiang, Direct synthesis of ethanol via CO2 hydrogenation using supported gold catalysts, Chem. Commun. 52 (2016) 14226–14229, https://doi.org/10.1039/c6cc08161d.
[121] K. Zheng, Y. Li, B. Liu, F. Jiang, Y. Xu, X. Liu, Ti-doped CeO2 Stabilized Single-Atom Rhodium Catalyst for Selective and Stable CO2 Hydrogenation to Ethanol, Angew. Chemie - Int. Ed. 61 (2022), https://doi.org/10.1002/anie.202210991.
[122] K. Zheng, Y. Li, B. Liu, J. Chen, Y. Xu, Z. Li, X. Liu, Phosphorus-substituted atomically dispersed Rh-N3P1 sites for efficient promotion in CO2 hydrogenation towards ethanol production, Appl. Catal. B Environ. 346 (2024) 123730, https://doi.org/10.1016/j.apcatb.2024.123730.
[123] X. Ye, C. Yang, X. Pan, J. Ma, Y. Zhang, Y. Ren, X. Liu, L. Li, Y. Huang, Highly selective hydrogenation of CO2 to ethanol via designed bifunctional Ir1-In2O3 single-atom catalyst, J. Am. Chem. Soc. 142 (2020) 19001–19005, https://doi.org/10.1021/jacs.0c08607.
[124] D. Yang, W. Pei, S. Zhou, J. Zhao, W. Ding, Y. Zhu, Controllable Conversion of CO2 on Non-Metallic Gold Clusters, Angew. Chemie - Int. Ed. 59 (2020) 1919–1924, https://doi.org/10.1002/anie.201913635.
[125] X. Ye, J. Ma, W. Yu, X. Pan, C. Yang, C. Wang, Q. Liu, Y. Huang, Construction of bifunctional single-atom catalysts on the optimized β-Mo2C surface for highly selective hydrogenation of CO2 into ethanol, J. Energy Chem. 67 (2022) 184–192, https://doi.org/10.1016/j.jechem.2021.10.017.
[126] M. Cui, Q. Qian, Z. He, Z. Zhang, J. Ma, T. Wu, G. Yang, B. Han, Bromide promoted hydrogenation of CO2 to higher alcohols using Ru-Co homogeneous catalyst, Chem. Sci. 7 (2016) 5200–5205, https://doi.org/10.1039/c6sc01314g.
[127] T. Lin, F. Yu, Y. An, T. Qin, L. Li, K. Gong, L. Zhong, Y. Sun, Cobalt Carbide Nanocatalysts for Efficient Syngas Conversion to Value-Added Chemicals with High Selectivity, Acc. Chem. Res. 54 (2021) 1961–1971, https://doi.org/10.1021/acs.accounts.0c00883.
[128] C. Scarfiello, K. Soulantica, S. Cayez, A. Durupt, G. Viau, N. Le Breton, A. K. Boudalis, F. Meunier, G. Clet, M. Barreau, D. Salusso, S. Zafeiratos, D.P. Minh, P. Serp, Modified Co/TiO2 catalysts for CO2 hydrogenation to fuels, J. Catal. 428 (2023), https://doi.org/10.1016/j.jcat.2023.115202.
[129] Y. Li, Z. Zhao, W. Lu, M. Jiang, C. Li, M. Zhao, L. Gong, S. Wang, L. Guo, Y. Lyu, L. Yan, H. Zhu, Y. Ding, Highly Selective Conversion of Syngas to Higher Oxygenates over Tandem Catalysts, ACS Catal. 11 (2021) 14791–14802, https://doi.org/10.1021/acscatal.1c04442.
[130] W. Li, X. Nie, X. Jiang, A. Zhang, F. Ding, M. Liu, Z. Liu, X. Guo, C. Song, ZrO2 support imparts superior activity and stability of Co catalysts for CO2 methanation, Appl. Catal. B Environ. 220 (2018) 397–408, https://doi.org/10.1016/j.apcatb.2017.08.048.
[131] P. Riani, G. Garbarino, T. Cavattoni, G. Busca, CO2 hydrogenation and ethanol steam reforming over Co/SiO2 catalysts: Deactivation and selectivity switches, Catal. Today. 365 (2021) 122–131, https://doi.org/10.1016/j.cattod.2020.05.002.
[132] S. Liu, Y. He, W. Fu, J. Ren, J. Chen, H. Chen, R. Sun, Z. Tang, C. Mebrahtu, F. Zeng, Synergy of Co0-Co2+ in cobalt-based catalysts for CO2 hydrogenation: Quantifying via reduced and exposed atoms fraction, Appl. Catal. A Gen. 670 (2024) 119549, https://doi.org/10.1016/j.apcata.2023.119549.
[133] W. Fu, S. Liu, Y. He, J. Chen, J. Ren, H. Chen, R. Sun, Z. Tang, C. Mebrahtu, F. Zeng, CO2 hydrogenation over CoAl based catalysts: Effects of cobalt-metal oxide interaction, Appl. Catal. A Gen. 678 (2024) 119720, https://doi.org/10.1016/j.apcata.2024.119720.
[134] C. Wang, J. Zhang, G. Qin, L. Wang, E. Zuidema, Q. Yang, S. Dang, C. Yang, J. Xiao, X. Meng, C. Mesters, F.S. Xiao, Direct Conversion of Syngas to Ethanol within Zeolite Crystals, Chem 6 (2020) 646–657, https://doi.org/10.1016/j.chempr.2019.12.007.
[135] E. Sheerin, G.K. Reddy, P. Smirniotis, Evaluation of Rh/CexTi1-xO2 catalysts for synthesis of oxygenates from syngas using XPS and TPR techniques, Catal. Today. 263 (2016) 75–83, https://doi.org/10.1016/j.cattod.2015.07.050.
[136] X. Huang, D. Teschner, M. Dimitrakopoulou, A. Fedorov, B. Frank, R. Kraehnert, F. Rosowski, H. Kaiser, S. Schunk, C. Kuretschka, R. Schlögl, M.G. Willinger, A. Trunschke, Atomic-Scale Observation of the Metal–Promoter Interaction in Rh-Based Syngas-Upgrading Catalysts, Angew. Chemie - Int. Ed. 58 (2019) 8709–8713, https://doi.org/10.1002/anie.201902750.
[137] T. Qin, T. Lin, X. Qi, C. Wang, L. Li, Z. Tang, L. Zhong, Y. Sun, Tuning chemical environment and synergistic relay reaction to promote higher alcohols synthesis via syngas conversion, Appl. Catal. B Environ. 285 (2021) 119840, https://doi.org/10.1016/j.apcatb.2020.119840.
[138] G. Prieto, S. Beijer, M.L. Smith, M. He, Y. Au, Z. Wang, D.A. Bruce, K.P. De Jong, J.J. Spivey, P.E. De Jongh, Design and synthesis of copper-cobalt catalysts for the selective conversion of synthesis gas to ethanol and higher alcohols, Angew. Chemie - Int. Ed. 53 (2014) 6397–6401, https://doi.org/10.1002/anie.201402680.
[139] J. Sun, Q. Cai, Y. Wan, S. Wan, L. Wang, J. Lin, D. Mei, Y. Wang, Promotional Effects of Cesium Promoter on Higher Alcohol Synthesis from Syngas over Cesium-Promoted Cu/ZnO/Al2O3 Catalysts, ACS Catal. 6 (2016) 5771–5785, https://doi.org/10.1021/acscatal.6b00935.
[140] H.T. Luk, C. Mondelli, S. Mitchell, S. Siol, J.A. Stewart, D. Curulla Ferre, J. Pérez-Ramírez, Role of Carbonaceous Supports and Potassium Promoter on Higher Alcohols Synthesis over Copper-Iron Catalysts, ACS Catal. 8 (2018) 9604−9618 Research. doi: 10.1021/acscatal.8b02714.
[141] Y. Li, W. Gao, M. Peng, J. Zhang, J. Sun, Y. Xu, S. Hong, X. Liu, X. Liu, M. Wei, B. Zhang, D. Ma, Interfacial Fe5C2-Cu catalysts toward low-pressure syngas conversion to long-chain alcohols, Nat. Commun. 11 (2020) 1–8, https://doi.org/10.1038/s41467-019-13691-4.
[142] K. Larmier, W.C. Liao, S. Tada, E. Lam, R. Verel, A. Bansode, A. Urakawa, A. Comas-Vives, C. Copéret, CO2-to-Methanol Hydrogenation on Zirconia-Supported Copper Nanoparticles: Reaction Intermediates and the Role of the Metal–Support Interface, Angew. Chemie - Int. Ed. 56 (2017) 2318–2323, https://doi.org/10.1002/anie.201610166.
[143] Y. Wang, S. Kattel, W. Gao, K. Li, P. Liu, J.G. Chen, H. Wang, Exploring the ternary interactions in Cu–ZnO–ZrO 2 catalysts for efficient CO2 hydrogenation to methanol, Nat. Commun. 10 (2019), https://doi.org/10.1038/s41467-019-09072-6.
[144] Y. Wang, W. Gao, K. Li, Y. Zheng, Z. Xie, W. Na, J.G. Chen, H. Wang, Strong Evidence of the Role of H2O in Affecting Methanol Selectivity from CO2 Hydrogenation over Cu-ZnO-ZrO2, Chem 6 (2020) 419–430, https://doi.org/10.1016/j.chempr.2019.10.023.
[145] H.T. Luk, C. Mondelli, D.C. Ferré, J.A. Stewart, J. Pérez-Ramírez, Status and prospects in higher alcohols synthesis from syngas, Chem. Soc. Rev. 46 (2017) 1358–1426, https://doi.org/10.1039/c6cs00324a.
[146] M. Takagawa, A. Okamoto, H. Fujimura, Y. Izawa, H. Arakawa, Ethanol synthesis from carbon dioxide and hydrogen, Stud. Surf. Sci. Catal. 114 (1998) 525–528, https://doi.org/10.1016/s0167-2991(98)80812-4.
[147] L. Ding, T. Shi, J. Gu, Y. Cui, Z. Zhang, C. Yang, T. Chen, M. Lin, P. Wang, N. Xue, L. Peng, X. Guo, Y. Zhu, Z. Chen, W. Ding, CO2 Hydrogenation to Ethanol over Cu@Na-Beta, Chem 6 (2020) 2673–2689, https://doi.org/10.1016/j.chempr.2020.07.001.
[148] D. Xu, H. Yang, X. Hong, G. Liu, S.C. Edman Tsang, Tandem Catalysis of Direct CO2 Hydrogenation to Higher Alcohols, ACS Catal. 11 (2021) 8978–8984, https://doi.org/10.1021/acscatal.1c01610.

[149] D. Xu, M. Ding, X. Hong, G. Liu, S.C.E. Tsang, Selective C2+ Alcohol Synthesis from Direct CO2 Hydrogenation over a Cs-Promoted Cu-Fe-Zn Catalyst, ACS Catal. 10 (2020) 5250–5260, https://doi.org/10.1021/acscatal.0c01184.
[150] D. Xu, M. Ding, X. Hong, G. Liu, Mechanistic aspects of the role of K promotion on Cu−Fe-based catalysts for higher alcohol synthesis from CO2 hydrogenation, ACS Catal. 10 (2020) 14516–14526, https://doi.org/10.1021/acscatal.0c03575.
[151] G. Zhang, G. Fan, L. Zheng, F. Li, Ga-Promoted CuCo-Based Catalysts for Efficient CO2Hydrogenation to Ethanol: The Key Synergistic Role of Cu-CoGaOxInterfacial Sites, ACS Appl. Mater. Interfaces. 14 (2022) 35569–35580, https://doi.org/10.1021/acsami.2c07252.
[152] C. Yang, B. Wang, Y. Wen, M. Fan, Y. Jia, S. Zhou, W. Huang, Composition control of CuFeZn catalyst derived by PDA and its effect on synthesis of C2+ alcohols from CO2, Fuel 327 (2022) 125055, https://doi.org/10.1016/j.fuel.2022.125055.
[153] H. Guo, S. Li, F. Peng, H. Zhang, L. Xiong, C. Huang, C. Wang, X. Chen, Roles Investigation of Promoters in K/Cu-Zn Catalyst and Higher Alcohols Synthesis from CO2 Hydrogenation over a Novel Two-Stage Bed Catalyst Combination System, Catal. Letters. 145 (2015) 620–630, https://doi.org/10.1007/s10562-014-1446-7.
[154] S. Santanta, M.T.M. Koper, H.M. Alisson, L.H. Vieira, E.M. Assaf, M. Assaf, J. F. Gomes, Ethanol formation from CO2 hydrogenation at atmospheric pressure using Cu catalysts: Water as a key component, Appl. Catal. b, Environ. 324 (2023) 122221, https://doi.org/10.1016/j.apcatb.2022.122221.
[155] Z. Si, L. Wang, Y. Han, J. Yu, Q. Ge, C. Zeng, J. Sun, Synthesis of Alkene and Ethanol in CO2 Hydrogenation on a Highly Active Sputtering CuNaFe Catalyst, ACS Sustain. Chem. Eng. 10 (2022) 14972–14979, https://doi.org/10.1021/acssuschemeng.2c05450.
[156] Y. Jia, B. Wang, Y. Wen, M. Fan, C. Yang, S. Zhou, Z. Cui, W. Huang, Mechanism of stability and deactivation of N-doped CuFeZn catalysts for C2+ alcohols synthesis by hydrogenation of CO2, Fuel Process. Technol. 250 (2023) 107901, https://doi.org/10.1016/j.fuproc.2023.107901.
[157] S. Zhou, Y. Wen, B. Wang, M. Fan, L. Ren, Z. Cui, W. Huang, J. Li, J. Guo, Regulation of CuFeZn catalysts by K3PO4 and its effect on CO2 hydrogenation to C2+ alcohols, Chem. Eng. J. 487 (2024) 150425, https://doi.org/10.1016/j.cej.2024.150425.
[158] Y. Wang, X. Zhang, X. Hong, G. Liu, Sulfate-Promoted Higher Alcohol Synthesis from CO2 Hydrogenation, ACS Sustain. Chem. Eng. 10 (2022) 8980–8987, https://doi.org/10.1021/acssuschemeng.2c02743.
[159] K. Okabe, H. Yamada, T. Hanaoka, T. Matsuzaki, H. Arakawa, Y. Abe, CO2 hydrogenation to alcohols over highly dispersed Co/SiO2 catalysts derived from acetate, Chem. Lett. (2001) 904–905, https://doi.org/10.1246/cl.2001.904.
[160] T. Witoon, T. Numpilai, S. Nijpanich, N. Chanlek, P. Kidkhunthod, C.K. Cheng, K. H. Ng, D.V.N. Vo, S. Ittisanronnachai, C. Wattanakit, M. Chareonpanich, J. Limtrakul, Enhanced CO2 hydrogenation to higher alcohols over K-Co promoted In2O3 catalysts, Chem. Eng. J. 431 (2022) 133211, https://doi.org/10.1016/j.cej.2021.133211.
[161] V.D. Lage, A. Le Valant, N. Bion, F.S. Toniolo, Tuning Co-Cu-Al catalysts and their reaction conditions on the CO2 hydrogenation reaction to higher alcohols under mild conditions, Chem. Eng. Sci. 281 (2023) 119208, https://doi.org/10.1016/j.ces.2023.119208.
[162] C. Yang, S. Liu, Y. Wang, J. Song, G. Wang, S. Wang, Z.J. Zhao, R. Mu, J. Gong, The Interplay between Structure and Product Selectivity of CO2 Hydrogenation, Angew. Chemie - Int. Ed. 58 (2019) 11242–11247, https://doi.org/10.1002/anie.201904649.
[163] S. Zhang, Z. Wu, X. Liu, Z. Shao, L. Xia, L. Zhong, H. Wang, Y. Sun, Tuning the interaction between Na and Co2C to promote selective CO2 hydrogenation to ethanol, Appl. Catal. B Environ. 293 (2021) 120207, https://doi.org/10.1016/j.apcatb.2021.120207.
[164] D.L.S. Nieskens, D. Ferrari, Y. Liu, R. Kolonko, The conversion of carbon dioxide and hydrogen into methanol and higher alcohols, Catal. Commun. 14 (2011) 111–113, https://doi.org/10.1016/j.catcom.2011.07.020.
[165] M. Irshad, H.J. Chun, M.K. Khan, H. Jo, S.K. Kim, J. Kim, Synthesis of n-butanol-rich C3+ alcohols by direct CO2 hydrogenation over a stable Cu–Co tandem catalyst, Appl. Catal. B Environ. 340 (2024) 123201, https://doi.org/10.1016/j.apcatb.2023.123201.
[166] K. An, S. Zhang, H. Wang, N. Li, Z. Zhang, Y. Liu, Co0 − Coδ+ active pairs tailored by Ga-Al-O spinel for CO2-to-ethanol synthesis, Chem. Eng. J. 433 (2022) 134606, https://doi.org/10.1016/j.cej.2022.134606.
[167] K. An, S. Zhang, J. Wang, Q. Liu, Z. Zhang, Y. Liu, A highly selective catalyst of Co/La4Ga2O9 for CO2 hydrogenation to ethanol, J. Energy Chem. 56 (2021) 486–495, https://doi.org/10.1016/j.jechem.2020.08.045.
[168] S. Zhang, X. Liu, Z. Shao, H. Wang, Y. Sun, Direct CO2 hydrogenation to ethanol over supported Co2C catalysts: Studies on support effects and mechanism, J. Catal. 382 (2020) 86–96, https://doi.org/10.1016/j.jcat.2019.11.038.
[169] S. Liu, H. Zhou, Q. Song, Z. Ma, Synthesis of higher alcohols from CO2 hydrogenation over Mo–Co–K sulfide-based catalysts, J. Taiwan Inst. Chem. Eng. 76 (2017) 18–26, https://doi.org/10.1016/j.jtice.2017.04.007.
[170] S. Liu, H. Zhou, L. Zhang, Z. Ma, Y. Wang, Activated Carbon-Supported Mo-Co-K Sulfide Catalysts for Synthesizing Higher Alcohols from CO2, Chem. Eng. Technol. 42 (2019) 962–970, https://doi.org/10.1002/ceat.201800401.
[171] J. Zhang, S. Lu, X. Su, S. Fan, Q. Ma, T. Zhao, Selective formation of light olefins from CO2 hydrogenation over Fe-Zn-K catalysts, J. CO2 Util. 12 (2015) 95–100, https://doi.org/10.1016/j.jcou.2015.05.004.
[172] T. Numpilai, T. Witoon, N. Chanlek, W. Limphirat, G. Bonura, M. Chareonpanich, J. Limtrakul, Structure–activity relationships of Fe-Co/K-Al2O3 catalysts calcined at different temperatures for CO2 hydrogenation to light olefins, Appl. Catal. A Gen. 547 (2017) 219–229, https://doi.org/10.1016/j.apcata.2017.09.006.
[173] X. Wang, J. Zhang, J. Chen, Q. Ma, S. Fan, T. sheng Zhao, Effect of preparation methods on the structure and catalytic performance of Fe-Zn/K catalysts for CO2 hydrogenation to light olefins, Chinese, J. Chem. Eng. 26 (2018) 761–767, https://doi.org/10.1016/j.cjche.2017.10.013.
[174] J. Wei, Q. Ge, R. Yao, Z. Wen, C. Fang, L. Guo, H. Xu, J. Sun, Directly converting CO2 into a gasoline fuel, Nat. Commun. 8 (2017) 1–8, https://doi.org/10.1038/ncomms15174.
[175] X. Cui, P. Gao, S. Li, C. Yang, Z. Liu, H. Wang, L. Zhong, Y. Sun, Selective Production of Aromatics Directly from Carbon Dioxide Hydrogenation, ACS Catal. 9 (2019) 3866–3876, https://doi.org/10.1021/acscatal.9b00640.
[176] N. Boreriboon, X. Jiang, C. Song, P. Prasassarakich, Fe-based bimetallic catalysts supported on TiO2 for selective CO2 hydrogenation to hydrocarbons, J. CO2 Util. 25 (2018) 330–337, https://doi.org/10.1016/j.jcou.2018.02.014.
[177] J. Liu, A. Zhang, M. Liu, S. Hu, F. Ding, C. Song, X. Guo, Fe-MOF-derived highly active catalysts for carbon dioxide hydrogenation to valuable hydrocarbons, J. CO2 Util. 21 (2017) 100–107, https://doi.org/10.1016/j.jcou.2017.06.011.
[178] J. Liang, J. Liu, L. Guo, W. Wang, C. Wang, W. Gao, X. Guo, Y. He, G. Yang, S. Yasuda, B. Liang, N. Tsubaki, CO2 hydrogenation over Fe-Co bimetallic catalysts with tunable selectivity through a graphene fencing approach, Nat. Commun. 15 (2024) 1–13, https://doi.org/10.1038/s41467-024-44763-9.
[179] A. Fedorov, H. Lund, V.A. Kondratenko, E.V. Kondratenko, D. Linke, Elucidating reaction pathways occurring in CO2 hydrogenation over Fe-based catalysts, Appl. Catal. B Environ. 328 (2023) 122505, https://doi.org/10.1016/j.apcatb.2023.122505.
[180] A.S. Skrypnik, S.A. Petrov, V.A. Kondratenko, Q. Yang, A.A. Matvienko, E. V. Kondratenko, Spatially resolved analysis of CO2 hydrogenation to higher hydrocarbons over alkali-metal promoted well-defined FexOyCz, J. Catal. 425 (2023) 286–295, https://doi.org/10.1016/j.jcat.2023.06.019.
[181] S. Li, H. Guo, C. Luo, H. Zhang, L. Xiong, X. Chen, L. Ma, Effect of iron promoter on structure and performance of K/Cu-Zn catalyst for higher alcohols synthesis from CO2 hydrogenation, Catal. Letters. 143 (2013) 345–355, https://doi.org/10.1007/s10562-013-0977-7.
[182] Q. Zhang, S. Wang, X. Shi, M. Dong, J. Chen, J. Zhang, J. Wang, W. Fan, Conversion of CO2 to higher alcohols on K-CuZnAl/Zr-CuFe composite, Appl. Catal. B Environ. 346 (2024) 123748, https://doi.org/10.1016/j.apcatb.2024.123748.
[183] T. Liu, D. Xu, M. Song, X. Hong, G. Liu, K-ZrO2 Interfaces Boost CO2 Hydrogenation to Higher Alcohols, ACS Catal. 13 (2023) 4667–4674, https://doi.org/10.1021/acscatal.3c00074.
[184] Q. Zhang, S. Wang, R. Geng, P. Wang, M. Dong, J. Wang, W. Fan, Hydrogenation of CO2 to higher alcohols on an efficient Cr-modified CuFe catalyst, Appl. Catal. B Environ. 337 (2023) 123013, https://doi.org/10.1016/j.apcatb.2023.123013.
[185] Y. Wang, Y. Zhou, X. Zhang, M. Wang, T. Liu, J. Wei, G. Zhang, X. Hong, G. Liu, PdFe Alloy-Fe5C2 interfaces for efficient CO2 hydrogenation to higher alcohols, Appl. Catal. B Environ. 345 (2024) 123691, https://doi.org/10.1016/j.apcatb.2024.123691.
[186] Y. Zhou, Y. Wang, H. Lu, T. Liu, X. Hong, G. Liu, Highly Dispersed K- and Pd-Comodified Fe Catalyst for CO2 Hydrogenation to Higher Alcohols, ACS Sustain. Chem. Eng. 12 (2024) 3322–3330, https://doi.org/10.1021/acssuschemeng.3c08044.
[187] J. Huang, G. Zhang, J. Zhu, M. Wang, F. Ding, C. Song, X. Guo, Boosting the Production of Higher Alcohols from CO2 and H2 over Mn- and K-Modified Iron Carbide, Ind. Eng. Chem. Res. 61 (2022) 7266–7274, https://doi.org/10.1021/acs.iecr.2c00720.
[188] X. Xi, F. Zeng, H. Zhang, X. Wu, J. Ren, T. Bisswanger, C. Stampfer, J.P. Hofmann, R. Palkovits, H.J. Heeres, CO2 hydrogenation to higher alcohols over K-promoted bimetallic Fe−in catalysts on a Ce−ZrO2 support, ACS Sustain. Chem. Eng. 9 (2021) 6235–6249, https://doi.org/10.1021/acssuschemeng.0c08760.
[189] D. Goud, S.R. Churipard, D. Bagchi, A.K. Singh, M. Riyaz, C.P. Vinod, S.C. Peter, Strain-Enhanced Phase Transformation of Iron Oxide for Higher Alcohol Production from CO2, ACS Catal. 12 (2022) 11118–11128, https://doi.org/10.1021/acscatal.2c03183.
[190] H. Kusama, K. Okabe, K. Sayama, H. Arakawa, Ethanol synthesis by catalytic hydrogenation of CO2 over Rh-Fe/SiO2 catalysts, Energy 22 (1997) 343–348, https://doi.org/10.1016/S0360-5442(96)00095-3.
[191] F. Zhang, W. Zhou, X. Xiong, Y. Wang, K. Cheng, J. Kang, Q. Zhang, Y. Wang, Selective Hydrogenation of CO2 to Ethanol over Sodium-Modified Rhodium Nanoparticles Embedded in Zeolite Silicalite-1, J. Phys. Chem. c. 125 (2021) 24429–24439, https://doi.org/10.1021/acs.jpcc.1c07862.
[192] G. Wang, R. Luo, C. Yang, J. Song, C. Xiong, H. Tian, Z.J. Zhao, R. Mu, J. Gong, Active sites in CO2 hydrogenation over confined VOx-Rh catalysts, Sci. China Chem. 62 (2019) 1710–1719, https://doi.org/10.1007/s11426-019-9590-6.
[193] S. Ji, F. Hong, D. Mao, Q. Guo, J. Yu, Enhanced ethanol synthesis from CO2 hydrogenation over Fe and Na co-modified Rh/CeO2 catalysts, Chem. Eng. J. 495 (2024) 153633, https://doi.org/10.1016/j.cej.2024.153633.
[194] B. Ouyang, S. Xiong, Y. Zhang, B. Liu, J. Li, The study of morphology effect of Pt/Co3O4 catalysts for higher alcohol synthesis from CO2 hydrogenation, Appl. Catal. A Gen. 543 (2017) 189–195, https://doi.org/10.1016/j.apcata.2017.06.031.
[195] Y. Lou, F. Jiang, W. Zhu, L. Wang, T. Yao, S. Wang, B. Yang, B. Yang, Y. Zhu, X. Liu, CeO2 supported Pd dimers boosting CO2 hydrogenation to ethanol, Appl. Catal. B Environ. 291 (2021) 120122, https://doi.org/10.1016/j.apcatb.2021.120122.

[196] A. Goryachev, A. Pustovarenko, G. Shterk, N.S. Alhajri, A. Jamal, M. Albuali, L. van Koppen, I.S. Khan, A. Russkikh, A. Ramirez, T. Shoinkhorova, E.J. M. Hensen, J. Gascon, A Multi-Parametric Catalyst Screening for CO2 Hydrogenation to Ethanol, ChemCatChem 13 (2021) 3324–3332, https://doi.org/10.1002/cctc.202100302.

[197] C. Zhou, A. Aitbekova, G. Liccardo, J. Oh, M. Stone, E.J. McShane, B. Werghi, S. Nathan, C. Song, J. Ciston, K. Bustillo, A.S. Hoffman, J. Hong, J. Perez-Aguilar, S. Bare, M. Cargnello, Steam-Assisted Selective CO2 Hydrogenation to Ethanol over Ru-In Catalysts, Angew. Chemie Int. Ed. (2024) e202406761, https://doi.org/10.1002/anie.202406761.

[198] C. Yang, R. Mu, G. Wang, J. Song, H. Tian, Z.J. Zhao, J. Gong, Hydroxyl-mediated ethanol selectivity of CO2 hydrogenation, Chem. Sci. 10 (2019) 3161–3167, https://doi.org/10.1039/c8sc05608k.

[199] K.K. Bando, K. Soga, K. Kunimori, H. Arakawa, Effect of Li additive on CO2 hydrogenation reactivity of zeolite supported Rh catalysts, Appl. Catal. A Gen. 175 (1998) 67–81, https://doi.org/10.1016/s0926-860x(98)00202-6.

[200] H. Kusama, K. Okabe, K. Sayama, H. Arakawa, CO2 hydrogenation to ethanol over promoted Rh/SiO2 catalysts, Catal. Today. 28 (1996) 261–266, https://doi.org/10.1016/0920-5861(95)00246-4.

[201] B. Ren, X. Dong, Y. Yu, G. Wen, M. Zhang, A density functional theory study on the carbon chain growth of ethanol formation on Cu-Co (111) and (211) surfaces, Appl. Surf. Sci. 412 (2017) 374–384, https://doi.org/10.1016/j.apsusc.2017.03.106.

[202] G. Wang, R. Zhang, B. Wang, Insight into the preference mechanism for C−C chain formation of C2 oxygenates and the effect of promoters in syngas conversion over Cu-based catalysts, Appl. Catal. A Gen. 466 (2013) 77–89, https://doi.org/10.1016/j.apcata.2013.06.042.

[203] X.C. Xu, J. Su, P. Tian, D. Fu, W. Dai, W. Mao, W.K. Yuan, J. Xu, Y.F. Han, First-principles study of C2 oxygenates synthesis directly from syngas over CoCu bimetallic catalysts, J. Phys. Chem. c. 119 (2015) 216–227, https://doi.org/10.1021/jp5065159.

[204] X. Sun, R. Zhang, B. Wang, Insights into the preference of CH x (x = 1-3) formation from CO hydrogenation on Cu(111) surface, Appl. Surf. Sci. 265 (2013) 720–730, https://doi.org/10.1016/j.apsusc.2012.11.091.

[205] G. Wang, R. Zhang, B. Wang, Insight into the Preference Mechanism of CHx (x =1−3) and C−C Chain Formation Involved in C2 Oxygenate Formation from Syngas on the Cu(110) Surface, J. Phys. Chem. c. 117 (2013) 6594–6606, https://doi.org/10.1016/j.apcata.2013.06.042.

[206] H. Zheng, R. Zhang, Z. Li, B. Wang, Insight into the mechanism and possibility of ethanol formation from syngas on Cu(100) surface, J. Mol. Catal. A Chem. 404–405 (2015) 115–130, https://doi.org/10.1016/j.molcata.2015.04.015.